TECHNISCHE UNIVERSITÄT MÜNCHEN

Lehrstuhl für Energiewirtschaft und Anwendungstechnik

Damping of Torsional Interaction Effects in Power Systems

Simon Schramm

Vollständiger Abdruck der von der Fakultät für Elektrotechnik und Informationstechnik der Technischen Universität München zur Erlangung des akademischen Grades eines

Doktor-Ingenieurs

genehmigten Dissertation.

Vorsitzender: Univ.-Prof. Dr.-Ing. Josef Kindersberger

Prüfer der Dissertation:

1. Univ.-Prof. Dr.-Ing. Ulrich Wagner
2. Univ.-Prof. Dr.-Ing. Rolf Witzmann
3. Prof. Dr.-Ing. Gerd Becker (Hochschule München)

Die Dissertation wurde am 21.01.2010 bei der Technischen Universität München eingereicht und durch die Fakultät für Elektrotechnik und Informationstechnik am 23.06.2010 angenommen.

Danksagung

Die vorliegende Dissertation entstand während meiner Tätigkeit als wissenschaftlicher Mitarbeiter im Bereich Hochleistungselektronik und Energiesysteme am Europäischen Forschungszentrum der Firma General Electric. Während dieser Zeit bin ich so vielen Menschen begegnet, die mir ihr Wissen und ihre Unterstützung zuteil werden ließen, dass es mir unmöglich erscheint, alle hier namentlich zu erwähnen.
Mein besonderer Dank gilt Herrn Professor Dr.-Ing. Ulrich Wagner, Leiter des Lehrstuhl für Energiewirtschaft und Anwendungstechnik der Technischen Universität München für die stete Unterstützung meiner Arbeit, die Anregungen und das kritischen Hinterfragen der angewandten Methodik und Ergebnisse.
Mein Dank gilt auch Herrn Professor Dr.-Ing. Rolf Witzmann für die Übernahme des Korreferats, und Herrn Professor Dr.-Ing. Josef Kindersberger für die Übernahme des Prüfungsvorsitzes.
Besonders möchte ich mich bei Herrn Professor Dr.-Ing. Gerd Becker und bei Herrn Professor Dr.-Ing. Oliver Mayer bedanken für die stetige, wertvolle Unterstützung in technischen und „anderen“ Fragen.
Ganz besonders möchte ich mich auch bei Herrn Dr.-Ing. Christof Sihler für die hervorragende Zusammenarbeit und Unterstützung während meiner ganzen Zeit bei General Electric bedanken. Er hat es immer sehr gut verstanden, mich vor anderen Aufgaben im Forschungszentrum zu bewahren, sodass ich mich auf diese Arbeit konzentrieren konnte.
Allen Mitarbeiterinnen und Mitarbeitern des Forschungszentrums und des Lehrstuhls für Energiewirtschaft und Anwendungstechnik möchte ich für die kollegiale Zusammenarbeit und Unterstützung danken.
Ganz herzlich möchte ich mich bei meiner Familie bedanken, die mich während dieser nicht immer einfachen Zeit durch ihre Unterstützung und Liebe getragen hat.

München, 03. Mai 2010
Simon Schramm

To My Family

Zusammenfassung

Drehzahlveränderliche Antriebe ermöglichen einen energieeffizienten Anlagenbetrieb. Die dazu erforderliche Leistungselektronik erzeugt Stromkomponenten mit (inter)harmonischen Frequenzanteilen. Große Antriebsstränge können geringe mechanische Dämpfungseigenschaften im Bereich ihrer Eigenfrequenzen aufweisen. Ein Übereinstimmen von interharmonischen Stromkomponenten mit mechanischen Eigenfrequenzen kann zur Anregung von Drehmomentschwingungen und damit zur Lebensdauerverkürzung des mechanischen Systems führen.

Schwerpunkt der Arbeit ist die Untersuchung einer Methode zur aktiven Dämpfung von periodisch angeregten Drehmomentschwingungen in Energiesystemen. Die entwickelte Methode erlaubt eine elektronisch einstellbare Erhöhung der Dämpfung eines elektrisch gekoppelten Systems, ohne dass Änderungen am mechanischen Design notwendig sind. Die entwickelte Methode wurde numerisch untersucht und an großen Antriebssystemen erfolgreich validiert.

Abstract

Variable speed-driven electric motor trains enable more energy efficient modes of operation. The variable speed operation is typically achieved by means of power electronic converters, which create harmonics and interharmonics. Mechanical drive trains for high power application have typically low inherent damping at their natural frequencies. Torsional interaction, a coincidence of electrically generated harmonics with (one or more) natural frequencies of a generator or motor train, can cause torsional oscillation issues, which may have a negative impact on the lifetime of a drive train.
Main focus of this thesis is the investigation of new countermeasures against torsional interactions. The developed approach is capable of increasing the overall damping behavior of mechanical drive trains at their sensitive natural frequencies, without modification of the mechanical train or power system. Thus, the applied damping becomes electronically adjustable. The approach has been numerically investigated by detailed simulation models and validated in test setups with large electric motor driven trains.

Contents

1

Introduction

Electric motor systems are by far the most important type of load in industry, e.g. in the EU they account for about 70% of the consumed electricity [1]. It is their wide use that makes motors particularly attractive for the application of efficiency improvements, especially those using power electronic devices to allow variable speed operation. Variable speed operation enables the largest energy savings in process industry applications, e.g. compressor applications with variable flow requirements, fluid-handling applications or in fan applications with variable cooling requirements. Driven by the high cost of electricity and the power handling capability of modern power electronic devices, mechanical drives and direct grid connected motors are increasingly being replaced by variable speed drives (VSDs). This trend started many years ago and it has now reached multi-megawatt drives. In these drive applications, VSDs were originally only applied as starter or helper motors for other prime movers, such as gas turbines. Higher efficiency, operational flexibility, speed controllability, lower annual maintenance costs, zero site air emissions or reduced noise levels are benefits of replacing a mechanical prime mover by power electronics-driven electrical machinery. But all power electronic designs produce harmonics with multiples of the fundamental frequency, multiples of the switching frequency, a combination of both frequencies and interharmonics. All these harmonics can produce pulsating torque components and possibly interact with rotor-shaft systems.

Torsional interaction due to harmonic excitation is a frequent topic in today's literature [2–5]. New developments in power electronic designs for large rotating machinery reduce the effect of pulsating torques with complex, multi-level arrangements or new control strategies. But torsional oscillations with significant impact on the lifetime of the

mechanical equipment can already be caused by electrical torque components with an amplitude of less than one percent of the nominal torque, if their frequency corresponds to one of the natural frequencies of the mechanical system.
Large drive trains typically have high moments of inertia, high torsional stiffness and low natural damping of torsional modes. The low mechanical damping in high power trains is one of the main reasons for torsional interaction between power system components and the mechanical drive train. If one of the natural frequencies of the mechanical drive train is excited to a torsional resonance, the resulting alternating mechanical torque can reach values that cause damage or fatigue in components of the rotor shaft system. Larger drive trains have multiple natural frequencies; therefore, a coincidence with significant electrical harmonics is more likely, e.g. while running up the train.
Torsional interaction can occur for power generation and motor units. Problems of and solutions for torsional interaction with large synchronous generator trains in utility applications have been discussed since the 1970's. The first natural frequencies (modes) are typically found at subsynchronous frequencies. Torsional oscillation can be excited by single events, e.g. faults in the power system, but also continuously by pulsating torque components, e.g. by subsynchronous resonance (SSR) phenomena in power systems [6].
The increasing trend of using large motors driven by power electronics has caused a new generation of torsional interaction phenomena. Issues can occur in the mechanical system driven by an electrical motor or in the power system supplying the electrical drive (VSD), especially in cases where the nominal power of the VSD is in the same order of magnitude as the nominal power of single synchronous generators in the power system. Some typical effects of uncontrolled torsional oscillation in large drive trains are failed couplings, broken shafts, and worn or fractured gear teeth in trains with gearboxes.

Examples for New Torsional Interaction Phenomena

Power generation trains installed close to power electronic devices with relevant nominal power can be found in many areas, especially in remote power systems with island-like structures, e.g. wind-farms or oil & gas industry power systems. Often, there are many power electronic loads from different manufacturers connected in direct proximity to each other. In such cases it is extremely difficult to link harmonic excitation of conventional units to dedicated VSDs, especially if they are all operated at different speeds, thus causing different pulsating torque components that vary with time.

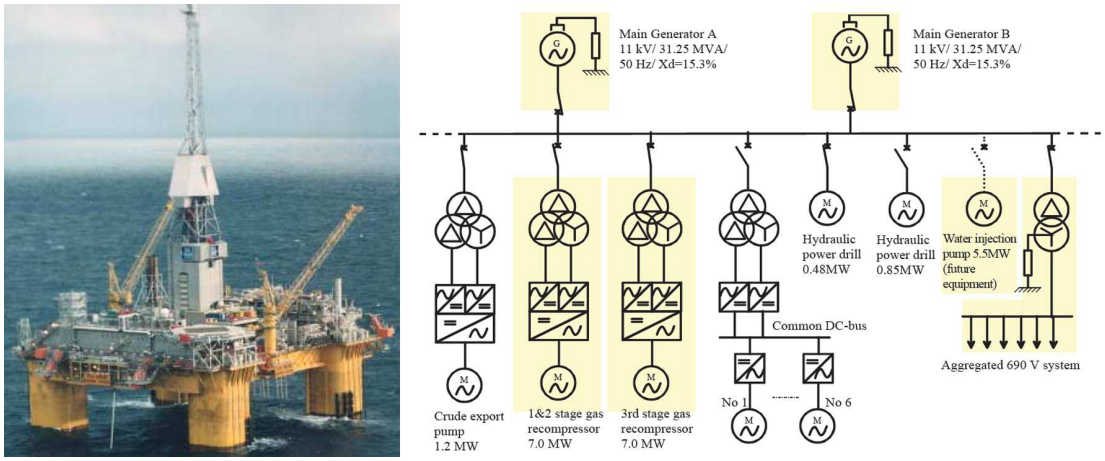

Figure 1.1: Typical island power system, powered by two gas turbine driven synchronous generators.

Figure 1.1 shows an existing power system arrangement that is typical for industrial applications of the process industry. There are several power electronic driven loads connected to the distribution bus fed by synchronous generators.

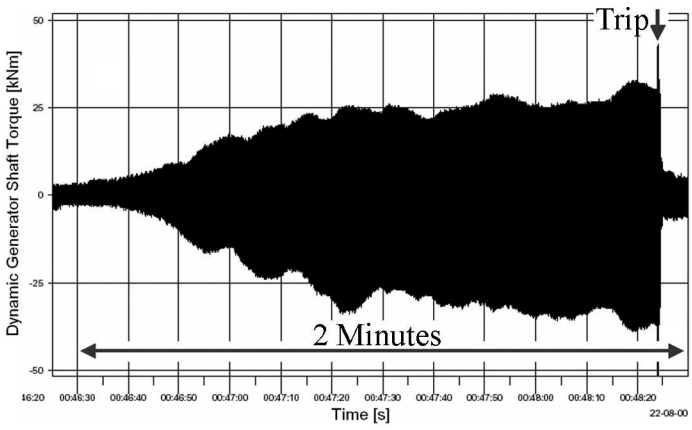

Figure 1.2: Torsional vibration level, measured on a synchronous generator as a result of electro-mechanical interaction with VSDs, leading to a protective trip of the generator [7].

Figure 1.2 shows the vibration level of a conventional generator caused by torsional interaction with VSDs. The pulsating torque component causing this resonance excitation must have been very low, because it took two minutes until a critical alternating torque level was reached and a protective trip of the generator was initiated, with the result of a system blackout.

A similar torsional interaction effect due to harmonic excitation can be observed with

electric drives, which enable variable speed operation of large motors. Figure 1.3 shows a measurement performed during string tests on a large compressor drive train while passing a critical speed. This case is quite similar to the first example, as there is typically no possibility of preventing the crossing of the critical speeds or even operation at critical speeds; the speed reference is typically set by process requirements.

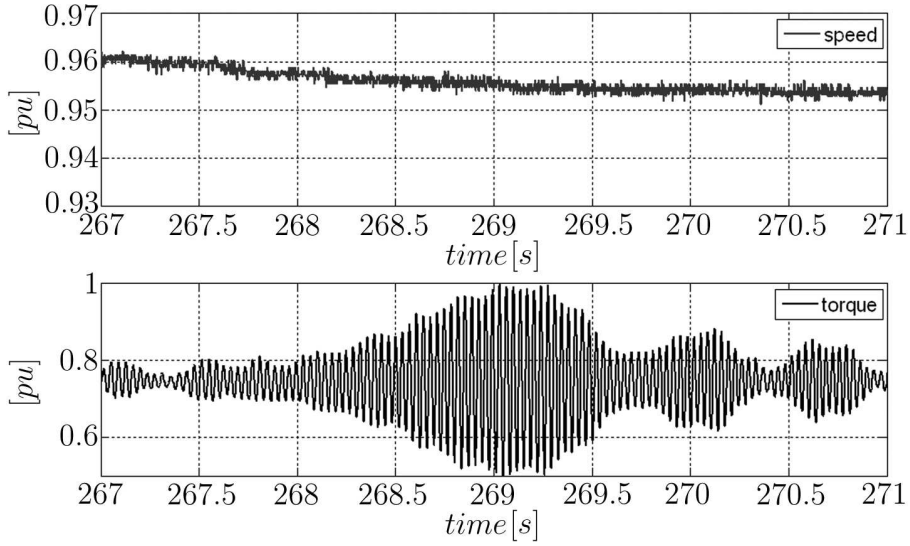

Figure 1.3: Measured shaft torque of a synchronous motor driven compressor drive train while passing a critical speed.

1.1 Thesis Objective

This thesis investigates new countermeasures against torsional interaction in power systems. Conventional countermeasures are typically based on avoiding excitation of resonances in the power system, e.g. using passive or active filters, or by mechanical approaches like improving the operational properties at critical speeds or moving natural mechanical frequencies out of the operation area. The new countermeasures are based on decreasing the sensitivity of large electrical machinery in the multi-megawatt range against torsional interaction caused by harmonic excitation. This is achieved by increasing the damping properties of the rotating equipment with power electronic devices. Torsional Mode Damping (TMD) as a countermeasure to torsional interactions will be investigated for different applications in island or island-like power systems feeding variable speed driven motors.

The investigated systems will be modeled with appropriate granularity in the power system, power electronics, electrical machinery and mechanical system to investigate and

estimate the effect of torsional interaction. Input parameters for these models are the mechanical design parameters of the drive train, the power system and drive system design together with all relevant controls. The simulation results will be validated and the simulation will be modified based on field measurements where available. The appropriate numerical simulation environments are used based on the application area and the focus of the investigation.

1.2 Thesis Structure

The thesis is split into three main chapters: Chapter 2 summarizes the theory and modeling aspects of coupled mechanical and electrical equipment relevant for torsional interaction understanding and analysis. The focus in the mechanical modeling section is the discussion of Q-factor determination and empiric (based on measurements) Q-factor values, which is the most critical property for large mechanical drive trains with respect to torsional interaction. The basic theory behind power electronics, especially their harmonic production, is also discussed in this chapter, as power electronic converters are the main source of harmonic excitation and torsional interaction.
Chapter 3 introduces the topic of torsional interaction by harmonic excitation in power systems. Typical sources of excitation in power systems are discussed; the relevant sources for harmonic excitation are investigated and possible impacts of torsional interaction are pointed out.
Chapter 4 and 5 are the main chapters in terms of the development and application of the novel damping devices. After giving an overview of existing solutions against torsional interaction, the thesis will propose new solutions, based on TMD, investigate the impact of TMD on relevant system designs and describe how TMD designs can be applied and optimized for different applications.

2

Modeling and Component Aspects

Numerical simulation is an important tool in science and engineering. A model must be sufficiently detailed but simple to understand and easy to manipulate. A model is typically defined by what is considered relevant. The modeling basis relevant for torsional interaction is described in the following chapter.

2.1 Mechanical Model

Torsional interaction (TI) is an interdisciplinary topic that involves mechanical and electrical engineering, as it occurs often in mechanical systems, but for electrical reasons. TI can occur in all drive train arrangements, but it is mainly critical for large rotating machinery with low inherent damping properties. The mechanical damping at a natural frequency is the critical parameter for the impact of TI. The determination of damping parameters mainly based on empiric knowledge will be discussed.
The analysis of the torsional behavior is mandatory for large drive trains, e.g. [8]. The basic theory and important tools will be discussed in this section. The main focus is on understanding and evaluating the torsional interaction of large drive trains.

2.1.1 Single Mass System

A typical way to represent a mechanical system is to use discrete elements for mass (m), spring (k) and damping (d). The masses of the system are concentrated on n masses,

which are connected by mass-less damping and spring components [9].

$$m\ddot{x} + d\dot{x} + kx = F(t) \tag{2.1}$$

Equation 2.1 represents Newton's law $\sum F = 0$. The eigenvalues of the equation can be calculated to:

$$s_{1/2} = -\frac{d}{2m} \pm \sqrt{\left(\frac{d}{2m}\right)^2 - \frac{k}{m}} \tag{2.2}$$

The natural frequency of an undamped system can be determined with $\omega_0 = \sqrt{\frac{k}{m}}$. The solutions of the differential equation are:

- $\left(\frac{d}{2m}\right)^2 - \frac{k}{m} > 0$, two real eigenvalues, $s_1 = \delta_1$, $s_2 = \delta_2$, the homogenous solution of the differential equation is then in the form of $x(t) = A \cdot e^{s_1 t} + B \cdot e^{s_2 t}$, aperiodic behavior without oscillation;
- $\left(\frac{d}{2m}\right)^2 - \frac{k}{m} = 0$, double negative eigenvalue $s_{1/2} = -\omega_0$ with the critical damping $d_{krit} = 2m\omega_0$, $x(t) = A \cdot e^{w_0 t}$, resulting in a periodic oscillation without damping;
- $\left(\frac{d}{2m}\right)^2 - \frac{k}{m} < 0$, a conjugate-complex pair $s_{1/2} = \delta \pm j\omega$, resulting in:

$$x(t) = e^{\delta t}\left(A \cdot e^{j\omega t} + B \cdot e^{-j\omega t}\right) \tag{2.3}$$

  where $e^{\delta t}$ represents the damping function with the damping coefficient $\delta = -\frac{d}{2m}$, the expression in brackets a periodic oscillation function.

Only the solution $\left(\frac{d}{2m}\right)^2 - \frac{k}{m} < 0$ is relevant in real applications and investigated within this thesis. Applying initial speed $\dot{x}(t = 0) = \dot{x}_0$ and initial angle $x(t = 0) = x_0$, the solution of the homogenous differential equation is then:

$$x_h(t) = e^{\delta t}\left[x_0 cos(\omega t) + \left(\frac{\dot{x}_0 - \delta \cdot x_0}{\omega}\right) sin(\omega t)\right] \tag{2.4}$$

The characteristic of this equation depends on the damping coefficient δ, which can be

- $\delta < 0$, the amplitude of the oscillation is decreasing over time.
- $\delta = 0$, the oscillation amplitude is constant, undamped oscillation.
- $\delta > 0$, the oscillation amplitude is negatively damped and increases with time.

Figure 2.1 illustrates the effect of different damping behaviors that can be observed with TI. The damping at the natural frequency is the key component for torsional interaction

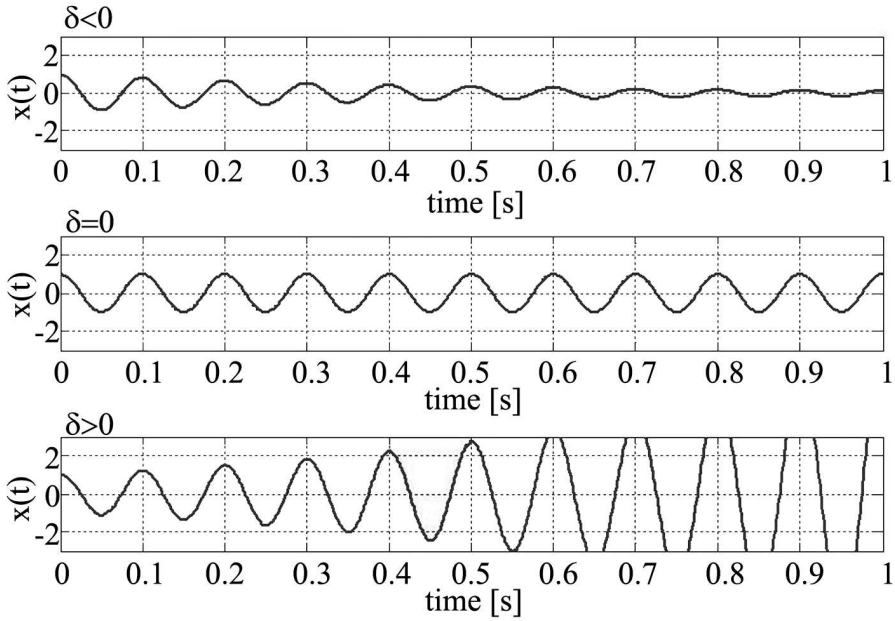

Figure 2.1: Impact of different damping coefficients on the resulting amplitude of oscillation. Case 3 ($\delta > 0$) is called negative damping ($d < 0$).

with large drive trains, as the mechanical inherent damping is very low at these frequencies, and potentially negatively influenced by non-linearity in the power system, as will be discussed in Chapter 2.1.3, 2.3 and 3.

2.1.2 Forced Oscillation

The partial solution of the differential equation depends on the type of external force $F(t)$. Distinguishing between non-periodic and periodic excitation will be made in the following section. These are the main types of excitation for torsional interaction (Chapter 3).

NON-PERIODIC EXCITATION

Step function-like behavior as non-periodic excitation can be observed with TI, e.g. with the torque response of a rotating drive train after an electrically close grid fault. A general step function $F(t)$ can be formulated with:

$$F(t) = \begin{cases} 0 & \text{for } t < 0 \\ \hat{F} & \text{for } t \geq 0 \end{cases} \tag{2.5}$$

The solution for the differential equation $m\ddot{x} + d\dot{x} + kx = F(t)$ can be formulated with $\dot{x}(t=0) = \dot{x}_0$ and $x(t=0) = x_0$ and $\zeta = \frac{\hat{F}}{m\omega_0^2}$ to:

$$x(t) = e^{\delta t}\left((x_0 - \zeta)cos(\omega t) + \frac{\dot{x} - \delta(x_0 - \zeta)}{\omega}sin(\omega t)\right) + \zeta \tag{2.6}$$

Equation 2.6 indicates that a step function applied to a mechanical system results in a static deflection ζ, followed by a transient response mainly described by the damping coefficient δ. This response is typical for torque steps acting on mechanical systems, e.g. the mechanical torque response of an electrically driven train after a trip event of the electrical system. Here, the system oscillates with a natural frequency ω_0 of the drive train; the decay is defined by the inherent mechanical damping of the mechanical system as shown in Figure 2.2.

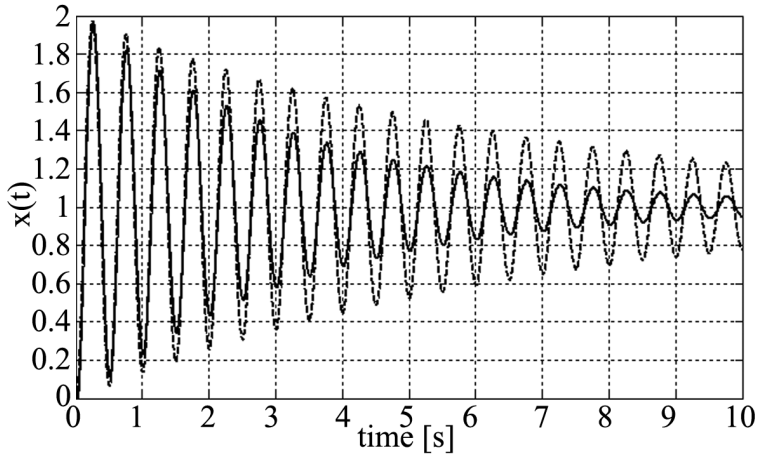

Figure 2.2: Time domain result of Equation 2.6 with $\zeta = 1$ and two different damping coefficients $\delta = -0.3$ (solid) and $\delta = -0.15$ (dashed) applied.

HARMONIC EXCITATION

Harmonic excitation is the main type of excitation relevant for TI within this thesis, and can be observed e.g. with pulsating torques generated by interharmonics of power electronic devices (Section 2.3) or imbalances in mechanical systems. The harmonic excitation function can be represented with a Fourier series:

$$F(t) = a_0 + \sum_{k=1}^{\infty} a_k cos(k\Omega t) + \sum_{k=1}^{\infty} b_k sin(k\Omega t) \tag{2.7}$$

A simplified method for finding the solution for the inhomogeneous differential equation is to reduce the number of harmonics to one, using $F(t) = \hat{F}cos(\Omega t)$ as source for harmonic

excitation. The particular solution can be written for ($\omega_0 \neq \Omega$) as:

$$x_p(t) = \frac{\hat{F}}{m} \frac{\left[(\Omega^2 - \omega_0^2)\left[cos(\Omega t) - e^{\delta t}\left(\frac{\delta}{\omega} sin(\omega t) + cos(\omega t)\right)\right] + 2\delta\left(\frac{\omega_0^2}{\omega} e^{\delta t} sin(\omega t) - \Omega sin(\Omega t)\right)\right]}{4\delta^2\Omega^2 + \left(\omega_0^2 - \Omega^2\right)^2} \tag{2.8}$$

with $x(t) = x_h(t) + x_p(t)$ ($x_h(t)$ - Equation 2.4). A second simplification is to neglect the damping behavior of the mechanical system, which can be appropriate for large drive trains; the differential equation is then reduced to $m\ddot{x} + kx = \hat{F}cos(\Omega t)$. The solution for $\omega_0 = \Omega$ can be written as:

$$x(t) = x_0 cos(\omega_0 t) + \frac{\dot{x}_0}{\omega_0} sin(\omega_0 t) + \frac{\hat{F}}{2m\omega_0} \cdot \mathbf{t} \cdot sin(\omega_0 t) \tag{2.9}$$

Harmonic excitation at the natural frequency results in an increasing deflection, proportional with time, dependent on amplitude of excitation $\hat{F}$, inertia m and exposure time t. Even small harmonic magnitudes e.g. interharmonics in the power system, can result in a large magnitude of alternating torque components of rotational equipment. The impact of the excitation frequency Ω and the damping ratio $D = \frac{d}{2\sqrt{mk}}$ can be observed in Figure 2.3, where the excitation frequency Ω is normalized by the natural frequency ω_0 on the x-axis and the absolute value of deflection $|\hat{x}(\Omega/\omega_0)|$ in the y-axis.
Expressing ω with the damping ratio D results in $\omega = \omega_0\sqrt{1 - D^2}$. $\Omega/\omega_0 = 1$ illustrates the resonant point or the natural frequency of the system (Figure 2.3). Large drive systems typically have very low damping ratios; they are very sensitive at the torsional natural frequencies. The value $|\hat{x}(\Omega/\omega_0)|$ is also called amplification factor, in the area of large drive systems also Q-factor.

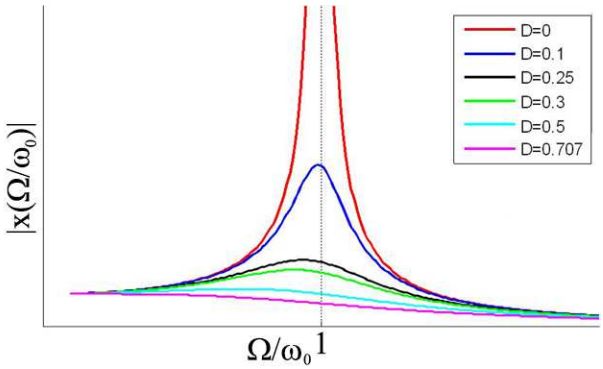

Figure 2.3: Amplification factor, dependent on damping ratio D and on frequency of excitation.

2.1.3 Q-Factor Determination

The mechanical damping is the most critical parameter for torsional interaction with large drive trains. The term "damping" denotes the combined effect of influences due to material damping, damping from windage, damping in bearings and electrical damping. A quantitative assessment of the magnitude of damping has been possible only on the basis of extensive measurements and tests [5]. The amplification factor caused by TI is mainly critical close to the natural frequency. Figure 2.3 shows that the dynamic response of mechanical systems is typically uncritical in frequency regions away from the resonance point. Mechanical engineers prefer the expression amplification factor or Q-factor instead of using, e.g., the damping ratio D, with $Q = \frac{1}{2D}$.
The Q-factor determination requires empiric knowledge; shaft material as well as shaft shear stress have significant impact on this value, which makes it difficult to calculate the effective Q-factor.
A convenient way to determine the amount of damping present in a system is to measure the rate of decay of a free oscillation, e.g. after a trip of a mechanical system, where the basic response of a mechanical system in the time domain is similar to Figure 2.2. The larger the damping, the higher will be the rate of decay. A measure of decay is the logarithmic decrement Λ, defined as the natural logarithm of the ratio of any n successive local maximum magnitudes x_1, x_2 Figure 2.4.

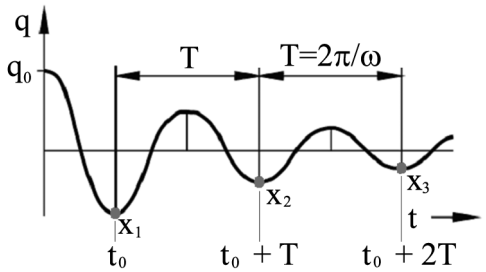

Figure 2.4: Logarithmic decrement determination based on time domain recording.

The expression for the logarithmic decrement applying Equation 2.4 with $x(t) = Ce^{\delta t}cos(\omega t + \phi)$ then results in:

$$n\Lambda = ln\frac{x_1}{x_2} = ln\frac{Ce^{\delta t_1}cos(\omega t_1 + \phi)}{Ce^{\delta(t_1+n\cdot\tau_d)}cos(\omega(t_1 + n\cdot\tau_d) + \phi)} \tag{2.10}$$

Using periodicity of the cos-function and the relation $\delta = -D\omega_0$ and $\omega = \omega_0\sqrt{1-D^2}$ results in the logarithmic decrement equal to:

$$\Lambda = \frac{1}{n} ln \frac{x1}{x2} = \frac{2\pi D}{\sqrt{1-D^2}} \tag{2.11}$$

The Q-factor can be calculated to:

$$Q = 1/\left(2\sqrt{\frac{\Lambda^2}{\Lambda^2 + 4\pi^2}}\right) \tag{2.12}$$

Large drive trains typically have small damping values, Equation 2.11 can be simplified to:

$$\Lambda = 2\pi D = \frac{\pi}{Q} = \frac{1}{n} ln \frac{x_1}{x_2} \tag{2.13}$$

The Q-factor can therefore be calculated to:

$$Q = \frac{n \cdot \pi}{ln \frac{x_1}{x_2}} \tag{2.14}$$

Empiric knowledge is essential for Q-factor determination. An empiric Q-factor relation for steam turbines units with eigenfrequencies between $8Hz$ and $150Hz$ is identified by $Q = \frac{f_{nat}}{0.10...0.16}$ (Figure 2.5)[i]. The Q-factor increases with increasing frequency.

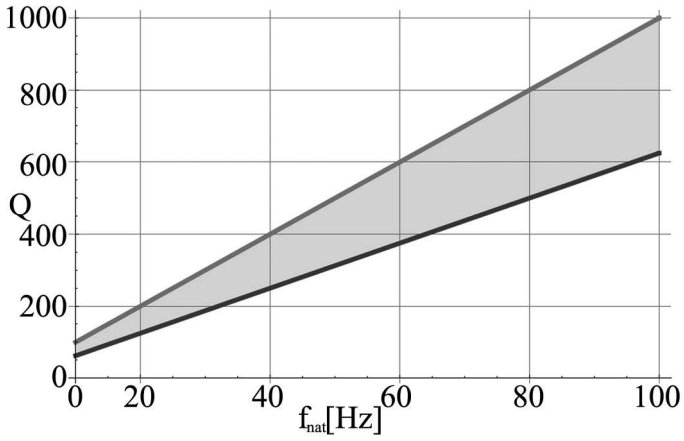

Figure 2.5: Q-factor for steam turbine units as function of natural frequency relevant for TI [10].

Another common way of expressing the damping of a mechanical system is to link the damping to the critical damping ($D = 1$, $d = d_{crit}$). A damping of $d = (1\%..2\%) \cdot d_{crit}$

[i] An oscillation decay based on Equation 2.10 between $1.38s$ (black) and $2.21s$ (gray) for a decay to half of the initial value, independent from the natural frequency has been measured for different units.

results in a Q-factor value between 25 and 50 for synchronous motor-driven turbomachinery ($D = \frac{d}{d_{crit}}$ and $Q = \frac{d_{crit}}{2d}$), reported in [11]. Measurements (e.g. Figure 2.6) have shown Q-factors between 100 and 1000 for large drive trains, which is more in line with Figure 2.5 and own experience during several measurements on large drive trains.

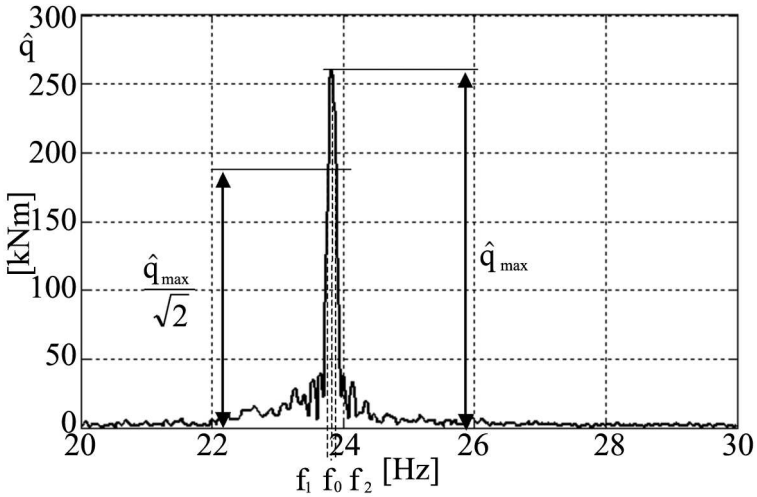

Figure 2.6: Measurement on a $144MVA$ generator after applying a step-load change [12]: A Q-factor of 200 can be calculated in the frequency domain with $Q = f_0/(f_2 - f_1)$.

Table 2.1 summarizes these amplification factors for synchronous machines driving turbomachinery and for power generation applications, together with the rated power of the synchronous units.

Application	Typical Nominal Power	Torsional Nat. Freq. of Interest	Q (conservative value)
Geared turbomachine	<50 MW	< 200 Hz	25-33
Ungeared turbomachine	<50 MW	< 200 Hz	40
Flywheel generator	150 MW	20-30 Hz	200
Power generation (utility steam turbines)	<1000 MW	8-150 Hz	400 (full load) to 4000 (light load)

Table 2.1: Summary of Q-factors reported for high power drive trains [13].

According to Table 2.1, generic values used for analysis of TI should be chosen with care, especially for new applications in the high power area because of the relatively wide spread of Q-factors. Conservative values derived from similar designs should be applied until measurement results become available.

The damping of a mechanical system can also be influenced by non-linear elements, e.g. gearboxes. The Q-factor of geared drive trains is typically lower than ungeared systems; a factor of two is mentioned in literature [11].

2.1.4 Multi-Mass System

A single mass-spring system is typically not suitable for investigating torsional interactions between electrical and mechanical systems. The minimum required complexity is to represent multiple mechanical components in the form of discrete spring, mass and damping elements (Figure 2.7) to obtain desired natural frequencies and damping of the mechanical system. The solution can usually be derived after cutting the mechanical model free.

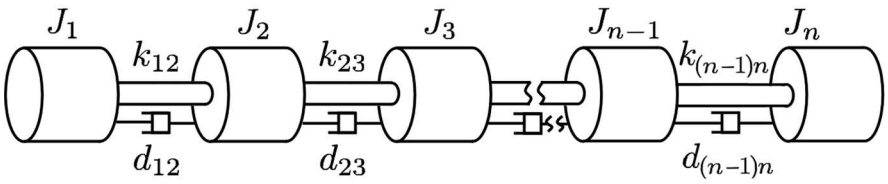

Figure 2.7: Mechanical multi-mass representation of a rotor-shaft system.

Rotor shaft systems are typically represented by the parameter J for the rotational moment of inertia, k and d stand for the rotational stiffness and damping. The rotational coordinate is ϕ (torsional angle). The complexity of the differential equation increases with the number of discrete elements, and it is advantageous to write it in matrix format. For a $n = 2$ system, the differential equation is:

$$\begin{bmatrix} J_1 & 0 \\ 0 & J_2 \end{bmatrix} \begin{Bmatrix} \ddot{\phi}_1 \\ \ddot{\phi}_2 \end{Bmatrix} + \begin{bmatrix} (d_1 + d_2) & -d_2 \\ -d_2 & (d_2 + d_3) \end{bmatrix} \begin{Bmatrix} \dot{\phi}_1 \\ \dot{\phi}_2 \end{Bmatrix} + \begin{bmatrix} (k_1 + k_2) & -k_2 \\ -k_2 & (k_2 + k_3) \end{bmatrix} \begin{Bmatrix} \phi_1 \\ \phi_2 \end{Bmatrix} = \begin{Bmatrix} 0 \\ 0 \end{Bmatrix} \tag{2.15}$$

The matrices are mass matrix (**J** , diagonal), damping matrix **D** and stiffness matrix **K** (symmetric about the diagonal). Thus, the square matrices are equal to their transpositions, e.g. $[J]^T = [J]$, $[D]^T = [D]$ and $[K]^T = [K]$. Equation 2.15 can be generalized in the form:

$$[\mathbf{J}] \cdot \left\{ \ddot{\phi} \right\} + [\mathbf{D}] \cdot \left\{ \dot{\phi} \right\} + [\mathbf{K}] \cdot \{\phi\} = [\mathbf{F}] \cdot \{u\} \tag{2.16}$$

where $\mathbf{J}$ can be written as:

$$\mathbf{J} = \begin{bmatrix} J_1 & 0 & \dots & 0 \\ 0 & J_2 & \dots & 0 \\ \vdots & \vdots & \ddots & \vdots \\ 0 & 0 & 0 & J_n \end{bmatrix} \tag{2.17}$$

The Γ matrix (Equation 2.18) can be transformed into the damping matrix $\mathbf{D}$ in replacing γ_x by d_x, and into the stiffness matrix $\mathbf{K}$ in replacing γ_x by k_x:

$$\Gamma = \begin{bmatrix} (\gamma_1 + \gamma_2) & -\gamma_2 & 0 & \dots & 0 & 0 \\ -\gamma_2 & (\gamma_2 + \gamma_3) & -\gamma_3 & \dots & 0 & 0 \\ \vdots & \vdots & \vdots & \vdots & \ddots & \vdots \\ 0 & 0 & 0 & 0 & -\gamma_{n-1} & (\gamma_{n-1} + \gamma_n) \end{bmatrix} \tag{2.18}$$

The left side of Equation 2.16 is the second order differential equation representing the mechanical system, and is given by the mechanical design of the system (see Chapter 2.1.1). Matrix $\mathbf{F}$ represents the external forces acting on the mechanical system, u represents the input vector of the system.
Equation 2.15 transformed into the well-known state space representation results in:

$$\begin{Bmatrix} \ddot{\phi} \\ \dot{\phi} \end{Bmatrix} = \begin{bmatrix} \mathbf{-D/J} & \mathbf{-K/J} \\ \mathbf{I} & \mathbf{0} \end{bmatrix} \cdot \begin{Bmatrix} \dot{\phi} \\ \phi \end{Bmatrix} + \begin{bmatrix} \mathbf{I/J} \\ \mathbf{0} \end{bmatrix} \cdot \begin{Bmatrix} \mathbf{0} \end{Bmatrix}$$
$$\begin{Bmatrix} \mathbf{y} \end{Bmatrix} = \begin{bmatrix} \mathbf{0} & \mathbf{I} \end{bmatrix} \cdot \begin{Bmatrix} \dot{\phi} \\ \phi \end{Bmatrix} \tag{2.19}$$

with identity matrix $\mathbf{I}$, rotational angle matrix $\phi = \begin{bmatrix} \phi_1 \\ \phi_2 \end{bmatrix}$, $\dot{\phi} = \begin{bmatrix} \dot{\phi}_1 \\ \dot{\phi}_2 \end{bmatrix}$ and $\ddot{\phi} = \begin{bmatrix} \ddot{\phi}_1 \\ \ddot{\phi}_2 \end{bmatrix}$. The homogenous Equation 2.15 results in an input vector u of zero, which is not the general case. The eigenvalues of a matrix are given by the values of the scalar parameter λ for which there exist non-trivial solutions.

$$\mathbf{A}\Phi = \lambda\Phi \tag{2.20}$$

The determinant (Equation 2.21) gives the characteristic equation with n solutions $\lambda = \lambda_1, \lambda_2, ..., \lambda_n$, the eigenvalues of state matrix A.

$$Det(\mathbf{A} - \lambda\mathbf{I}) = 0 \tag{2.21}$$

The determination of the eigenvalues of the system is important for the modal analysis (Chapter 2.1.5), as it represents the natural frequencies of the mechanical system. For any eigenvalue λ_i the n-column vector Φ_i, which satisfies Equation 2.20, is called the right eigenvector of $\mathbf{A}$ associated with the eigenvalue λ_i. The eigenvector has the form:

$$\Phi_i = \begin{bmatrix} \Phi_{1,i} \\ \Phi_{2,i} \\ \vdots \\ \Phi_{n,i} \end{bmatrix}$$

It gives the "mode shape" which is the relative activity of a state variable in a given mode of the mechanical system (see Figure 2.8).

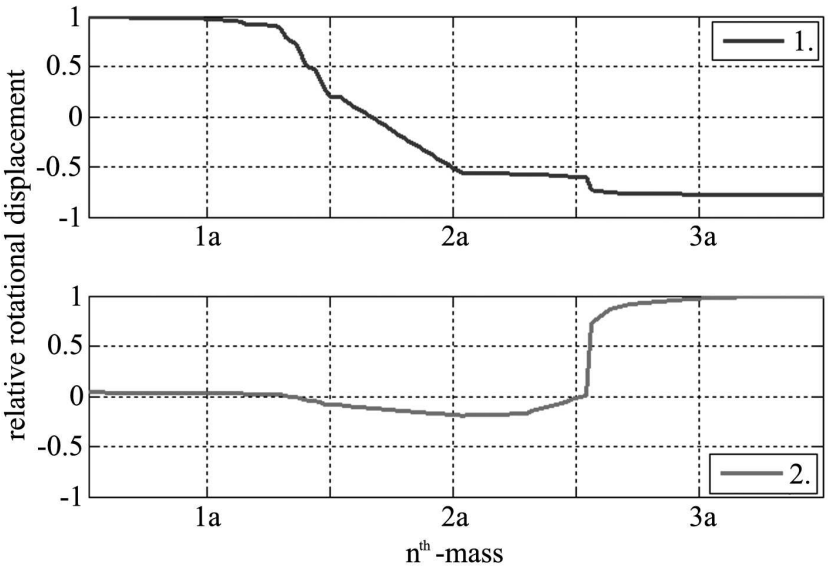

Figure 2.8: Example of mode shape for a mechanical system. The x-axis represents the location of three discrete masses (1a, 2a, 3a), the y-axis the related normalized displacement at each mass.

Some important conclusions can be drawn from the mode shape representation (Figure 2.8): The polarity of the displacement indicates the parts oscillating against each other, e.g. blue curve (1^{st} mode): mass 1 (positive displacement) against mass 2 and 3 (negative). The larger the displacement distance to the x-axis, the higher the sensitivity to be excited, e.g. the small distance from mass 1 and mass 2 in the red curve (2^{nd} mode) to the abscissa means that the second mode cannot be easily excited from location 1. The best sensing location can be determined by evaluating the slope of the mode shapes: Mode 1 can be best measured between mass 1 and mass 2, mode 2 between mass 2 and mass 3.

2.1.5 Modal Analysis

Modal analysis is an important design tool for understanding the behavior of a mechanical system at its natural frequencies, and is part of the torsional analysis, which is e.g. specified in [8] for compressors in the Oil & Gas industry. The modal analysis allows decoupling an n^{th}-order mechanical system into n first order systems with its parameters (a) modal stiffness, (b) modal damping, (c) eigenfrequency and (d) mode shape.
Finding a transformation matrix $\mathbf{X}$, which allows a transformation of stiffness and damping matrix into equivalent diagonal matrixes, finally representing a decoupled mechanical system, is the usual task to be performed. The modal analysis can be obtained by calculating the eigenvalues from the homogenous part of the second order differential Equation 2.16, (see Equation 2.2), and results after some steps into:

$$\mathbf{XJX}^{-1} \cdot \mathbf{X}\ddot{\phi} + \mathbf{XDX}^{-1} \cdot \mathbf{X}\dot{\phi} + \mathbf{XKX} \cdot \mathbf{X}\phi = 0 \tag{2.22}$$

Newly transformed modal parameters with a diagonal form can be introduced, resulting together with new variables for angle, angle speed and angle acceleration into:

$$\mathbf{J}_m \cdot \ddot{\theta} + \mathbf{D}_m \cdot \dot{\theta} + \mathbf{K}_m \cdot \theta = 0 \tag{2.23}$$

The result is a decoupled system with the ability to determine mode shapes or modal damping at each natural frequency separately. The approach of decoupling the differential equation corresponding to the physical mechanical system into decoupled equations, applied to the state space representation can basically be written as:

$$\dot{z} = \Lambda z \tag{2.24}$$

The important difference between Equation 2.24 and the standard state space representation (Equation 2.19) is that Λ is a diagonal matrix whereas $\mathbf{A}$, in general, is non-diagonal. Equation 2.24 represents n uncoupled first order differential equations.
An old and practical modal analysis approach is to apply the iterative "Holzer [14]" method to a discrete mechanical model. It can be used to calculate natural frequencies and mode shapes of a torsional system:

$$\begin{aligned} \phi_{f,n+1} &= \phi_{f,n} - T_{f,n}/K_n \\ T_{f,n+1} &= T_{f,n} + \omega_f^2 \cdot J_{n+1} \cdot \phi_{f,n+1} \end{aligned} \tag{2.25}$$

The starting condition of this algorithm is a unity amplitude at one end of the system, $\phi_{f,1} = 1$ and progressively calculated speed and angular displacement at the other end. The initial torque is calculated with $T_{f,1} = \omega_f^2 \cdot J_1$. The quantities of concern are the torsional displacement ϕ of each mass considered, the torque T carried by each shaft, index n represents the mass position J_n along the structure and $\omega = 2\pi f$ for the frequency applied. Scanning with incremental frequencies f in the described iterative concept identifies the natural frequencies of the system:
The natural frequencies are the frequencies at which the torque at the n_{th} mass is calculated to be equal to zero, $T_{f,end} = 0$, assuming that no external torque is applied. Figure 2.9 indicates the result of the iterative Holzer algorithm to an example multi-mass system. The zero crossings are indicated with dots, they represent the natural frequencies of the investigated system.

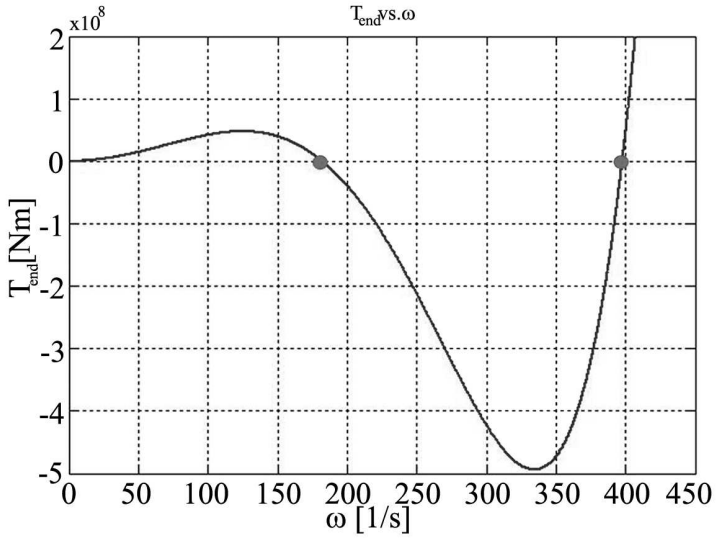

Figure 2.9: Applying the iterative Holzer algorithm to a mechanical system represented with three discrete masses. The natural frequencies are calculated to be $\omega_1 = 182\ [rad/s]$ and $\omega_2 = 397\ [rad/s]$(where $T_{f,end} = 0$ is fulfilled).

The related mode shapes can be found by printing the displacement ϕ_n for each of the natural frequencies (see Figure 2.8).
Equation 2.25 can be adapted, e.g. by modifying the transfer-matrix representation, to also include the damping values at each location of the shaft. Since the torsional damping in large drive trains is low, as discussed in Section 2.1.3, the resulting eigenfrequencies and mode shapes will not significantly deviate from the results calculated without modification of Equation 2.25.

2.1.6 Model Reduction

Simulation lives from simplification. It is not necessary to use a finite element representation of the mechanical model for the analysis of TI, as the frequencies of interest are typically up to or around the synchronous frequency. It is therefore recommended to reduce complex mechanical systems, so as to be suitable for application in combined electromechanical simulation environments, to limit the computational effort required with an appropriate granularity of the mechanical representation. There are several methods available for a degree-of-freedom reduction for torsional systems. An iterative method is the reduction approach introduced by RIVIN [15] and DI [16]. A torsional model with a high degree of freedom can be subdivided into subsystems with one of the two representations indicated in Figure 2.10: either a subsystem including two torsional springs associated with one rotational inertia J_k (type a) or two inertias connected by one torsional spring k_{Tk} (type b). A n^{th} order torsional system can than be split into n subsystems of type a and $(n-1)$ subsystems of type b.

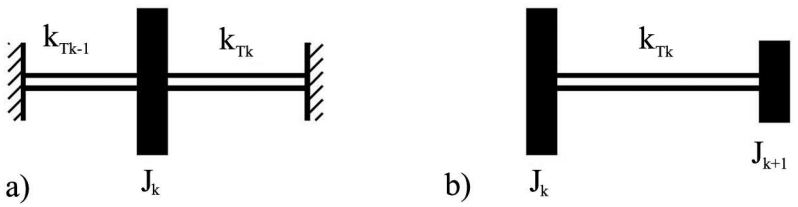

Figure 2.10: Two different types of subsystem of a reduced torsional model.

The eigenfrequencies for all subsystems $k = 1, 2, ..., n-1$ and $k_{T0} = k_{T(n+1)} = 0$ can be calculated based on Equation 2.2 with:

$$\omega_{ak}^2 = \frac{k_{T(k-1)}+k_{Tk}}{J_k}; \qquad \omega_{bk}^2 = \frac{k_{Tk}(J_k+J_{k+1})}{J_k J_{k+1}}; \tag{2.26}$$

Equation 2.26 results in $2n-1$ different natural frequencies for the subsystems. The maximum of all identified subsystem natural frequencies represents the most rigid subsystem:

$$\omega_{k-max}^2 = MAX_{k=1..n}\left[\omega_{ak}^2, \omega_{bk}^2\right] \tag{2.27}$$

A partial model reduction will be applied to the subsystem identified in Equation 2.27; it will be split to the closest connected subsystems. Therefore, after each reduction step the degree of freedom of the torsional system will decrease, until the desired degree of freedom or maximum remaining eigenfrequency is reached.

2.2 Electrical Machine

The electrical machine is the interface between the electrical power system and the mechanical drive train. The two most important ways of applying torque with electrical machinery in the high power area are: (a) asynchronous, stator and rotor have different "rotational" speeds, a field is induced from stator to rotor or from rotor to stator; and (b) synchronous, flux linkage between stator and rotor, generated from independent sources in stator and rotor, e.g. by current sources. The electrical machine models used in this thesis are represented as quasi-stationary; the electromagnetic transients are typically much faster than the mechanical time constants involved with torsional dynamics.

2.2.1 Induction Machine

The most commonly used small to medium sized motor is the induction or asynchronous machine because of the clear advantages: simple and robust machine design, self startability, and comparably low initial cost. Induction machines in the high power range are rare, but they exist [17]. More reactive power consumption and higher losses compared to synchronous machines limit applications in the multi-megawatt range.
One special example of an induction machine in large drive trains is the doubly fed induction machine (DFIM) used with variable speed wind turbines. The design varies slightly from the standard induction machine in that it has access to the rotor windings to manipulate the effective rotor current frequency. The dynamic behavior of a field-oriented, controlled, doubly fed induction machine is close to that of a synchronous machine as long as the frequency of interest is within the bandwidth of the current control, which is at least around $50Hz$.
A conventional induction machine acts on pulsating torque components in the lower frequency range with a nearly proportional torque-slip characteristic, providing additional damping of non-fundamental frequency components to the mechanical drive train. The dynamic characteristic of an induction machine derived in [18] results in:

$$\ddot{M} + \left(2s_k + \frac{\dddot{\phi}}{2\Omega^2}\right)\dot{M}\Omega + \left((s_k^2 + s^2)\Omega^2 + \frac{\ddot{\phi}s_k}{2}\right)M = 2M_k s_k s\Omega^2 \tag{2.28}$$

The variables are torque M, synchronous speed Ω, angular motor speed $\dot{\phi}$, slip s and the two parameters defining the torque-slip characteristic are the stall torque M_k and stall slip s_k.

Equation 2.28 linearized and reduced to the static case ($\ddot{\phi} = 0,\ \dot{M} = 0,\ \ddot{M} = 0$) results in:

$$M = 2M_k \frac{s_k s}{s_k^2 + s^2} \tag{2.29}$$

the well-known Kloss equation.

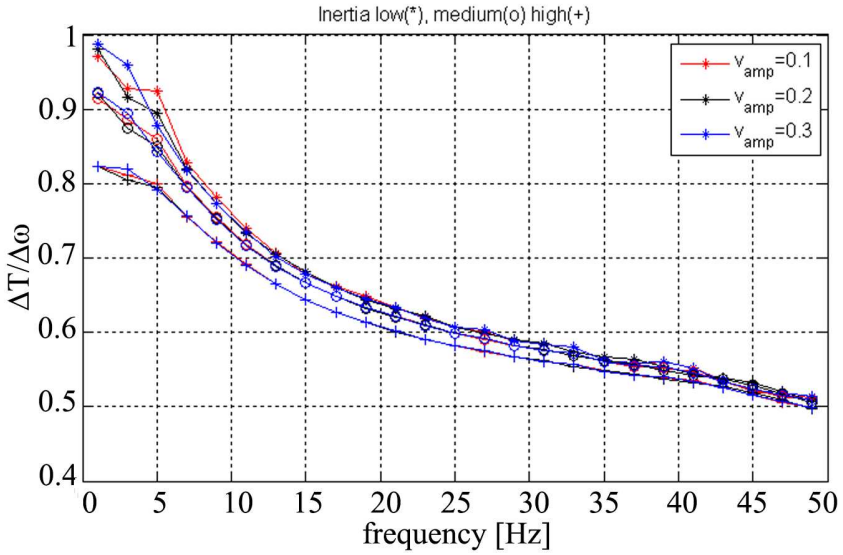

Figure 2.11: Damping effect of the slip of an induction machine, dependent on the frequency of the pulsating torque components. The different colors indicate different modulation amplitudes, '*','o' and '+' different inertia values.

Figure 2.11 illustrates the effect of the pulsating torque frequency on the damping effect introduced by the slip of an induction machine based on Equation 2.28. The damping effect of the slip reduces with higher pulsating torque frequency. The amplitude of the pulsating torque has limited effect on the damping, as long as the stall torque is not reached. This curve was derived as an electrical torque response to a change in machine speed (Figure 2.12):

$$D_e(f) = \frac{\Delta T(f)}{\Delta \omega(f)} \tag{2.30}$$

The frequency axis (Figure 2.11) is related to the rotational frame of the electrical machine, the effective pulsating torque components have to be calculated as sideband of the nominal electrical frequency. The slip value is equivalent to the losses of the induction machine; large drive trains have comparably low slip values, resulting in a large torque/slip ratio, representing a relatively stiff electro-mechanical connection with limited damping property.

2.2.2 Synchronous Machine

The synchronous machine is the most important electrical machine for power generation, but also for motoring of high power loads. The conventional synchronous design allows the control of reactive power by adjustment of the excitation voltage, and more important for high power applications, a higher efficiency compared to the induction design [19]. (a) Slip-ring or (b) brushless and (c) permanent magnet excitation systems are the main solutions for the exciter system. Disadvantages are lower reliability, especially for higher operational speeds with slip rings (a) or a more complex motor construction due to the presence of two windings on the stator and for the rotating diodes (b) [17]. The permanent magnet synchronous machine (c) is the main driver for the utilization of the synchronous machinery in the lower multi-megawatt power range, e.g. in wind turbines, with higher complexity for the control of this type of machine. The rotor always rotates with synchronous speed, resulting in a start-up challenge, which can be mitigated by using a starting inverter or a starting (induction) machine or winding. Using induction-windings results in well-known torsional interaction during start-up, caused by a match between pulsating torques and natural frequencies of the drive train because of the typical asymmetrical rotor design, salient poles generating torque output as a function of the rotor position. The frequency of the torque pulsation is the difference in frequency between the stator and the rotor, known as slip speed for induction type machines. The net result of this is a torque pulsation that occurs at twice the slip frequency, which is defined as:

$$f_{slip} = f_1 \frac{n_s - n}{n_s} \tag{2.31}$$

to be:

$$T_{puls}(n) = 2f_{slip} = 2f_1 \frac{n_s - n}{n_s} \tag{2.32}$$

The pulsating torque (Equation 2.32) can be eliminated with using a starting inverter, which is an elegant but rather expensive means of reducing the motor torques only during start-up, e.g. as described in Chapter 2.3. This type of torsional interaction will not be discussed further in this document. A direct startup of a synchronous machine in the described way is relatively seldom.

The torque of a synchronous machine is nearly sinusoidal. The rotor lags behind the rotating field with the (electrical) angle Θ.

$$T = T_{max} sin(\Theta) \tag{2.33}$$

The relation torque/angle is the same as a spring characteristic of the air-gap torque. Some design modifications allow uncritical operation by adding damping elements to the characteristics of the synchronous machine [20]:

1. Asynchronous damping moment, similar to the induction machine where the rotor slips to the stator winding. The asynchronous damping moment provides the major contribution for the damping torque, mainly for higher load levels; but it is very low for no-load operation.

2. The synchronous damping moment, caused by pulsating currents in the armature because of angular oscillation; this term is always negative, relevant for low load operation, where a continuous oscillation can be observed for large synchronous generators.

3. Alternating damping moment, because of interaction between armature and (electrical) angle, positive for generation, negative for motoring.

The positive damping of the asynchronous damping (1) has the highest influence on the damping of the synchronous machine, and is typically amplified by the mechanical damping provided by the load characteristic, typically higher damping for higher load operation. The resistance in the damping winding is usually higher compared to that in the induction machine design, resulting in a smaller overall damping effect; a factor 10 times smaller has been reported in [4].

2.2.3 Torque Modulation

Electrical machinery converts electrical into mechanical, typically rotational, energy or vice versa. Rotating quantities like torque can be expressed in terms of stationary, but also in terms of rotational frame. The Park coordinate transformation can be used to link harmonic currents e.g. produced in power converters to pulsating torque components. The impact of the non-fundamental frequency components on the mechanical drive train depends on the dynamic performance of the electrical and mechanical design. The relevant electrical dynamics have already been discussed in Sections 2.2.1 and 2.2.2. The mechanical dynamics are influenced by the drive train inertia J, which is accelerated by the imbalance between the applied air-gap and mechanical torque:

$$T_m - T_e = J\frac{d\omega_m}{dt} \tag{2.34}$$

The full electromechanical relationship can be identified in Figure 2.12.

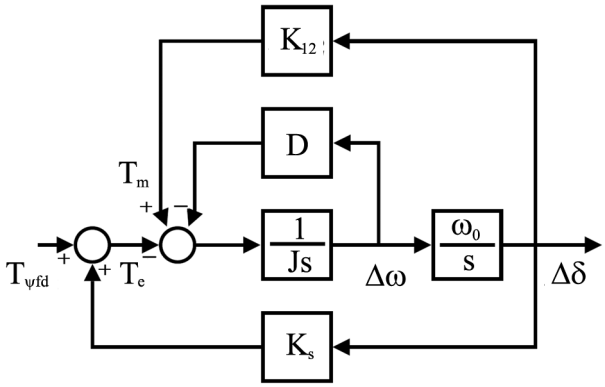

Figure 2.12: Equation of motion for an electromechanical system: T_m applies to the mechanical torque, K_{12} represents the mechanical stiffness coefficient, D the mechanical damping coefficient, and K_s the synchronization torque coefficient.

The equation of motion can be written to:

$$\dot{\Delta\omega} = \frac{1}{J}\left(K_{12}\Delta\delta - D\Delta\omega - T_e\right) \tag{2.35}$$

Hence, the higher the frequency component, the lower the magnitude of acceleration (Figure 2.13). The electrical dynamics have a similar characteristic, influenced by the effective inductance of the electrical machine and the associated time constants $\tau(\omega) = L_{eff}(\omega)/R$.

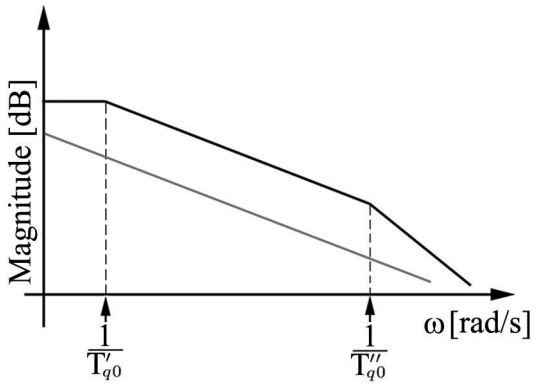

Figure 2.13: Transfer functions: influence of the electrical machine - stator to field (black) and drive train inertia (gray) [6].

High frequency variations in the field voltage are not reflected in the stator flux linkage

and hence other stator quantities, they do not result in considerable pulsating torque components [6].

2.3 Power Electronic Devices

Power electronic devices play an increasing role in modern electrification scenarios. They allow higher flexibility and higher efficiency, e.g. with variable speed operation in drive train applications replacing conventional fixed speed electrical and non-electrical drives (e.g. gas-turbines). The Electric Power Research Institute (EPRI) estimates, that 60% to 65% of generated electrical energy in the US are consumed in motor drives. Most of the machines operate at light load most of the time. Motor efficiency can be improved by as much as 30% by reduced flux operation instead of operating with rated flux [21]. Power electronics is also widely used in transmission, e.g. for High Voltage DC (HVDC)-Transmission or Flexible AC Transmission (FACTS). The focus in this document is (a) the impact of power electronic designs used in high power applications with respect to TI, and (b) the use of different designs for the active damping approach (Chapter 5). Two principle converter designs are relevant in applications of high power electronics:

1. Voltage source converters, operating with a DC-voltage always with one polarity and supported by a DC-capacitor. The power reversal takes place through reversal of the DC-current polarity.

2. Current source converters, operating with a DC-current always at one polarity and supported by a DC-reactor. The power reversal takes place through reversal of the DC-voltage polarity.

Figure 2.14 summarizes the two principle design options and indicates fundamental differences in the capability of the design. A second way of distinguishing the power electronic devices used in the high power area is to distinguish at the semiconductor level between a self-commutated and line-commutated inverter type. The valves of Line-Commutated Inverter (LCI) have only turn-on control capability; turn-off depends on the current zero crossing as per circuit and system conditions. The valves of a self-commutated converter have turn-on and turn-off capability. Devices such as Gate Turn-Off Thyristor (GTO), Integrated Gate Bipolar Transistor (IGBT) and Integrated Gate-Commutated Thyristor (IGCT) and similar devices have turn-on and turn-off capability. A property comparison of the main types of power electronic converters, relevant for high power applications, is summarized in Table 2.2. It explains why line commutated converters are still attractive

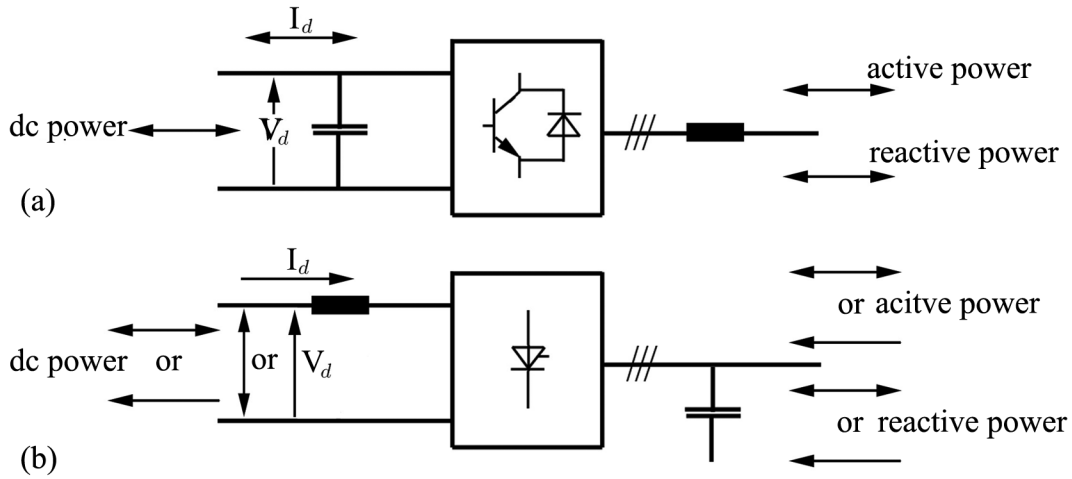

Figure 2.14: (a) Voltage source converter design, (b) Current source converter design [22].

Characteristic	Line-Commutated	Self-Commutated
Design Options	Current Source	Voltage- or Current Source
Dynamic Performance	Medium	High
Rating	1-80 MW	Up to 8 MW per Module
Efficiency	High	Medium
Reliability	High	Medium
System Cost	Low	High
Complexity	Low	High
Reactive Power	Consumption	Consumption or Production
Power Quality	Low-Medium	Medium-High
Torsional Interaction	High	Medium
Footprint	Low	Medium

Table 2.2: Relative comparison between line-commutated and self-commutated inverter type [23–25].

for high power applications. Switching devices always produce harmonics, which can excite torsional natural frequencies, independent from the power electronics design, if the generated harmonics are in coincidence with one of the torsional natural frequencies of the mechanical drive train. It is essential to know the frequency and amplitude of the generated harmonics to estimate the impact on the torsional behavior of the system.
Conventional countermeasures to the torsional interaction with power electronic devices are based on increasing the frequency of low order torque harmonics (e.g. by increasing the converter switching frequency) or decreasing their amplitude (e.g. by multi-level converter topologies or by increasing the effective commutation inductance of load-commutated converter). The fundamentals for harmonics production are discussed in the following chapters.

2.3.1 Line-Commutated Inverter (LCI)

Line-commutated inverters are well known in the high power area because of their simplicity, proven reliability and practically unlimited output power, but also because of limited dynamic performance. Typical LCIs in the high power range are based on a 6 or 12-pulse design. It will be shown in the following subsections, that the pulse number significantly influences the location and amplitude of the produced harmonics and interharmonics.

LCI CONTROL

The control of line-commutated converters will be discussed briefly in order to understand the major aspects of the LCI operation. Figure 2.15 indicates a principle control diagram of a load-commutated converter. The components indicated in red belong to a successfully implemented torsional mode damping extension developed and discussed within this thesis (Section 4.2.2 and 5.3.2).

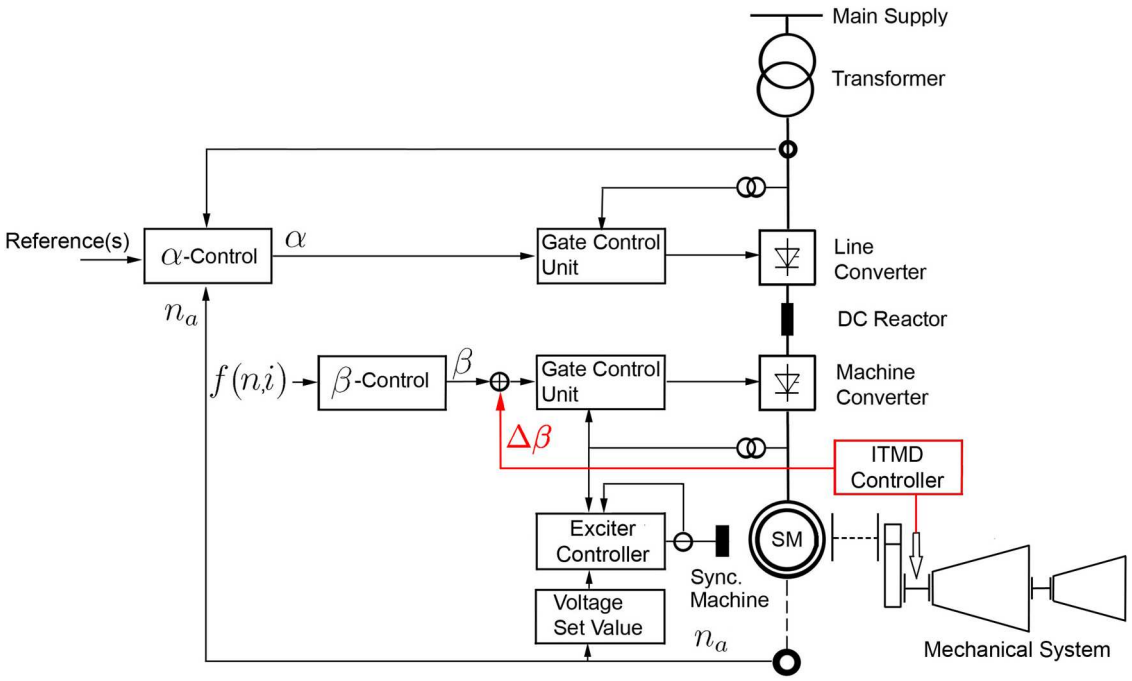

Figure 2.15: Principle control diagram of a load-commutated inverter.

There are two bridges to be controlled, the line side converter - rectifier (r) and the machine side converter - inverter (i). The rectifier firing angle, which is basically used to adjust the power flow from the grid to the DC-link, is also called α-angle. The inverter firing angle, adjusting the power flow from the DC-link to the electrical machine, is also called β-angle. The rectifier controls the DC-link current to remain constant (current

source converter type). Its value depends on the desired torque level of the connected electrical machine; a superior speed control sets the current reference. The steady state and dynamic behavior of the converter is highly nonlinear [26]. A change in the firing angle command becomes delayed before becoming effective in the power circuit; the delay is between $0ms..\frac{20}{6}ms$ for a 6-pulse system with $50Hz$ grid frequency. A typical approach is to approximate the delay with $T_T = 1.67ms$ for the given control design example (Figure 2.16). The control dynamics are influenced by the time constant given by the commutation inductance, $\tau = \sum \frac{L_k}{R}$ and by the period firing delay between $0...T_{pulse}$, higher pulse numbers allow faster controllability. The focus in this section is mainly on the current control loop controlling the α-angle. This loop can influence the operation of the damping loop, which will be discussed in Section 5.3.2.

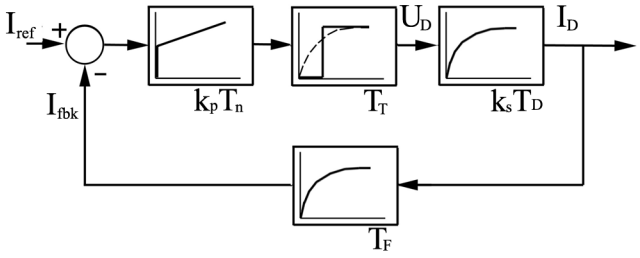

Figure 2.16: Simplified block diagram for an LCI current control, with k_p and T_n as current control settings, T_T as averaged firing delay time, k_s and T_D defining a first order DC-link time constant, and T_F as first order feedback time constant.

Figure 2.16 can be used to derive control parameters for the current control loop. The open loop transfer function can be formulated to:

$$F_{OL}(s) = \frac{k_p(1+sT_n)}{sT_n} \cdot \frac{1}{1+sT_e} \cdot \frac{k_s}{1+sT_D} \tag{2.36}$$

$T_e = T_T + T_F$, $k_s = \frac{1}{R_D}$, $T_D = \frac{L_D}{R_D}$;
The classical approach of the "symmetrical optimum" then results in:

$$T_n = T_D, \quad k_p = \frac{T_n}{4D_c^2 k_s T_e} \tag{2.37}$$

The current control performance can be varied with D_c, e.g. $D_c = 0.5$ for fast, $D_c = 0.9$ for a slow current control performance.
The inverter open-loop control affects the power factor of the connected electrical machine. A typical approach is to maintain the power factor at a high level to minimize the losses

and current rating of the equipment. The power balance between the AC and the DC system is given and can be calculated, neglecting the converter losses, to be:

$$P = 3 \cdot V_{LN} I_L cos\phi = V_d I_d = (V_{d0} cos\alpha) I_d \tag{2.38}$$

Hence, the power factor is proportional to the firing angle:

$$cos\phi \sim cos\alpha \tag{2.39}$$

Equation 2.38 and thus Equation 2.39 can be applied for both rectifier firing angle α and inverter side firing angle β. The β-angle value is typically derived from a table and influenced by the actual speed and torque of the connected electrical machine (no feedback control of β-angle).

LCI HARMONICS

Harmonics produced by power electronic devices are the major source of a harmonic excitation of torsional oscillations. The harmonics can result in pulsating torque components affecting the torsional behavior of a sensitive drive train (comparable large Q-factor), if the frequencies are close or match the natural frequency of the train. Harmonics are generated on the DC-side of the converter, the DC-link voltage has AC-voltage components (DC-Harmonics), and on the AC-side of the converter, where the current includes multiples of the fundamental frequency.

Both harmonics are linked by the firing pulse clock, which acts like a modulator known from the amplitude modulation theory.

DC-Link-Harmonics

On the DC-side of the converter, the output voltage is of a form, which depends on the pulse number, angle of delay α and angle of commutation γ. The output voltage consists of a DC-voltage with superimposed harmonics; which can be calculated by applying the Fourier transformation.

The ν^{th} harmonic can be calculated for uncontrolled valves with p as pole number of the inverter bridge (e.g. $p = 6$) to be:

$$|a_\nu| = U_d \cdot \frac{2}{\nu^2 - 1} \tag{2.40}$$

for $\nu = p \cdot k$ and $(k = 0, 1, 2, ...)$. The amplitude of the ν^{th} harmonic for controlled circuits can be written as:

$$u_\nu = U_d \cdot \frac{\sqrt{2}}{\nu^2 - 1} \sqrt{\nu^2 - (\nu^2 - 1) cos^2 \alpha} \tag{2.41}$$

with α as firing angle. The maximum harmonic magnitude can be observed for a firing angle equal to 90^o, which represents no load operation. Figure 2.17 indicates the normalized harmonic amplitude for a 6-pulse design, dependent on the firing angle of the inverter. Equation 2.41 shows that the magnitude of the produced harmonic decreases with higher order of ν.

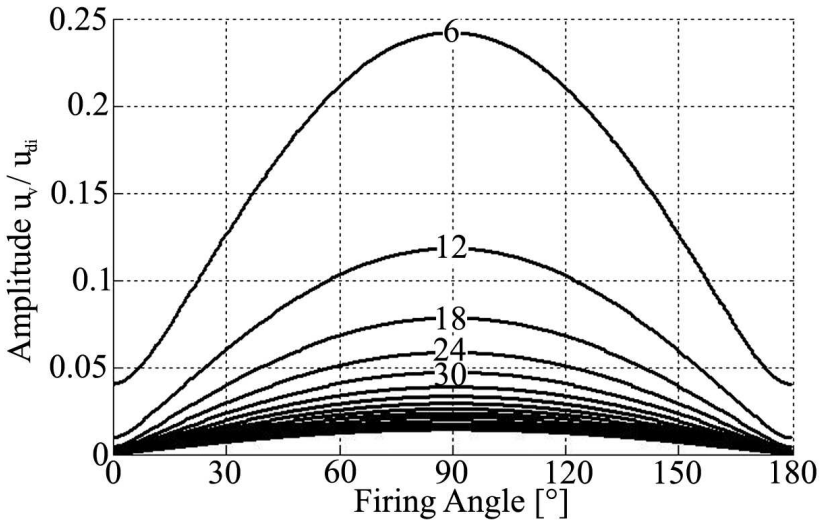

Figure 2.17: Amplitude of harmonics $n = 6, 12, ..$ of a 6-pulse inverter design, dependent on the firing angle α.

The firing angle dependency of the produced harmonic is an indication of why torsional interaction is more likely to occur during light load operation, where the firing angle is closer to 90^o.

Another "degree of freedom" in terms of harmonic magnitude is the commutation angle γ. It can be formulated with:

$$\gamma = arcos(cos\alpha - 2d_x) - \alpha \tag{2.42}$$

where $d_x = \frac{1}{2} \frac{2X_k I_d}{\sqrt{2} U_k}$ includes the values having impact on the commutation time: commutation inductance $X_k = \omega L_k$, current I_d and commutation voltage U_k. For a small

commutation angle γ, the harmonic magnitude increases with increasing firing angle α until $\alpha >= 90^o$, see Figure 2.17. For a constant angle α, the harmonics decrease with increasing commutation angle γ and reach a first minimum at, approximately $\gamma = \pi/\nu$, e.g. for a 6-pulse design at $\gamma = 30^o$.

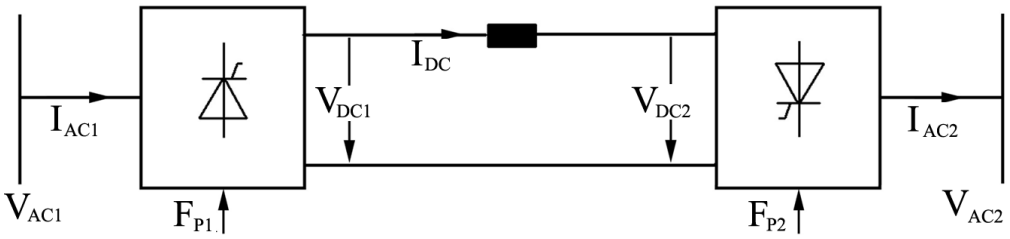

Figure 2.18: LCI one-line diagram with rectifier (1) and inverter (2) bridge and DC-link reactor.

Figure 2.18 indicates two DC-link voltages V_{DC1} and V_{DC2}, which contain harmonics at:

$$f_{\nu x} = k \cdot p \cdot f_x \tag{2.43}$$

dependent on the frequency f_x of the AC-voltages V_{AC1} and V_{AC2}. Harmonics based on Equation 2.43 are called integer (k) pulsating torque component if superimposed in the air-gap torque of an electrical machine.
Another set of harmonics in the DC-link is produced if the frequencies on both AC-sides are not equal, e.g. in case of variable speed operation, where the grid frequency f_r is nearly constant and the machine side frequency f_i depends on the desired rotational speed of the electrical machine and the pole-pair number. In case of asynchronous power systems, it depends on the second grid frequency f_i. The DC-link current consists of $i_{DC} = \frac{V_{DC1,dc} - V_{DC2,dc}}{R_{DC}}$, the DC-component and of an AC-component responsible for an interharmonic content in the DC-link:

$$i_{AC} = \frac{1}{L_{DC}} \int V_{DC1,ac} - V_{DC2,ac} dt \tag{2.44}$$

A non-infinite DC-link inductance is the reason for the interharmonics, Equation 2.44, which does not perfectly decouple the two AC-systems. The interharmonics are therefore

present in both AC-systems. The resulting interharmonics are in the form:

$$f_{\nu\,12} = |k \cdot p \cdot f_1 \pm m \cdot p \cdot f_2| \tag{2.45}$$

The frequencies f_1,f_2 of both AC-systems are multiplied with the independent integer variables $k, m = 1, 2, 3, ...$ and the effective pulse number of the utilized converter bridge p. The harmonics, also called non-integer harmonics, are the main reason for TI between power electronics-driven systems and conventional rotating machinery, which transform them into pulsating torque components. Some of them are in the lower frequency range, and they vary with varying frequency, so that a large number of frequencies can be excited by this set of harmonics (see also Figure 2.19). Equation 2.45 will be derived in the next subchapter. A design criterion for modern LCIs in high power applications is the production of interharmonics with magnitudes as low as possible, less than one percent of the nominal power can be achieved. But this can still cause relevant torsional excitation [27]. This low level of pulsating torque production has also been observed in air-gap torque measurements during tests performed on a $30MW$ O&G train driven by an LCI.

AC-Side Harmonics

Current harmonics produced on the AC-side of the converter can be derived from the typically rectangular like current shape, as shown in [22]. The generated harmonics are in the order of:

$$n = p \cdot k \pm 1 \tag{2.46}$$

where n is the harmonic order, $k = 1, 2, 3, ...$ and p the pulse number of the inverter bridge. Higher harmonics and higher pulse numbers result in lower magnitudes; the n^{th} harmonic has an amplitude of:

$$I_n = \frac{I_1}{n} \tag{2.47}$$

The commutation process mainly influences the higher frequency harmonics to be smaller, as the wave shape is slightly closer to a sine wave.

Equation 2.40 indicates DC-harmonics for $\nu = k \cdot p$ and $k = 0, 1, 2, ...$, and for the same converter on the AC-side (Equation 2.46) AC-harmonics with $n = p \cdot k \pm 1$. The bridge acts as a modulator, with the firing pulse clock as modulator. The interharmonics discussed in Equation 2.44 can be derived on the AC-current side. Figure 2.18 gives the nomenclature:

Inverter 1 is not fully decoupled from inverter 2 by the DC-link inductor, and can therefore see the harmonics produced by inverter 2. The total current on inverter 1 can therefore be written as:

$$\begin{aligned} i_{AC} = \tfrac{2\sqrt{3}}{\pi}\left(cos(\omega_1 t) - \tfrac{1}{5}cos(5\omega_1 t) + \tfrac{1}{7}cos(7\omega_1 t) - \tfrac{1}{11}cos(11\omega_1 t) + ...\right) \cdot \\ \{I_d + A_6 sin(6\omega_2 t + \phi_6) + A_{12} sin(12\omega_2 t + \phi_{12}) + A_{18} sin(18\omega_2 t + \phi_{18}) + ...\} \end{aligned} \tag{2.48}$$

with $A_\nu = \frac{a_\nu}{Z_{DC}}$ from Equation 2.40 and Z_{DC} as DC-link impedance. Using the trigonometric identity $cos(A)sin(B) = \frac{1}{2}\left[sin(A+B) - sin(A-B)\right]$, Equation 2.48 can also be written as:

$$\begin{aligned} i_{AC} = i_{ph} + \tfrac{\sqrt{3}}{\pi} A_6 \left[sin(\omega_1 t + 6\omega_2 t + \phi_6) - sin(\omega_1 t - 6\omega_2 t - \phi_6)\right] \quad (a) \\ -\tfrac{\sqrt{3}}{\pi}\tfrac{A_6}{5}\left[sin(5\omega_1 t + 6\omega_2 t + \phi_6) - sin(5\omega_1 t - 6\omega_2 t - \phi_6)\right] \quad (b) \\ +\tfrac{\sqrt{3}}{\pi}\tfrac{A_6}{7}\left[sin(7\omega_1 t + 6\omega_2 t + \phi_6) - sin(7\omega_1 t - 6\omega_2 t - \phi_6)\right] \quad (c) \\ +\tfrac{\sqrt{3}}{\pi} A_{12}\left[sin(\omega_1 t + 12\omega_2 t + \phi_{12}) - sin(\omega_1 t - 12\omega_2 t - \phi_{12})\right] \quad (d) \\ -\tfrac{\sqrt{3}}{\pi}\tfrac{A_{12}}{5}\left[sin(5\omega_1 t + 12\omega_2 t + \phi_{12}) - sin(5\omega_1 t - 12\omega_2 t - \phi_{12})\right] \quad (e) \\ +\tfrac{\sqrt{3}}{\pi}\tfrac{A_{12}}{7}\left[sin(7\omega_1 t + 12\omega_2 t + \phi_{12}) - sin(7\omega_1 t - 12\omega_2 t - \phi_{12})\right] \quad (f) \\ ...etc. \end{aligned} \tag{2.49}$$

with i_{ph} as the Fourier series based on Equation 2.46. Equation 2.49 illustrates selected components of the current harmonics for a six pulse converter feeding into the power system, which can potentially result in pulsating torque components. As an example, (b) and (c) of Equation 2.49 will be modulated into the components $f_{6.6} = |6 \cdot f_1 \pm 6 \cdot f_2|$ based on Equation 2.45 after the modulation of the electrical machine. The current harmonics introduced into the power system can be better analyzed in graphical form with the Campbell diagram. Figure 2.19 shows a typical Campbell diagram for a 6-pulse system, including integer and non-integer pulsating torque components. The $6f_{1,2}, 12f_{1,2}$ components are based on the current waveform.

The intersection of integer harmonics (Equation 2.43) with relevant torsional natural frequencies of the system can generally be avoided within the operation speed range. The intersection of non-integer harmonics with torsional natural frequencies of the mechanical system cannot be excluded if the drive train is design to operate below and above a motor supply frequency of approximately the grid frequency, which is typically the case. And all harmonics and interharmonics are also present on the grid side of the converter. They can potentially interact with natural frequencies of electrically close connected power generation systems (synchronous generators).

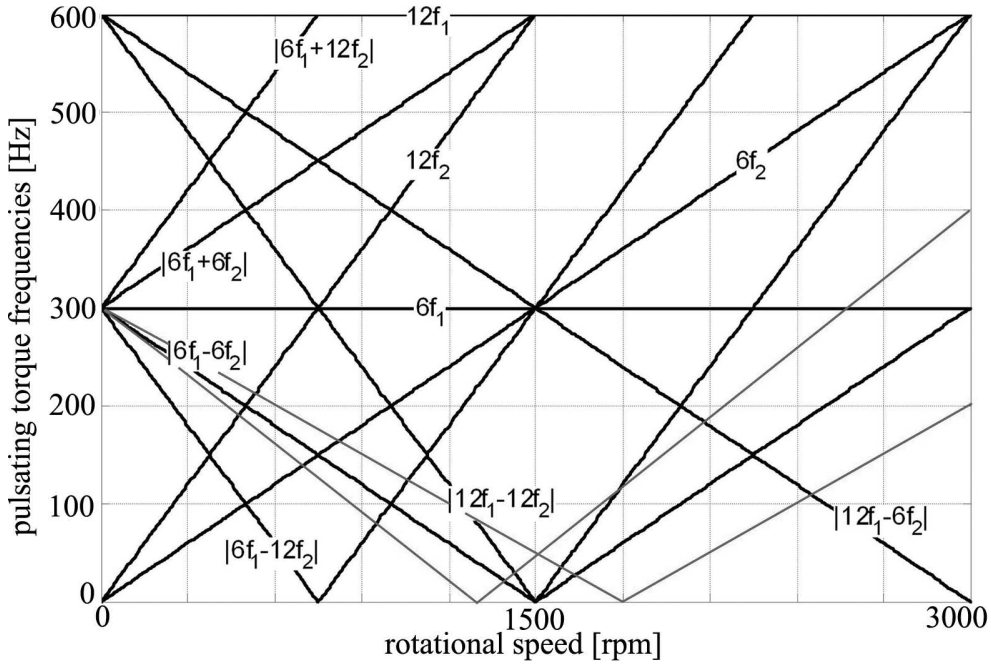

Figure 2.19: Campbell Diagram of pulsating torque components generated from inter-harmonics and harmonics (Equation 2.49). The two gray lines indicate the current harmonic $|6f_1 - 5f_2|$ and $|6f_1 - 7f_2|$, which are transformed into a pulsating torque component of $|6f_1 - 6f_2|$.

2.3.2 Self-Commutated Inverter

Self-Commutated Inverters have some significant advantages over line-commutated inverter types, as summarized in Table 2.2.

They are known to produce significantly less torque ripple than line-commutated inverters, which is one critical item for TI in addition to others such as exposure time of excitation and proximity between a generated harmonic and a natural frequency of the drive train. Self-commutated inverters are still reported as one source of torsional excitation, e.g. in [28]. Conventional countermeasures to the TI with power electronic devices are based on increasing the frequency of low order torque harmonics (e.g. by increasing the converter switching frequency) or by utilizing different control schemes e.g. using Pulse-Width Modulation (PWM) or hysteresis control instead of square wave. Converter losses are typically the limitation, which are very critical in high power electronic applications. The amplitude of low-order torque harmonics can also be reduced by multi-level converter topologies, where the resulting wave shape is closer to the desired sine wave compared to, e.g., two level designs. The control complexity as well as the reliability decreases with an increasing number of devices.

HARMONICS

The integer pulsating torque component of the fundamental frequency can always cross a natural frequency of a mechanical system, e.g. during start up. Additionally, the square wave operation has fundamental disadvantages as discussed in Chapter 2.3.1 for LCIs. The "advanced" PWM operation produces harmonics basically described by:

$$k_1 n \pm k_2 \tag{2.50}$$

with k_1 as frequency multiplier, e.g. a carrier frequency $f_c = 540Hz$ at a power system with $f_1 = 60Hz$ results in $k_1 = 9$. The variables n and k_2 are integers. A typical harmonic spectrum for PWM operation is shown in Figure 2.20.

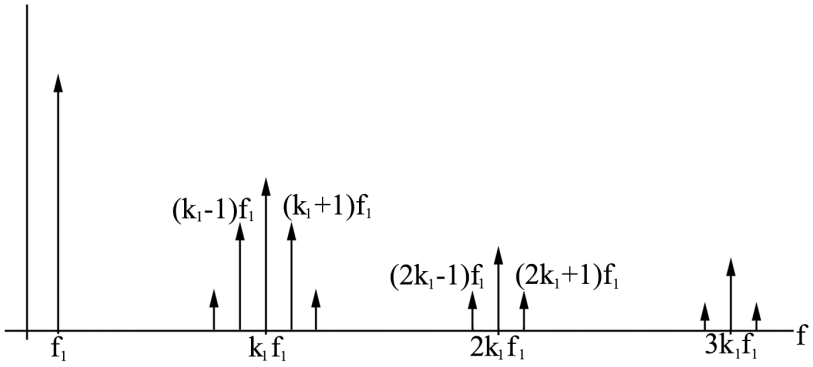

Figure 2.20: Typical PWM harmonic spectrum with synchronous switching strategy and fundamental frequency f_1.

In general, the harmonic frequencies can be relatively high, and passive filters can be used to attenuate the amplitudes. However, lower frequency harmonics, also called beat harmonics or beat frequencies, can be present and more difficult to reduce with passive filters since they are closer to the required voltage bandwidth. These beat components can occur at frequencies both above and below the fundamental frequency. Many converters operate with a synchronous PWM strategy, where the carrier frequency is a fixed integer multiple of the output fundamental frequency of the converter. However, this is not desirable when operating at low fundamental frequencies since the switching frequency is constrained to low values leading to poor harmonic performance.

Harmonics can also be produced in addition to the theory due to the influence of the modulator design, e.g. spectrum smearing of the modulator due to distorted measurements, but also by control internals like the sampling process, feedback filtering, DC-link component design or cabling, as reported recently, e.g. in [3].

2.4 Summary - Modeling and Component Aspects

The critical parameter for multi-megawatt drive trains coupled to or electrically close to power electronic converter is the damping of the mechanical system at its natural frequencies. Low torsional damping parameters (large Q-factors) result into a very sensitive response to harmonic excitation (Section 2.1.3). Such excitation can easily be caused by harmonics and interharmonics produced from power conversion units.

A coincidence of electrically generated harmonics with a natural frequency of a large drive train can result in significant torsional excitation. The most relevant parameter of the electrical excitation source is its frequency (proximity to critical natural frequencies) and the exposure time of excitation, not its magnitude. Therefore, a greater electrical excitation source, if not located close to a mechanical resonant frequency, will have less impact on the shaft than a smaller excitation localized at or near that resonant frequency. None of the existing converter topologies available for high power applications, voltage source and current source converter, can generally be excluded from producing harmonics and interharmonics. Both are potential sources for torsional interaction.

3

Torsional Interaction Analysis

Definition of the Torsional Interaction (TI) phenomenon with turbine generators:
"Torsional interaction occurs when the electrically induced subsynchronous torque in the generator is close to one of the torsional natural modes of the turbine generator shaft. When this happens, generator rotor oscillations build up and this motion induces armature voltage components at both subsynchronous and super synchronous frequencies" [29].

3.1 Sources of Excitation for Torsional Oscillations

Excitation of torsional oscillation always follows the same principle, a disturbance in the torque-balance between the mechanical system, e.g. compressor load or gas turbine, and the electrical machine, e.g. motor or generator. These disturbances can be in the form of step functions but also discrete frequencies, exciting the natural frequency of the drive train. The magnitude of a resonant vibration depends on the proximity of the stimulating frequency and a natural frequency, on the magnitude and duration of the excitation, and on the damping of the excited natural mode [30]. The impact of non-local "excitation sources" on large rotational equipment depends on the effective electric impedance between the source of disturbance and the rotating machinery.
The main disturbances responsible for TI in rotating equipment are grid events [31], harmonics produced by power conversion, interaction between electrical and mechanical resonances (subsynchronous resonances which are out of the scope of this thesis) and improper operation of equipment. TI can lead to increased material fatigue, system

outages due to trip, or instantaneous damage of the drive train (see Section 3.2).

3.1.1 Grid Events

Lightning strikes into the transmission system can lead to short circuits, resulting in one-, two- or three-phase faults, a major disturbance in the power system. High voltage created from a high current injection can be a source of excitation, if non-linear devices like transformer saturation limit those high voltages. Over-voltages also occur during normal or abnormal switching operation e.g. in medium- and high-voltage systems with vacuum switches which are known for very steep over-voltages because of their very fast switching capability. Generally, planned and unplanned switching operation of loaded lines and units result in an impedance change in the power system and act, therefore, like a step function for the power system and the connected units. These events can excite torsional oscillations (Equation 2.6, Figure 2.2). Examples are short circuits, trip and reconnection of transmission lines, but also failed synchronization of synchronous machines [32].

3.1.2 Torsional Interaction with Large Power System Unit Controls

Large grid-connected equipment having fast regulating controls is another potential source of torsional interaction, as it can affect the damping of torsional vibration on generator shafts. This phenomenon is also referred to as Sub-Synchronous Torsional Interaction (SSTI). Interaction with generator excitation controls, e.g. with a power system stabilizer (PSS) acting through the excitation system have been reported in the past [33]. Those PSS are typically tuned to a certain frequency and use an available speed measurement e.g. from the generator end of a drive train. The stabilizing function is typically designed to provide zero phase shift at the frequency to be stabilized. The applied filter can, as will be discussed in the Chapter 4, act as a negative damping for frequencies other than the stabilized natural frequency. This results in the instability of that mode, even if the feedback magnitude at the mode is attenuated by the applied filter. Using very high gain in the exciter control, to keep the terminal voltage within a limited band, can also lead to torsional instability due to higher frequency components in the voltage signal.
The speed governor of generation units can interact with torsional modes if the bandwidth of the governor allows action in the range of natural frequencies. Filter design and tuning are the keys in tuning the controls so that they do not interact with natural frequencies, which can lead to instability.

Power conversion devices, with e.g. constant power control as in HVDC transmission, have been reported to be a source of torsional excitation: Turbine-generator rotor motion, in addition to the constant rotational speed, causes variation in both magnitude and phase angle of the AC-voltage. A line-commutated HVDC system connected and therefore locked to this AC-voltage modifies the apparent firing angle away from the steady state phase shift because of equidistant firing angle control. This affects both direct current and voltage, and thereby the transferred DC-power transferred. The closed loop controls on direct current, direct voltage or firing angle react to correct for these changes, impacting magnitude and phase in the DC-transferred power, with the frequency of the initial rotor motion. The ultimate effect of the change in DC-power is a change in generator air-gap torque. The impact of the interaction depends on the strength of the AC-system compared to the DC-system, and on the electric distance between the turbine-generator and the HVDC system [34], [35].
The Unified Interaction Factor (UIF) [36] has been established as an important design factor used in preliminary studies to identify potential SSTI based on large-scale interaction studies. The UIF value allows one to decide whether more detailed studies of SSTI are needed.

3.1.3 Harmonics Produced Due to Power Conversion

Harmonics are produced with all kind of power electronic devices, as already discussed in Section 2.3. These harmonics are distributed through the connected power system, dependent on the impedance distribution to connected units like electrical machinery. They can transform the harmonics with non-fundamental frequency through the air-gap torque (Section 2.2) and, in case of coincidence of the pulsating torque components with eigenfrequencies of the mechanical system; they can excite these natural frequencies.
Figure 3.1 represents a Campbell diagram for a 12-pulse LCI, including electrical frequencies (solid), which are mostly dependent on the rotational speed of the drive train; and mechanical frequencies (dashed) representing the eigenfrequencies of the drive train, which are typically fixed over the whole operational speed range. The intersection of electrical and mechanical frequencies are called critical speeds; they can result in torsional interaction, dependent on the amplitude of the pulsating torque (electrical), the mode shape at this frequency and the effective modal damping.
This effect occurs especially in island-like power systems as shown in Figure 3.2, where several power electronic loads are connected close to similar sized generation units. In this case, the magnitude of the harmonics produced can be large enough to significantly

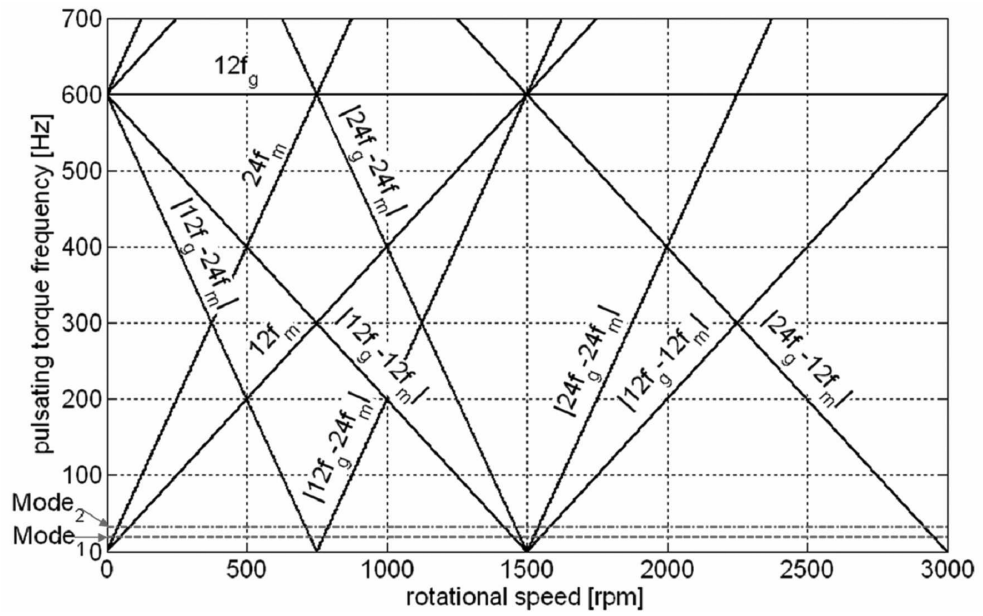

Figure 3.1: Campbell diagram: relevant electrically generated frequencies for a 12-puls design (black) together with relevant natural frequencies of the mechanical system, indicated with $Mode_1$ / $Mode_2$ (gray - dashed).

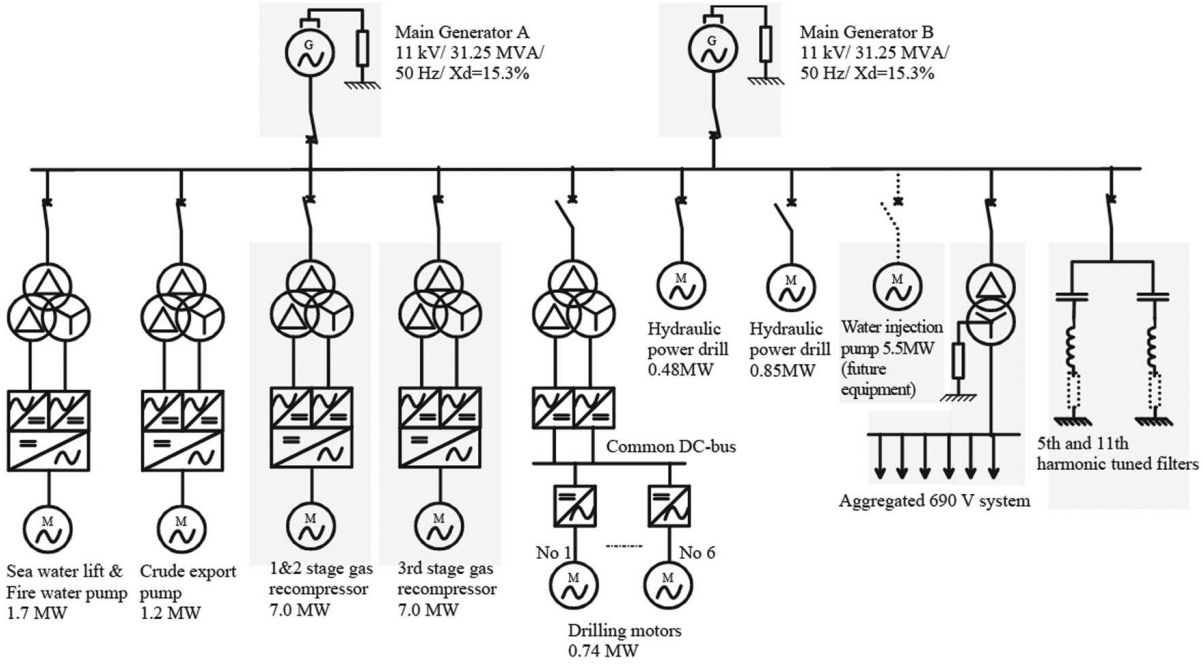

Figure 3.2: Island power system with high penetration power conversion loads [7].

excite the mechanical drive train of the power generation units, which are typically based on synchronous generators. Power outages or broken shafts can be the consequence.

3.1.4 Subsynchronous Resonance

The subsynchronous resonance is a special case of TI. An electrical resonance at a frequency f_{er} interacts with a mechanical natural frequency of a drive train $f - f_{er}$ and can result in a resonance catastrophe. Subsynchronous resonances typically happen with series capacitor-compensated transmission systems forming, with generator inductances, an electrical resonance circuit. A small voltage induced by rotor oscillation can result in large subsynchronous currents, which will produce an oscillatory component of rotor torque. The phase of the rotor torque is such that it enhances the rotor oscillation, like a positive feedback loop, so that the coupled electromechanical system will experience rapidly growing oscillations.

3.1.5 Excitation Due to Load Variation

So far, only electrical sources that excite torsional oscillation of rotating machinery have been described, mainly because the natural frequencies typically begin in the high one-digit frequency range and the load characteristic, which has typically low bandwidth, is therefore not capable of exciting these natural frequencies. An exception can be wind turbines, where statistically fast wind variations, but also the "shadow effect" of the pylon acting on the blades and subsequently on the rotating drive train, results in a torque variation. A frequency spectrum of typical wind speed variations is shown in Figure 3.3, calculated with a Von Karman Wind Turbulence distribution including roughness of the area around the wind turbine or a standard deviation of the wind speed distribution. The dominant frequency components are located in section A; section C includes relevant frequencies for torsional excitation, which have almost negligible contribution.

Another potential excitation can be found in geared drive trains in which the gear mesh can generate higher frequency torque components. It is also found in the operation of unbalanced drive trains producing pulsating torque elements with multiples of the mechanical rotational speed. And there are several situations with combustion engines that can lead to torsional vibration problems [38]: engine misfire, pressure imbalance, ignition problems, leaks or instability of the control.

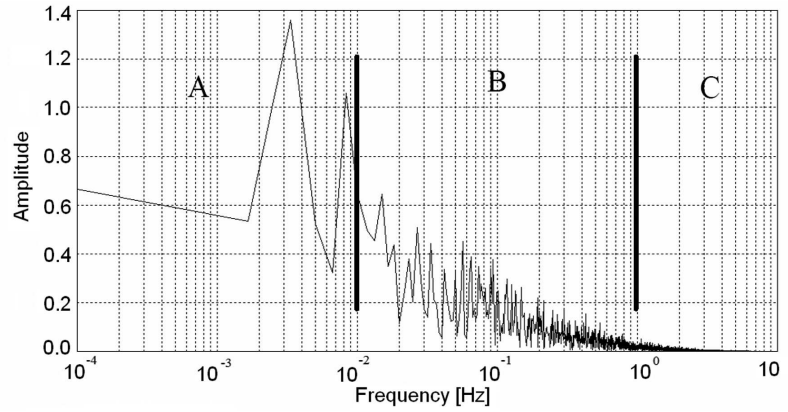

Figure 3.3: Wind speed variation in frequency domain [37]

3.1.6 Torsional Interaction Between Closed Coupled Units

Another not uncommon scenario for TI is the interaction between electrically close (connected through low impedance) coupled units. Figure 3.2 indicates two identical generation units connected to the same busbar, which couples those two machines through the electrical system. The eigenfrequencies and eigenvectors (Figure 3.4) of the two or, in general n units are calculated to understand the principle reaction to torsional excitation. The network strength influences the electrical stiffness, which connects the mechanical system. The electrical stiffness adds another mode to the mechanical modes of the system (subplot 1 - Figure 3.4).

The relation between electrical network strength X and mechanical stiffness k can be found with $k \sim 1/X$. A stronger system (smaller X) results in higher stiffness. The resistive part of the grid impedance influences the damping of the additional mode. One significant question for the understanding of the interaction is the cause of excitation: (a) if one of the generators is excited from the mechanical side, than this generator can oscillate e.g. against the other generator, with an anti-phase oscillation (subplot 3 - Figure 3.4). (b) If there is an external excitation then both generators oscillate probably in-phase (subplot 2 - Figure 3.4). The closed coupled torsional interaction could be potentially of interest as wind farms usually have many wind turbines of an equal type. Most state-of-the-art wind turbines in the MW class are connected to the grid via power electronic converters, which have the advantage of effectively decoupling the mechanical system from the power system for frequency components within the bandwidth of the torque controller. But there are wind turbine designs operating variable speed without power electronics, e.g. a hydrodynamic torque converter connected to a medium voltage synchronous generator [39].

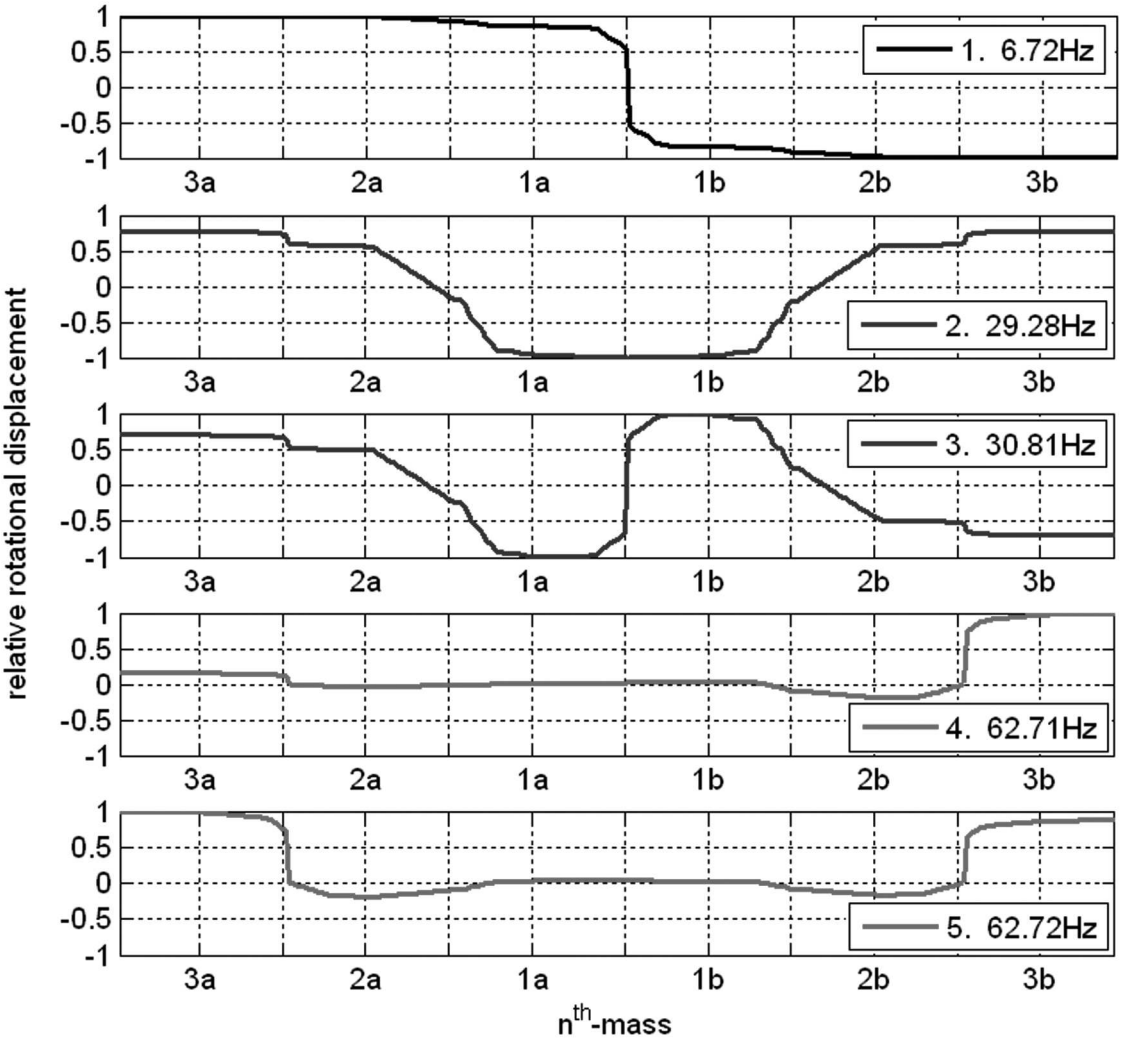

Figure 3.4: Combined mode shape of two (a, b) electrically close coupled units of type Figure 2.8. Both units have three main masses (1, 2, 3). The original 2^{nd} natural frequency (subplots(4,5)) is not significantly influenced from the network parameter, as there is no strong coupling of this mode to the electrical machine (distance between mode shape and x-axis for $1a$ and $1b$).

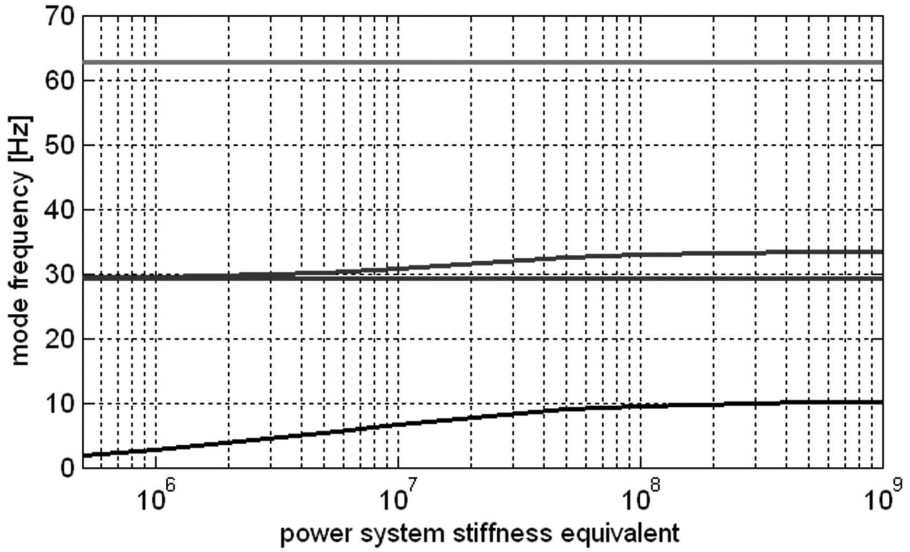

Figure 3.5: Mode frequency dependent on system strength, represented in a power system equivalent. Mode 1 is the system mode, where both units oscillate against each other (black).

Figure 3.5 indicates the dependency of the eigenmodes of two electrically close generators on the electrical coupling between the generators. A low coupling (low stiffness) results in equal eigenfrequency of the in-phase and anti-phase modes. The difference between the modes increases with increased stiffness of the electrical coupling of the system.

3.2 Impact of Torsional Interaction

Lifetime reduction is one major impact of TI, as alternating load cycles can have significant influence on the remaining lifetime of the mechanical system. But there are other factors to be considered with TI. For instance, expensive equipment is protected against TI, and may have to be tripped at a certain level of vibration, with the possible consequence of system outages, as reported in [7].

3.2.1 Lifetime Reduction

A broken turbo generator shaft was the first incident in which the impact of subsynchronous resonances, a kind of TI, was recognized [40]. Broken shafts as a result of TI represent worst-case lifetime reduction, and can hardly be found in literature. But it is quite common in industry not to publish severe damages.
The majority of known TI's impact the lifetime of a system because of the increased stress

at shaft sections and couplings of rotating machinery. Components usually fail because of fatigue. Fatigue is defined as failure at relatively low stress levels caused by repeated load cycling [41]. The alternating torque amplitude, the average value of the cycles and the number of load cycles, influences the lifetime consumption of mechanical shafts. Typical alternating torque limits for drive trains in the multi-megawatt range are below 20% to 30% of the static torque rating. Fatigue damage from torsional vibration is cumulative over many events. TI can frequently induce relatively small torsional vibration in addition to the static (nominal) torque, so that high generator shaft lifetime expenditure can quickly be accumulated.
The assessment of the impact is mainly based on empiric knowledge and numerous material tests. There are several monitoring systems which estimate the shaft fatigue damage including loss-of-life per event and cumulative loss-of-life for planning maintenance or inspection while damage is minimal, to prevent more costly repairs [42]. Those systems are only utilized with very expensive generator units in power plants, e.g. with ratings above $100MW$.
A common approach in industry to guarantee a certain lifetime with alternating torques during operation is to over-dimension the shaft to sustain higher alternating torques. But there are economical limits for over-engineering large rotor shaft systems, especially at high rated power levels.

3.2.2 Loss of Production

Large generation units with comparably high Q-factor are typically equipped with monitoring and protection mechanism, to disconnect the electrical machine as a consequence of uncontrolled excitation of torsional oscillations, to prevent mechanical damage, such as failed couplings or broken shafts. Examples for protective devices are torsional motion relay, armature current relay or unit tripping logic schemes [5].
Protection schemes mainly based on vibration measurements are applied for synchronous motor driven compressor trains in the multi-megawatt range. They trip the total compression system after certain level of alternating torque is reached (Figure 1.2). The protection algorithm can be quite complex, as many criteria have to be considered to prevent unwanted system trips.

3.2.3 Vibration - Noise

Torsional interaction can cause torsional vibration, which can be transferred via a gearbox into lateral vibrations. These vibrations can potentially cause high sound pressure levels,

which can exceed stringent environmental requirements, e.g. for systems installed in densely populated areas with low-noise requirements. Problems are known e.g. for wind turbines, where gear-mesh excitation could potentially excite acoustic resonances resulting in high noise pressure levels.

3.3 Summary - Torsional Interaction Analysis

The consideration of torsional interaction is important for high power systems, in industrial as well as in power generation applications. Torsional interaction directly affects the operation of the system only in a minority of cases, e.g. in cases with subsynchronous resonances, where the system can be damaged within seconds or with system blackouts due to a protective shut down of generation units.
More frequent are effects that are identified after months or years because of broken shafts or damaged gearboxes. The reason is mainly the unknown stress in the mechanical shaft due to torsional interaction because of lack of appropriate sensors connected to the shaft (Section 5.1). Some industries, like Oil & Gas, require a torsional analysis in the design phase e.g. for centrifugal compressor systems.
But it is not always possible to prevent excitation of torsional interaction during operation, especially with growing complexity in industrial power systems due to an increased percentage of power electronic loads.

4

Damping of Torsional Interaction Effects in Power Systems

Torsional interaction resulting in excitation of torsional oscillation can be observed mainly in large rotating machinery. Countermeasures have been discussed for decades [43] because of fatigue and subsequent structural failure of the equipment, but also because of noise generation (Section 3.2). The focus of this chapter is on damping of torsional oscillations in large drive trains for industrial or utility applications, since large drive trains have typically low damping properties and low natural frequencies.
In case of large drive trains with low damping properties, it is impossible to design an overall system, which operates in all conditions without experiencing any of the discussed effects at the natural frequency of the drive train. This makes it necessary to apply countermeasures against TI to the system, to prevent fatigue effects and to stay operational over the specified lifetime of the system.

4.1 State of the Art - Countermeasures against TI

Large drive trains have unique properties compared to other mechanical systems:

1. Low inherent damping, high Q-values, as discussed in previous sections
2. Natural frequencies in the subsynchronous range
3. High initial and operational costs

It is very challenging to apply new damping strategies because of the technical properties mentioned and a conservative operational attitude of the drive train owners. Hence the existing solutions for active damping in the area of large drive trains are quite limited.

4.1.1 Passive Countermeasures

Passive countermeasures have advantages in reliability terms, but are limited in possible application, are less flexible and have typically higher initial costs. They have to be considered in the design process to be applied, retrofit solutions are quire rare. One can distinguish between mechanical and electrical counter-measures:
A very common countermeasure against TI is to **Shift Resonant Frequencies** by modifying the drive train stiffness and/or inertia, e.g. by changing the shaft material, diameter or overall length, mainly during the design phase. This can be done when the expected frequency spectrum of pulsating torques is known, e.g. with known electrical resonance frequencies in the power system, which is fixed as long as there are no changes in the system. [38] reported several cases where adding a flywheel to the main shaft resolved the problem of torsional interaction, at the expense of changing the mechanical design of the drive train. This approach works only for relevant harmonics with fixed frequency component. **Viscous dampers** are often used in reciprocating engines to help limit torsional vibration and crankshaft stresses. A viscous damper consists of a flywheel that rotates inside the housing, which contains a viscous fluid such as silicon oil that provides a shear motion of the fluid between the internal flywheel and damper housing. The damping characteristics can be adjusted by changing the internal clearances between the housing and flywheel. Adding **Soft Couplings** with damping components, usually rubber, can achieve an increase in the overall system damping of a mechanical drive train [38] plus detuning the torsional natural frequency of the shaft. The coupling is termed "soft" because it typically has a lower torsional stiffness than the shafts it is connected to. Soft couplings are not preferred because of increased maintenance, and they are not available for drive trains in the multi-megawatt range [41].
Another mechanical approach is a **Passive Absorber** with inertia J_a, stiffness k_a and damping d_a, attached to a primary mechanical system. It is tuned to absorb the energy of an undesired critical frequency with $\omega_c = \sqrt{k_a/J_a}$, which cannot fully be achieved because of the presence of the damping value d_a. The mechanical properties of a passive damping device cannot be adjusted, resulting in a very narrow and fixed interval of operating frequency to be damped. The passive damping device coupled to the original mechanical design adds another degree of freedom to the primary structure, with an addi-

tional natural frequency of the overall system. A theoretical elimination of the undesired critical frequency ω_c results therefore in two new natural frequencies, appearing typically as sidebands of the undesired natural frequency. The distance to the "old" natural frequency depends on the physical dimensions of the passive damping device. Numerous variations and improvements to the passive absorber structure can be found in the literature, e.g. in [44], [45]. They deal with ideal resonators by active elimination of d_a, but also with actively tuned absorber devices with superimposed angle dependent reactions (varying effective k_a) or acceleration-dependent reactions (varying effective J_a), for a wide frequency operation up to damping all frequencies in a certain band. All partially passive methods need additional components attached to the primary mechanical system, which is typically undesirable for high power rotational drive trains.

A **Static Blocking Filter** made up of LC-tank circuits inserted in series with the device to be protected can be tuned to contribute positive resistance with frequencies, which are coincident with the complement of the torsional natural frequencies. In essence, the filter isolates the machine from the system at the critical natural frequency. This hardware is expensive, and can't be applied e.g. to power electronics-driven electrical machinery [43].

A similar approach is a **Line Filter**, which can protect a conventional unit from torsional interaction when the source of the problem is a single line, but it loses its effectiveness with changes in the power system.

A **Bypass Damping Filter** based on a resistor in series with a parallel combination of a reactor and a capacitor are tuned to have very high impedance at system frequency, and relatively low impedance at the complement of the torsional natural frequency of the conventional unit to be protected.

All filters have the drawback that this kind of equipment is limited in flexibility, requires design changes to the existing power system, and becomes expensive at high voltages levels.

4.1.2 Active Countermeasures

The active countermeasures can also be divided into mechanical and electrical countermeasures. The active electrical countermeasures typically try to avoid the coincidence between complementary electrical and torsional natural frequencies in the system, or they try to eliminate the complementary electrical frequency components, e.g. by means of control or a specific switching algorithm for power electronic devices, especially with voltage source converters. Active mechanical countermeasures improve the mechanical system at the natural frequency to be less sensitive at those points.

Resonant Frequency Avoidance is the main approach against torsional excitation of natural frequencies for large variable-speed drive trains, to avoid operation at critical speeds. It can be achieved by reducing the allowable operational range of the system, or by quickly bypassing any determined resonant speed by adding a dead-band in the control logic at these points, thus exciting the natural frequencies for only a very limited time. The problem with the approach is that the process typically sets the reference speed. The process can ask the variable-speed drive to operate at the excluded speed, resulting in a toggling around the critical speed due to the exclusion.

Active Compensation can be applied, when the disturbance has a periodic character and continuously excites the structure in steady state. This forced vibration attenuation problem can be addressed by introducing a controlled excitation moment to the mechanical design with appropriate amplitudes and phase angles at the disturbing frequency. The feed-forward control allows a theoretical cancellation of the disturbance at the sensor location, $f_{dist}(t) = f_{comp}(t)$. The practical realization results in a relatively complex controller, including adaptive control paths, because of the importance of gain and phase matching the disturbance, to prevent the vibration canceling system becoming the major disturbance. The active compensation approach is well understood and applied, for example, in the area of noise canceling in numerous applications. The difference to torsional interaction is the disturbance amplitude and the effect on the surrounding system. Noise canceling applied, as in the car industry, is tuned to eliminate unwanted noise in the automotive cabin at the passengers heads. The noise has significant amplitude, which directly influences driver satisfaction. The disturbance in torsional interaction effects is typically a frequency component in the air-gap torque corresponding to a natural frequency of a drive train with comparably little amplitude, e.g. below one percent of the nominal torque. The unwanted effect is not the air-gap torque but the reaction of the drive train to that disturbance.

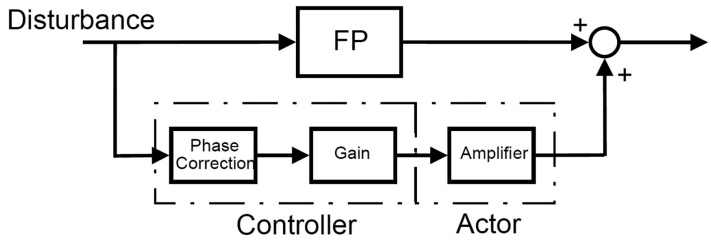

Figure 4.1: Active compensation block diagram including forward path (FP).

Active compensation is one method applied in the **Active Damping of Torsional Oscillation in Low Power Applications** e.g. servo drive applications. The disturbance can mainly be found in the mechanical system (Section 3.1.5). Harmonics and interharmonics produced by the servo-drive power electronic converter are typically not critical (no torsional interaction effect) because of significantly better damping properties (Section 2.1.3) of the mechanical system at its natural frequencies. Natural frequencies can be relevant up to the Kilohertz range for servo-drive applications. The comparably lower stiffness requirement of lower power drive trains allows observing torsional oscillation by means of high precision speed or acceleration sensing equipment. This signal can be fed through the high dynamic converter control to cancel out the effect of the disturbance (Figure 4.1, summation point). Mainly sensing, complex signal processing and different control implementation into dynamically controlled power electronic systems are discussed in literature. The first two aspects are also relevant for high power applications, but typical industrial high power converters cannot be controlled as dynamic as low power servo drives, which makes it difficult to apply already available methods for low power systems into the high power application area. Already the effect of a torsional oscillation is different at lower power level. For instance in the printing industry, the main objective of reducing torsional oscillations is to increase the product or process quality, not to achieve the desired lifetime of the mechanical system (Section 3.2).

A conventional **Dynamic Stabilizer**, which was developed as a countermeasure to SSR in power systems, consists of thyristor-modulated shunt reactors. It is connected to the isolated phase bus of the protected synchronous generator. It responds to a measured oscillation of the conventional generator around a quiescent operation point. In the absence of rotor oscillation, the quiescent operation of the stabilizer is like a continuous reactive load. It can't be applied to power electronics-driven electrical machinery; the voltage at the motor terminals is usually distorted and thus difficult to synchronize to. Drawbacks of dynamic stabilizers are the reactive and active power consumption (losses), the production of harmonics and its associated high costs.

An **Active Damping Control via Exciter Controller** is a very sophisticated approach to active damping of torsional oscillation. It has been developed for large synchronous generators. A damping reference, based on external measurements such as rotational speed, AC-bus frequency or acceleration power, is added to the exciter control [46]. The controller has to produce an electrical torque component on the rotor (by modulation of the generator flux), which is in phase with the speed variation to provide additional damping to the mechanical system. The control has to compensate for gain and phase of the excitation system, power system and the generator, as these components influence the

effect of the generator flux on the resulting torque [47]. The typical frequencies of application are in the range of approximately $0.2Hz$ to $2.5Hz$, sufficient for very large generation units. Higher natural frequencies can hardly be addressed because of time constraints of the exciter converter and the exciter implementation, especially for rotating exciter.

4.2 New Damping Approach

None of the available approaches (Section 4.1) is capable of enabling electrically driven multi-megawatt trains and power generation units to operate in their designed way without being possibly affected by torsional interactions. Large drive trains have very limited damping properties (Section 2.1.3). This makes them very sensitive to torsional interaction. The approach introduced and developed within this section decreases the inherent sensitivity of the mechanical system and thus allows operation of such multi-megawatt drive trains without the negative effects discussed in Section 3.2.
The damping method chosen for application with large drive trains can be derived from Newton's equation of motion:

$$[\mathbf{J}] \cdot \left\{\ddot{\phi}\right\} + [\mathbf{D}] \cdot \left\{\dot{\phi}\right\} + [\mathbf{K}] \cdot \{\phi\} = [\mathbf{B}] \cdot \{u\} \tag{4.1}$$

where **J** represents the systems matrix of inertia, **D** the damping matrix and **K** the stiffness matrix. The part of the equation to the left of the equal sign describes the mechanical system with its properties, as described in the Chapter 2. The matrix **B**, on the right side of the equation, represents all input components acting on the mechanical system, including pulsating torque components. The basic approach of the developed active damping method is to modify **B** in such a way that it behaves like an increased damping matrix **D** on the mechanical system, but only at the natural frequencies of the system, where an increased damping is required. This is achieved by basically modulating active power at the natural frequency of the sensitive drive train.
The developed method is a mechatronic control approach. It utilizes a mechanical feedback signal to introduce limited damping power, and it has the capability to compensate for dead times typically existing in large converters without significant loss of damping performance. It provides a very robust design for slight natural frequency variation and mistuning although it modulates active power exactly at the resonant frequencies of the mechanical system. It operates only at the natural frequency of the sensitive drive train, and allows high damping performance with very limited power. More than one mode

can be damped simultaneously based on superposition, but dependent on the controllability of that mode. This can be analyzed by the introduced mode shape characteristic of the mechanical structure. This restriction is, typically, not a limitation, because all modes excited by the electrical machine can also be damped by the same machine with the developed method. One kind of realization utilizes an existing small DC-link storage device (inductor or capacitor) for generating active power at the natural frequency of the mechanical system in order to use it as damping power. The damping power is than per se not an energy loss. The new damping scheme can be integrated into existing large drive topologies, but it can also be applied by means of low cost separate devices. Figure 4.2 gives a very good insight into the fundamental functionality.

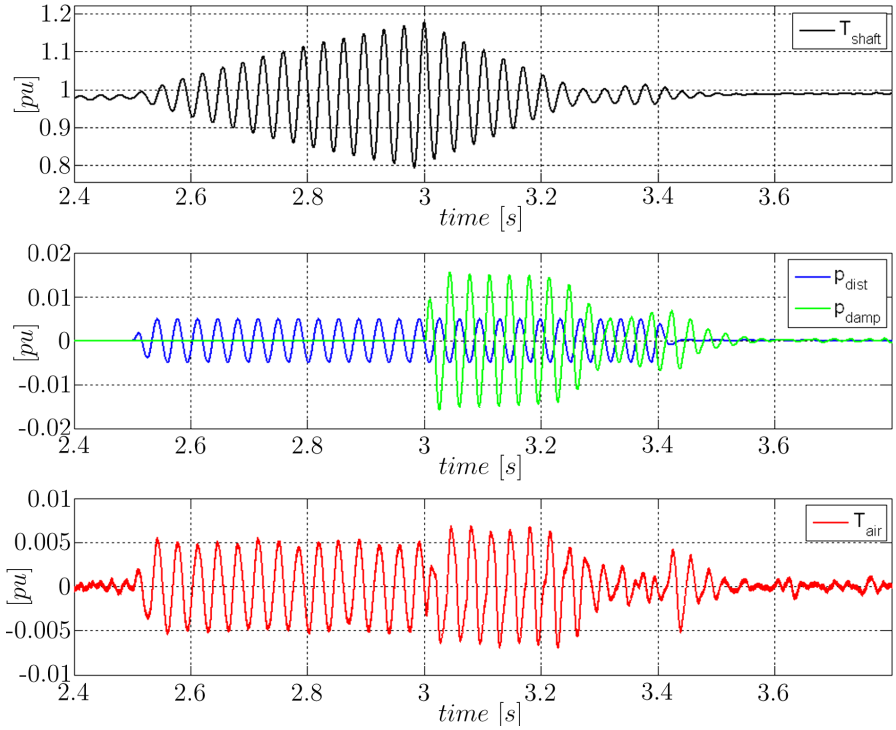

Figure 4.2: Electromechanical simulation: Effect of Torsional Mode Damping applied to a large compression train. P_{dist} - Active power exciting torsional oscillation ("disturbance power"). T_{shaft} - Effective shaft torque of the mechanical system. P_{damp} - Active power at the natural frequency, exchanged between the sensitive drive train and the damping converter ("damping power"). T_{air} - Air-gap torque component at the natural frequency of the mechanical system.

The black line - T_{shaft} - in the upper subplot indicates the measured shaft torque from the mechanical system which is used as an input signal for the control. It shows the reaction of the drive train to a pulsating torque introduced by means of the air-gap torque. The corresponding electrical power is indicated in blue on the second subplot - P_{dist}. The

mechanical damping of the drive train is not sufficient; the alternating torque increases until the active damping is enabled ($t \geq 3s$). The damping controller adds another component - P_{damp} - green - with effective $+90^o$ (Figure 4.3) phase shift to the mechanical torque and reduces the alternating torque component over time (as compared to compensation, which would try to eliminate the alternating torque components immediately), until the oscillating torque component reaches an acceptable limit. Active power is modulated at the natural frequency of the sensitive drive train. The reduction of alternating torque components over time allows the implementation also with low bandwidth controlled systems. After the disturbance disappears, the damping component decays and the oscillation in the measured torque almost disappears. The damping controller is designed to stay enabled at all times. The principle indicated in Figure 4.2 is only for demonstration and tuning purposes of the controller. It can easily be recognized that the damping controller, when enabled, acts like an increased natural damping of the mechanical drive train and is electronically adjustable. The effective air-gap-torque (red) shows that the air-gap-torque is not compensated to zero at any time when enabled. The damping power compensates the disturbance power only when the disturbance reaches a steady state amplitude and phase (Figure 4.2 - $3.3s < t < 3.4s$.). But this has rarely been observed in the numerous measurements performed while testing this active damping method.

4.2.1 Active Damping Topology

The block diagram in Figure 4.4 represents the mechanical structure of a two mass system with an additional, simplified damping circuit. The damping loop acts based on a torque measurement of the shaft T_T between the two masses represented by J_1 and J_2. Two variables, an additional delay time T_{del} and a gain V, can be adjusted to provide an additional damping component to the air-gap torque T_1.
The adapted transfer-function between the air-gap torque T_1 and the shaft T_T can generally be formulated with:

$$\frac{T_T}{T_1} = \frac{(\frac{d}{k}s+1)(T_{del}s+1)}{\frac{1}{k}\frac{J_1J_2}{J_1+J_2}T_{del}s^3 + \left(\frac{1}{k}\frac{J_1J_2}{J_1+J_2} + \frac{d}{k}T_{del}\right)s^2 + \left(\frac{d}{k}\left(1-\frac{VJ_2}{J_1+J_2}\right)+T_{del}\right)s + \left(1-\frac{VJ_2}{J_1+J_2}\right)} \tag{4.2}$$

This equation does not reflect the full implementation, as there is much more complexity in between the measurement and the air-gap torque response of the electrical machine, e.g. the power system and the non-linear behavior of the large drive. It shows a control system description, the active damping is adjusted with appropriate values for V and T_{del}.

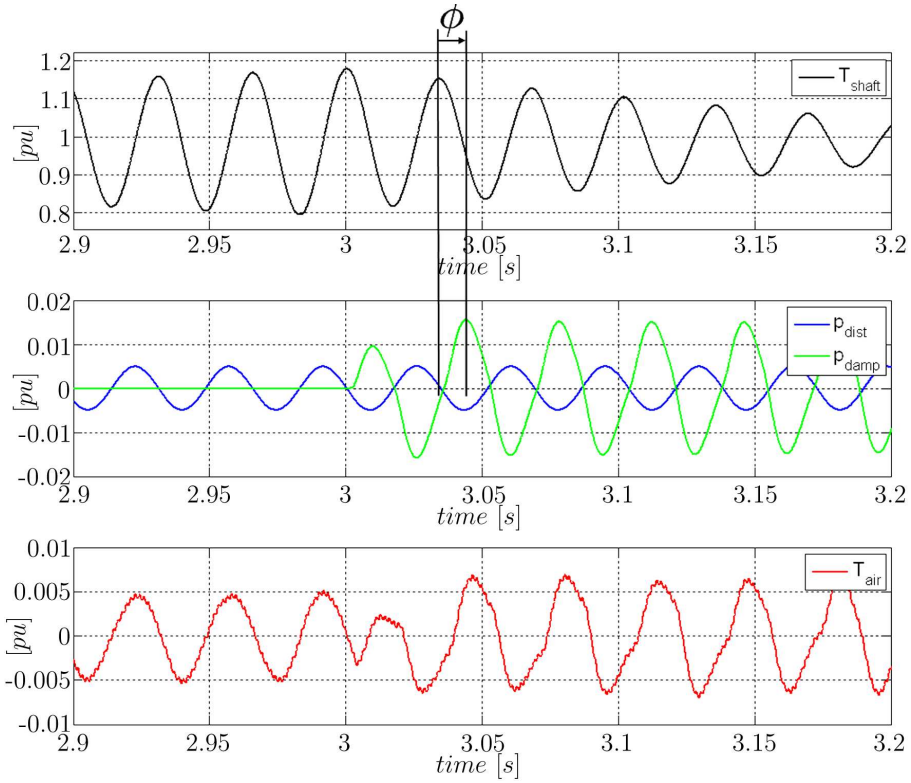

Figure 4.3: Zoom of Figure 4.2: Damping torque acting with $\varphi = +\frac{\pi}{2}$ phase at ω_{nat} between shaft torque T_{shaft} and effective damping power P_{damp}.

Figure 4.5 can be used to determine the required phase relations between pulsating torque component and damping component. As already mentioned in previous sections, the principle approach is to add a $+90^o$ phase shift to the open-loop system response to achieve damping behavior.

For explanation purposes, T_d can be initially understood as a pulsating torque component acting on the air-gap torque and exciting the mechanical system at the desired natural frequency. The open-loop transfer-function $G_{mdd}(s)$ between the assumed pulsating torque T_d and the natural damping component proportional to the speed of the mechanical system T_{md} can be calculated with:

$$G_{mdd}(s) = \frac{T_{md}}{T_d} = \frac{D}{Js}, \quad \varphi(G_{mdd}(s)) = -\frac{\pi}{2} \tag{4.3}$$

The delay $\varphi(G_{mdd}(s))$ calculated in Equation 4.3 refers to a pulsating torque component exciting the mechanical system, adding a negative damping component to the natural damping of the mechanical system. A positive damping component requires therefore a

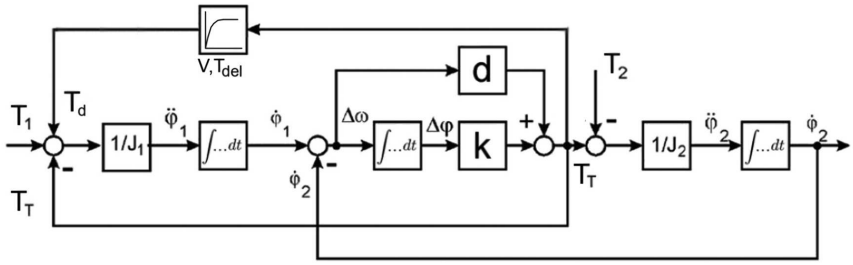

Figure 4.4: Mechanical model representation with theoretical active damping loop

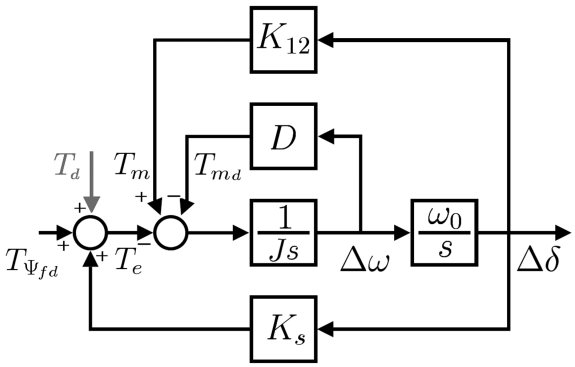

Figure 4.5: Active damping component T_d acting through the air-gap torque on the mechanical system.

phase shift between the introduced pulsating damping torque and the natural damping of:

$$\varphi(G_{mdd}(s)) \stackrel{!}{=} +\frac{\pi}{2} \tag{4.4}$$

These relations can also be observed in the demonstration plot (Figure 4.3). The single sine periodicity of the oscillating torque component allows the utilization of the damping structure also with topologies including delay or dead-time behavior; the positive damping torque can also be achieved with a delay of:

$$\varphi(G_{mdd}(s)) \stackrel{!}{=} \frac{\pi}{2} + n \cdot 2\pi \tag{4.5}$$

with $n = 0, 1, 2, ...$ The influence of the delayed damping on the damping performance depends mainly on the natural damping of the mechanical system, and can be almost neglected for large systems because of their low natural damping. When applying a delayed damping power, it is not possible to completely eliminate torsional oscillations.

But this is not needed in high power drive trains where small torsional oscillations are well within the specification limits.

4.2.2 Implementation of the Active Damping Method

Two main designs have been identified to be suitable as a platform for the implementation of the damping structure:

- Integrated into a power conversion system utilizing the available hardware to provide damping to the variable speed driven electrical machine, on the machine side of the converter.
- Integrated into a power conversion system, but acting on the grid side of the converter. This implementation requires care that it does not impact the connected variable speed drive train by the damping power modulated with the grid.
- A separate power conversion device dedicated to generate active damping power, to produce air-gap torque harmonics acting as increased natural damping.

More details to the hardware implementation aspects will be given in Chapter 5. The implementation of the damping structure itself can be divided into three parts:

1. Measurement in the mechanical system providing an analog input signal ("In")
2. Data processing
3. Analog output and interface to converter control ("Out")

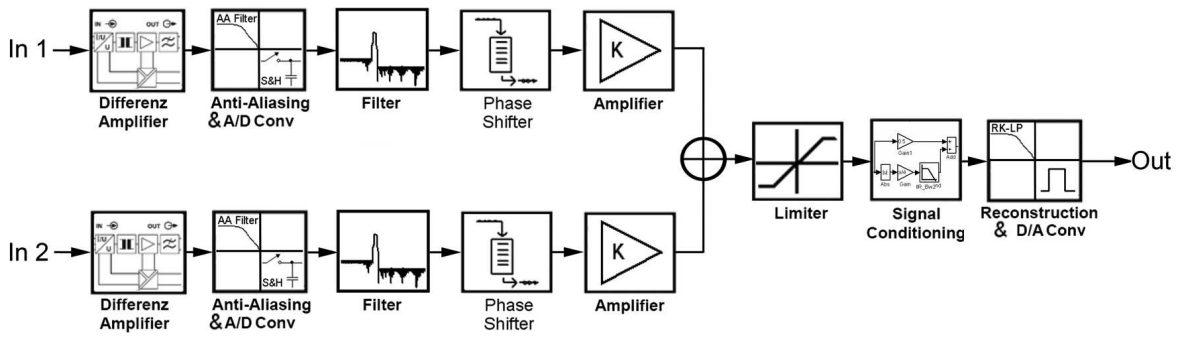

Figure 4.6: Block diagram of the principle damping circuit implementation, e.g. for damping of two natural frequencies.

The main components for the torsional mode damping structure are (Figure 4.6):

- The filter isolates the signal component around the desired natural frequencies from the measured input. The filter could be in the simplest implementation a 2^{nd} order high-low pass combination with zero phase at the natural frequencies. Better signal isolation results can be achieved with more complex filter methods, like Kalman-filter or observer based structures utilizing a decoupled system structure as discussed in Section 2.1.5 based on air-gap-torque calculation; or a synthetic generation of the feedback signal with a Phase Lock Loop (PLL) like structure detecting the phase and amplitude of the alternating torque at the desired natural frequency.

- The phase shift block, typically a memory block with successively writing and reading addresses in an endless loop, the reading address offset can be dynamically adjusted to allow adjustable time delays, required for compensation of converter, power system and mechanical system time delays.

- The gain block compensating for the attenuation of other blocks, but mainly to adjust the desired degree of damping, to set the alternating torque response of the system in steady state with active damping enabled.

- The limiter allowing stable operation even with high-adjusted gains without disturbing the operation of the power electronic device.

The interface to the power electronic converter is also an important part of the damping loop, especially the point of connection (POC) inside the existing control structure. The converter control can have a significant influence on the performance of the damping loop, because of (a) possible small variable delays between the introduced signal at the POC and the pulsating torque components in the air-gap torque, and (b) because of the internal control structure probably fighting against the introduced "disturbing" damping signal. A careful design is therefore necessary, and will be demonstrated for a self-commutated inverter and a line-commutated inverter implementation.

4.2.3 Tuning of the Active Damping Method

Large equipment is typically expensive to purchase and to operate. The tuning of the active damping system requires, therefore, a careful strategy to satisfy the customer with appropriate damping performance in an appropriate tuning time. Theoretically, an unlimited positive feedback loop would be capable of destroying the whole drive train in very little time, dependent on the closed loop gain. Therefore, in practical applications, the

closed loop gain is limited to small values by means of an output-limiter (Section 4.2.2). Two main approaches have been identified to satisfy this need:

1. Excitation-Wait-Damping (EWD): the damping controller operates in open loop configuration. It excites the mechanical system at the natural frequency for a limited time to uncritical alternating torque values. The loop will be closed for another limited time to apply damping to the system after a short waiting period.

2. Limited Damping (LD): the damping controller operates in closed loop configuration for a limited time. The introduced delay utilizing the phase shift block will be modified until a negative damping can be observed, indicating an upper or lower border for delay time. This modification will be done in both delay time directions, increased and decreased. The ideal delay time for this operation point is than exactly in the middle.

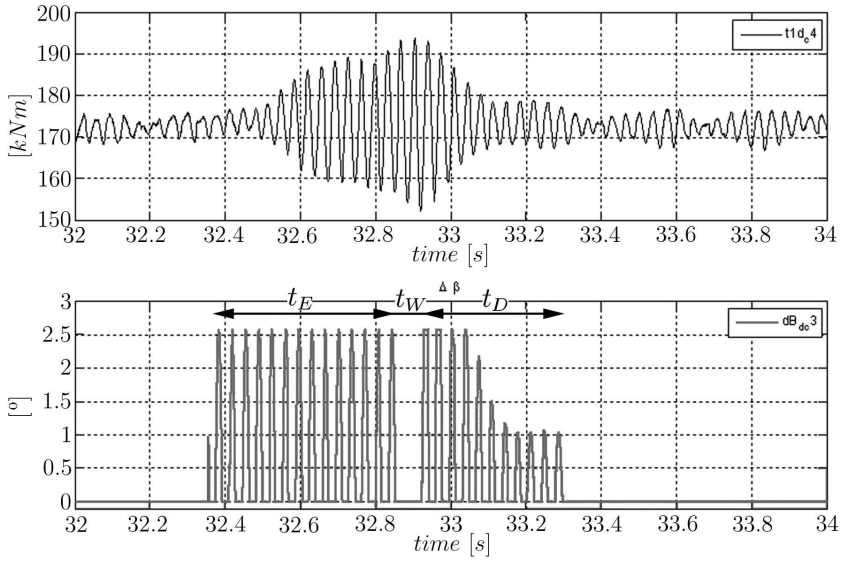

Figure 4.7: Tuning of the active damping structure with the EWD approach: measured torque (plot 1 - black), unipolar modulated damping signal (plot 2 - gray).

Both approaches have several advantages: EWD allows the interface to the power converter and to the electrical machine to be checked by exciting the natural frequency of the mechanical system for an adjustable time and with adjustable gain until uncritical values are reached. The effect of the excitation can be identified in the torque measurements (Figure 4.7). It shows also the capability of the active damping implementation, between 40..80 kNm/s increasing alternating torque rates have been measured during the string

test. LD can be more easily applied for mechanical systems connected to electrical machinery exposed to relatively high air-gap torque noise, where it is difficult to distinguish between self-made excitation (with EWD excitation to uncritical values) or excitation due to the noise in the pulsating air-gap torque, e.g. caused by an electrical drive.

4.2.4 Sensitivity and Gain Margin Analysis

Gain and phase margins are measures for the stability of a control loop. It can be derived e.g. by calculating the bode plot, see Figure 4.8. The feedback loop is stable for magnitudes $|\beta A| > 1$, if the associated phase is between $-180^o < \beta A < 0^o$. A phase $\beta A < -180^o$ would result in unstable operation of a positive feedback loop.

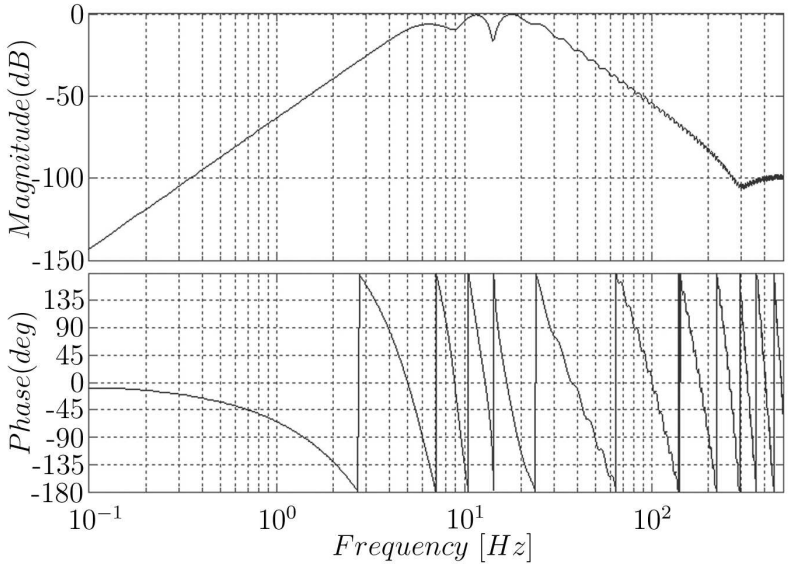

Figure 4.8: Transfer-function example of a potential damping circuit, with three damping circuits in parallel (Subsection 5.5.3).

Another measure of stability is the phase margin value, the phase at which the magnitude reaches $0\,dB$, a gain of 1. The phase should have some distance from -180^o to provide a stability margin for the control loop. Figure 4.8 shows the transfer function of a damping control tuned to provide damping for three modes simultaneously. This is challenging because of the dead times and the associated phase behavior introduced into the closed loops. The limiter block as a non-linear element, an important part of the damping control loop, is not considered in the gain margin analysis. Therefore it was obvious that it would be useful to verify the gain margin analysis with gain variation in a full simulation model to have a clear understanding of the stability of the closed loop control. The full simulation

results show a significant gain margin of factor 10 and larger for a single damping loop with the proposed control scheme. This was also verified in measurements. The reasons for the high gain margin are the limitation of the output signal, and the quality of the sensing input because of the usage of a torque measurement. The torque measurement or a signal representing shaft torque is a very important requirement of the damping structure for large drive trains (Section 5.1). The drive trains have high surface stress and high stiffness, resulting in low resolution of dynamic elements in the conventional high-end speed measurements.

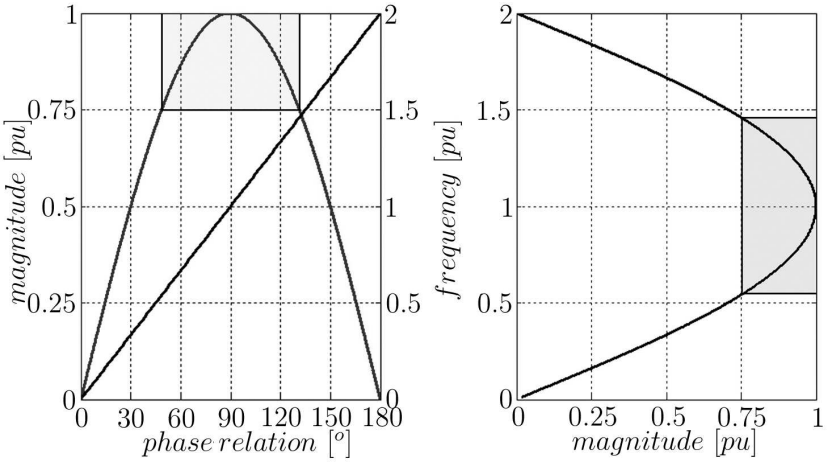

Figure 4.9: Sensitivity of the control loop to phase variation due to variation of natural frequencies or due to imperfectly tuned controls. A damping efficiency better 75% is indicated in gray boxes.

Another factor in terms of stability is the sensitivity of the damping loop to the natural frequency variation of the mechanical system (Figure 4.9). This variation can occur e.g. in wind turbines, where the inertia of the blades depends on the pitch angle of the rotor. But it can also "occur" with an imperfectly tuned damping loop.
A perfectly tuned damping circuit would have a phase relation of $+90^o$ between measured torque and damping power, see Equation 4.4. But the damping loop provides damping as long as the phase shift is between 0^o and 180^o.
Figure 4.9 gives a good insight into the sensitivity of the proposed damping loop to frequency misalignment. The non-linear graph in the left corner indicates the change in magnitude of the control circuit because of phase misalignment. A frequency variation expressed in per unit (p.u.), based on the real natural frequency of concern, as a black line in the left plot could be the reason for the phase alignment. The right side of the plot shows it merged, the reduction in damping magnitude due to frequency variation, e.g. the damping loop is tuned to $10Hz$, the natural frequency of the mechanical system

$11Hz$ ($1.1p.u.$), effecting the damping gain with $0.988p.u.$, a negligible gain reduction of 1.2%. The damping loop would be unstable for frequencies with $f_{nat} \geq 2 \cdot f_{tun}$. Although the control system has low sensitivity to parameter changes, the mechanical system is very sensitive to the frequency of the modulated power (system with high amplification factor Q, see Figure 2.6). The mechanical sensitivity is critical for a synthetic calculated signal representing the shaft torque, e.g. by utilizing imperfectly tuned observer models, and uncritical when acting based on a direct measurement from the mechanical system.

4.3 Summary - Damping of Torsional Interaction Effects in Power Systems

Several approaches as state of the art countermeasures against torsional interaction have been discussed within this chapter. Most of the passive countermeasures can only be applied where fixed harmonics cause torsional oscillations, not for variable speed operation, and are typically difficult to be applied in high power drive trains. The discussed active countermeasures can usually be found for different power levels: dynamic stabilizer and exciter control modification in very large generation units, with significantly lower bandwidth and higher costs due to required modification in the electrical system. Active compensation as well as other complex control approaches are typically available for low power applications in the kW range and usually require a sufficient dynamic control and corresponding power electronic hardware, which is not applied to industrial high power drive systems.

A new method to increase the damping property of mechanical systems has been introduced in this chapter. It utilizes power electronic devices to exchange active power at the measured and isolated natural frequency of a drive train with sensitivity to torsional excitations. The method is implemented in such a way that the mechanical system behaves like with an increased mechanical damping. The damping property is thus electronically adjustable by modifying control loop settings. The principle implementation of the developed damping loop is illustrated, and the relevant blocks are discussed. Tuning approaches are introduced, which are very important for the implementation into real systems. The proposed damping circuit operates with a measured natural frequency of the mechanical system but without risks for the mechanical system because the applied damping power is always limited to small values, by means of a limiter at the interface to the converter control. The developed method has shown very low sensitivity to parameter changes and provides a very high gain margin, larger than 10 was verified in field measurements.

5

Fields of Application for the Active Damping Approach

The active damping system acts as an increased natural damping for the mechanical drive train, and can be applied in different ways. A power electronic device is always needed to modulate active power through the winding of an electrical machine. There are in general two options:

1. There is no power electronic device available electrically close to the drive train that includes an electrical machine.

2. There is already a power electronic device available, which can be used for the modulation of active power. The requirements for this power electronic device will be discussed in the second part of this chapter.

The potential hardware implementation with two independent options is indicated in Figure 5.1. The sensors measuring the mechanical torque of the desired drive train are located based on the mode shapes of the drive train, and are connected to the "TMD" box including, among others, the damping circuit (Figure 4.6). Only one out of two indicated solutions is needed to provide additional damping to the conventional generation units: (1) the separate device controlled with the gray line or (2) the integrated solution, utilizing available converter(s), indicated with numbered dots. There is only a single separate unit shown, but two potential converters for integrating the damping functionality into existing units, marked with numbered dots. The number of required units depends on the necessary damping power level (which is typically less than 1% of the nominal power)

and on the redundancy requirements for the damping solution. Both damping options will be discussed in this section.

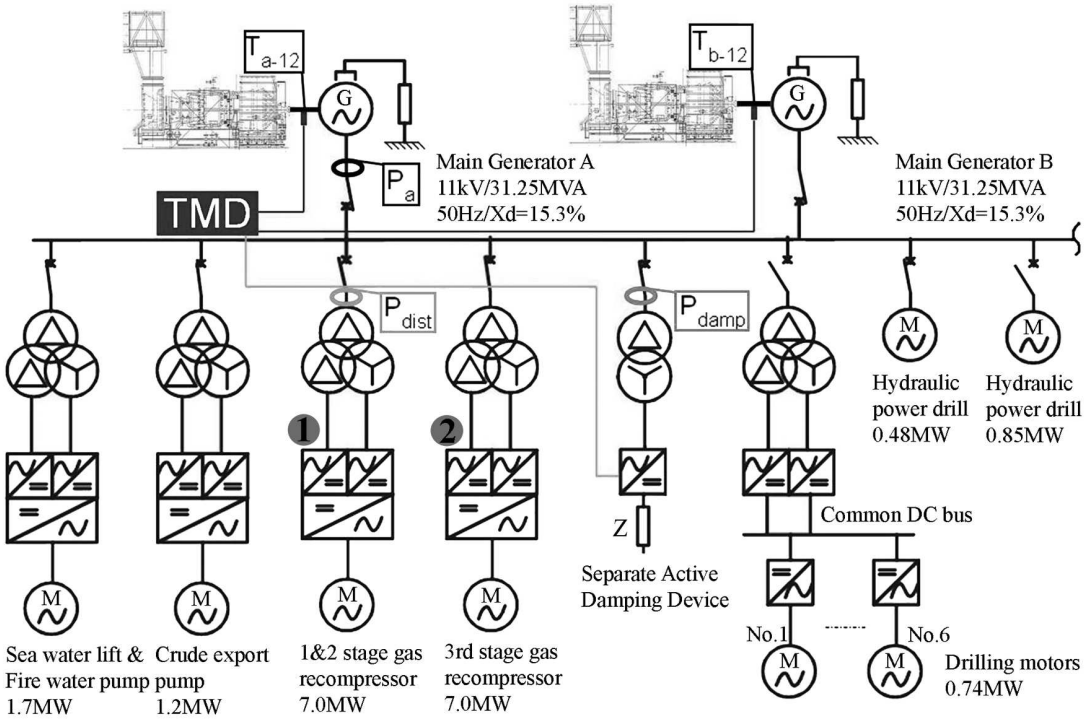

Figure 5.1: Island power system (introduced in Section 3), equipped with a torsional mode damping option to increase the damping properties of both generator drive trains. One of the available power converters (1) or (2), or a separate damping converter can be utilized for this purpose.

The availability of a power electronic system for an active damping implementation depends on (a) the feasibility and effort for modifying this system, (b) the hourly availability, and also (c) the reliability of the desired active damping solution. The electrically close requirement implies low impedance between the damping device and the mechanical drive train compared to the other impedances connected to the same node, to conduct most of the modulated active power to the desired mechanical system. A weak grid connection results in relatively high impedance values, one reason why the active damping solution is perfectly suited for island like power system structures.

Reliability is an important aspect in the active damping approach. Relying on an actively damping system that is unavailable can lead to severe outages (see Section 3.2). Being able to observe the availability of the active damping device could be a requirement. Different levels of reliability can be imagined: A watch dog controlling the availability of the damping control; or a redundant measurement detecting the vibration of the mechanical system, can set an alarm with abnormal values. A stronger reliability requirement might

be necessary: a redundant damping solution. A $n-1$ reliability requires at least n devices online to provide active damping on demand. The effort for the implementation into existing systems then depends on the availability of suitable designs. The separate device (Chapter 5.2) solution can be built relatively easily as a redundant design.

5.1 Monitoring of Torsional Oscillations

Sensing of a torsional oscillation is a critical requirement for the implementation of the developed damping method. Standard equipment used for analyzing lateral vibrations, such as accelerometers and proximity probes, are not able to measure torsional vibrations. Depending on the shape of the torsional mode and the stiffness of the motor coupling, even high-resolution motor speed measurements may not be able to accurately measure such vibrations, also due to the comparably small torsion angle at a certain level of alternating torque. In string tests, torsional oscillation measurements are typically based on measuring the shaft torque, e.g., by a full-bridge strain gage system with telemetry. If the shaft torque has to be monitored over long time periods or if the torque signal is used in a control system, long-term stable measurement methods have to be applied.

Examples for suitable sensing systems are continuous duty (CD) torque-meters for permanent installation, which are offered by a variety of vendors. The most widespread CD sensing technology is based on measuring the twist over a coupling spool, and there are more than 800 installations worldwide using this approach with many millions of operating hours accumulated.

To achieve absolute accuracy of the torque measurement in the order of one percent full scale, such torque-meters must be integrated into the mechanical system design, typically during the design stage. Therefore it can be costly to apply this type of torque-meter as a retrofit.

However, for torsional mode damping applications, an absolute accuracy of one percent full scale is not needed. The most important measured signals in this type of feedback control system are the frequency and phase of a measured oscillation. An accuracy of $\sim 5\%$ is sufficient for torsional mode damping, based on own experience. Therefore, alternative non-contact sensing methods with high long-term stability may be more attractive. As an example, toothed-wheel based monitoring systems sensing the speed on both ends of a drive train have a long history of measuring torsional vibrations continuously on utility-class generating machines.

Proper transduction of the pulses from the sensors, plus knowledge of the torsional mode shapes, is adequate for detecting torsional vibrations sufficient for both protection and

damping [48]. This type of sensing and monitoring system has been used in several dozens of applications with synchronous generators over the last 30 years. Recently, in another power system application, a magnetostrictive torque sensing system was installed to monitor the shaft torque at the couplings of two large flywheel generators [49]. The absolute accuracy of the torque sensors in this application is only in the lower percent range, but still suited for retrofit applications because it does not require attachment to the rotating shaft or modification of the existing train.
It is an ongoing effort to improve existing torsional vibration sensor systems with both, improved sensing devices, but also with model based approaches to better detect the phase and amplitude of the torsional oscillation.

5.2 Separate Active Damping Device

A separate active damping device can be utilized when there are no or no suitable existing power electronic devices available electrically close to the mechanical system. Many different design options are feasible for exchanging active power at the natural frequency of the mechanical drive train between the mechanical system and the separate device. The separate device always consists of three parts: a separate power conversion module, a load and a control system including the damping control structure. The vibration sensing in the mechanical system is assumed to be solved.
A general overview about power electronic converter has already been given in Section 2.3. Both designs (self- and line-commutated converter types) are principally applicable, dependent on rating, dynamic performance or reliability requirements. Only one conversion from AC to DC is typically necessary to be able to modulate the desired active power as needed for the active damping (Figure 4.2).

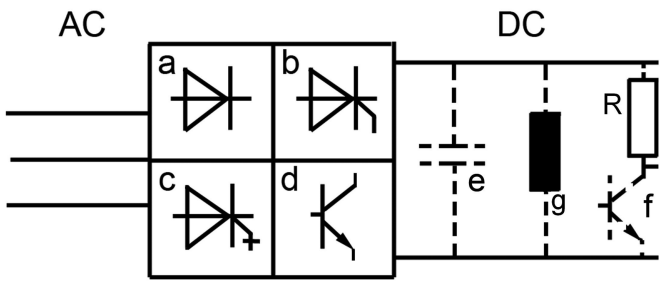

Figure 5.2: Design options for the separate active damping device. Options a and b indicate line-commutated converter types, option c and d self commutated converter types.

Figure 5.2 gives multiple design options: Devices (a) and (b) indicate the line-commutated converter design, whereas (c) and (d) are self-commutated semiconductor devices. The capacitor (e) is typically needed for voltage source DC-link types, where also the break chopper design (f) can be applied. The inductor (g) is used with current source converters. Table 5.1 summarizes and evaluates the different options:

	e	f	g	Converter Control Reference	Harmonics production	Cost Effective	Control Complexity	Reliability
a	-	x	-	I	O	+	+	++
b	-	-	x	I	-	O	+	+
c	x	x	x	I/V	+	O	O	O
d	x	x	-	V	++	O	-	O

Table 5.1: Evaluation of different options for the separate damping device.

As already mentioned, the main purpose of the active damping device is to modulate active power with the mechanical drive train. Any device type (R, L, C) would be suited as "load" in the hardware of the active damping device, indicated in Figure 5.1 with Z as impedance, where the active power is modulated.
They are utilized as short-term storage devices (energy buffer storage). The energy stored in the component can be calculated with $E_{ind} = \frac{1}{2}LI^2$ for the inductor, $E_{cap} = \frac{1}{2}CU^2$ for the capacitor and $P_{res} = UI$ for the active power dissipated into heat for the resistive component. Modulating active power means charging or discharging the storage device (except for the resistive component, where modulating active power corresponds to a modulation of the dissipated power). No reactive power is needed per se for operating the different kind of storage devices. Converter options (a) and (b) require some reactive power because of commutation reasons, but not because of the connected R, L or C. Operational constrains or high dynamic performance requirements could result into reactive power consumption for certain configurations, e.g. while keeping an inductive coil charged (constant DC-current), in standby operation mode [50]. Solutions based on capacitive storage do not consume reactive power during standby (constant DC-voltage) [51].
Several aspects have to be considered for estimation of the required damping power, and will be discussed based on the scenario given in Figure 5.1: The size of a single generator is $\sim 30MW$. The damping device for that generator would therefore be designed to $\sim 300kW$ peak power, as one percent of the nominal power of the sensitive drive train is

typically sufficient for damping torsional oscillation based on the developed method within this thesis. The required energy capability of the capacitor and inductor depends on the active power modulation frequency, which is equal to the natural frequency of the sensitive system, and assumed to be at $\sim 30Hz$, resulting into a period of $33.3ms$. The energy stored in the capacitor or inductor can be estimated to $E_{storage} = 300kW \cdot 16.7ms = 5kJ$. A capacitor operated between $1000V$ DC and $1500V$ DC (690V AC supply - converter option (d)) would require a minimum size of $\sim 8mF$, an inductor $\sim 111mH$ at a maximum current of $300A$ (converter option (b) or (c)). A resistor needs to be rated to dissipate $300kW$ peak, or $150kW$ RMS. The size of the resistor is mainly defined by the duration of damping operation. A continuous operation of $10s$ at maximum power would require dissipating $1.5MWs$ for the resistive operation. A suitable resistor with a total weight of $20kg$ can dissipate this energy. The bandwidth of the pure resistive element is the highest compared with the other two options.

The preferred device will be chosen mainly based on reliability and economic aspects, dependent on the expected disturbance power in terms of duration and amplitude. Do the variable speed drives potentially operate at speeds critical of the generation unit? What is the size of the variable speed drives? How long do they potentially operate at that speed? Utilizing L or C for the separate damping unit is only beneficial in cases where a torsional interaction can be present for long periods of time. They have lower reliability numbers as compared to pure resistive components, probably higher control complexity and higher investment costs. L and C are partially utilized in the form of an already available DC-link inductor or capacitor in case of the integrated damping solution described in Section 5.3. The resistive load is, for many cases, the easiest from a control complexity, cost and safety point of view, in case of applying a separate damping device [52].

High redundancy can be achieved e.g. with design (a) or (d) and several "break chopper" modules (f) in parallel, switching an interleaved pattern, or with n individual units.

The control can be state-of-the-art PWM with third harmonic injection for the inverter of type (c) and (d), controlling the DC-link voltage or current; PWM for the break chopper (f) option controlled by a current reference, and current control for the line-commutated option (b). The reference for the power electronic converter is always derived from the active damping control (Chapter 4.2.2), and can be modified to achieve lower harmonic content beside the desired active damping power at non-fundamental frequency, e.g. by modulating $\sqrt{i_{des}}$ because of $P_d = i_{des}(t)^2 R$, to achieve modulated power only at the desired frequency.

5.3 Integrated Active Damping Device

Power electronic devices are one reason for exciting torsional oscillations (Section 2.3). The probability of having power electronic devices close to compromised mechanical drive trains is high. One approach proposed in this document is therefore the use of the available power electronic devices to provide active damping power for the mechanical drive train. It is not meant to eliminate the harmonics generated by the device, but to add an independent component achieving the increased natural damping of the mechanical system. Two different active damping approaches for different mechanical systems are indicated in Figure 5.1. The first solution uses the active front-end of the converter to exchange active damping power with the sensitive generator connected with the power system in-between; the second is to provide active damping to the mechanical system which is directly connected on the machine side and driven by a synchronous motor. Here, both converter bridges can be used to provide the required active damping power, as shown in Section 5.5.1. An important precondition for using existing power conversion hardware to provide active damping power to a mechanical system is that the normal operation of the drive system, especially the utilized power electronic devices, is not influenced by the additional damping loop. This can typically be assured by the very limited active damping power requirements, e.g. one percent of the nominal power of the drive system.

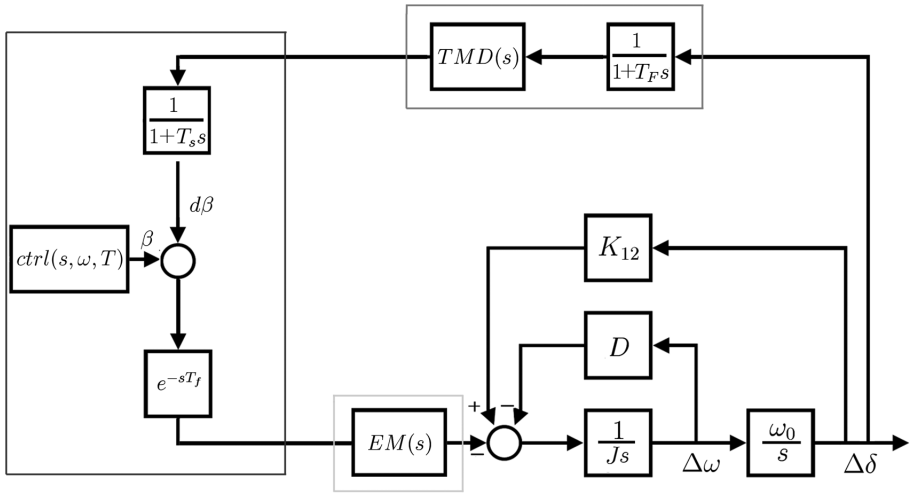

Figure 5.3: System design with system components influencing the performance of an active damping loop.

The interface and the implementation into an existing control structure are key for the utilization of existing hardware for providing active damping power. Figure 5.3 gives a good insight into the different components, which significantly influence the active damping loop. The interface has to be designed with a sufficient bandwidth to allow the active damping power modulation. The implementation into the existing control structure depends on the available converter type. A potential interaction between the existing control structure and the additional damping loop has to be considered during the design phase to prevent malfunctions of the damping circuit because of certain control functionalities working against the introduced damping signal. There is typically no choice of selecting self-commutated or line-commutated converters for the implementation of the active damping loop, especially not for drive trains connected to the motor side of the converter. Generally, both converter types can be used for implementation of the developed damping loop. If both converter types are available, e.g. for grid side active damping implementation, the power level of the converters, operational aspects or the effort for implementation needs do be evaluated for a final decision. The inherent operation of the converter, to drive a variable speed drive train, must not be influenced by the additional functionality.

5.3.1 Self-Commutated Converter Implementation

A very high percentage of self-commutated converters are based on a voltage source converter topology (Section 2.3). The following implementation aspects are therefore based on this topology, but are not limited to this type of self-commutated converter. Typical voltage source converters have some degree of freedom (e.g. modulation strategy) that can be utilized during the design phase to reduce or prevent a continuous excitation of dedicated frequencies. But it may still be necessary to implement the developed damping loop into a voltage source converter, especially with very sensitive mechanical trains or if a retrofit solution is required. A voltage source converter is typically designed to provide a comparably high dynamic performance, which can only be achieved with sufficient control bandwidth. This simplifies on the one hand the implementation of the active damping loop, e.g. in adding the signal to the torque reference for a machine side implementation (Figure 5.4). But it also requires considering higher level controls potentially counteracting this implementation and thus reducing the effect of the damping loop.
An active damping loop implementation for the purpose of providing damping power to synchronous generators connected on the grid side of the converter can also be implemented. One example is to utilize the DC-voltage control (or active current control) to

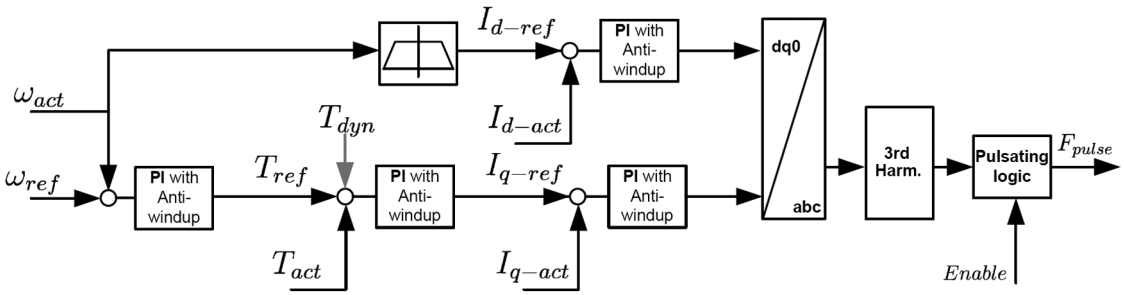

Figure 5.4: Typical block diagram for a voltage source converter type - machine side - with independent speed, torque and current control implementation [26].

modulate active power between the sensitive generator train and the DC-Link capacitor of the damping converter. Another solution is to modulate active power between the sensitive generator train and the connected variable speed driven train.

Figure 5.5 illustrates the results of a combined electro-mechanical simulation, including a full model of a three-level voltage source converter driving a high-speed compressor induction machine with field-oriented control.

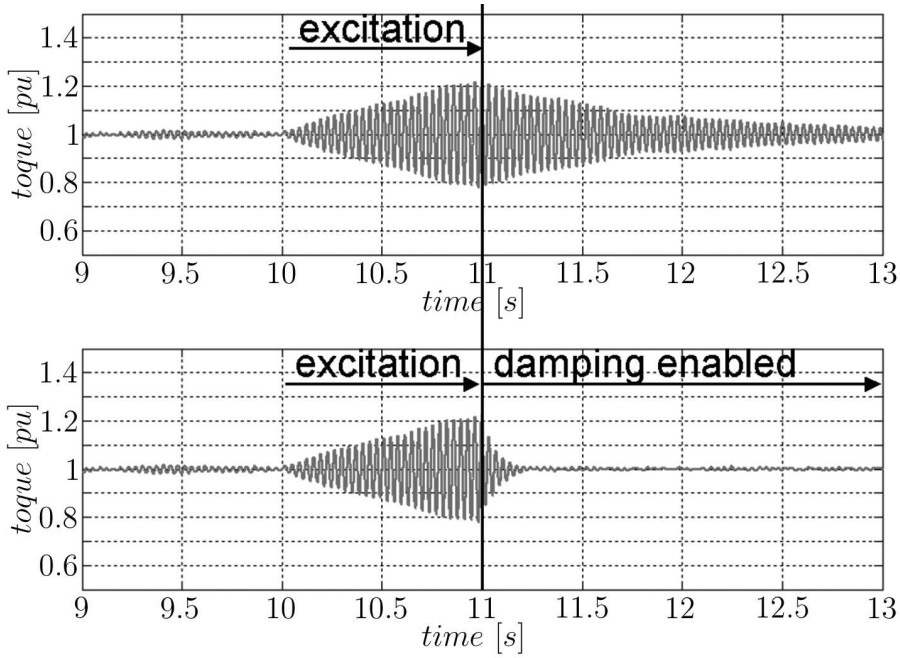

Figure 5.5: Three level voltage source converter driving a high speed induction machine: active damping loop disabled (1) and enabled (2).

The mechanical system is assumed to be excited from the electrical system at a natural frequency between $10s < t < 11s$. Subplot 1 indicates the shaft torque measurement with

a disabled active damping loop. The effective Q-factor is $Q_{eff} \sim 80$, and it is influenced by various control settings, but also by the damping properties introduced with the induction machine slip. In comparison, subplot 2 illustrates results from a simulation with the developed active damping control enabled and implemented as indicated in Figure 5.4. The effective Q-factor is changed to $Q_{eff} \sim 7$ for the total system, as soon as the active damping is enabled ($t > 11s$). This active damping result is achieved with a maximum torque reference modulation of 1%. The system was excited in both simulations with a torque reference modulation of 0.2%.

5.3.2 Line-Commutated Converter Implementation

The line-commutated inverter is still very attractive in the high power range, as explained in Section 2.3.1. The limitation of this design relevant for the implementation of an active damping scheme is the low bandwidth of the implemented controls because of the inherent commutation only once per period and semiconductor. A torsional mode damping implementation for a variable speed application will be demonstrated within this section.

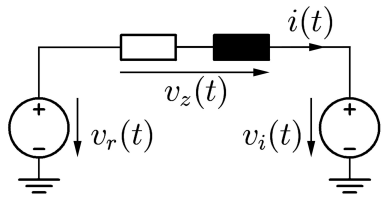

Figure 5.6: Principle voltage and current relation for a load-commutated inverter, with rectifier (r) and inverter (i).

The principle relation between voltage and current for a load-commutated inverter are shown in Figure 5.6. The magnitude of the fundamental voltages on the rectifier and inverter side can be calculated with:

$$v_r(t) = k \cdot V_{ACr} cos\alpha \tag{5.1}$$

$$v_i(t) = k \cdot V_{ACi} cos\beta \tag{5.2}$$

with α as rectifier, β as inverter firing angle,$V_{ACr,i}$ the voltage magnitude on rectifier and inverter side, and $k = \frac{3\sqrt{2}}{\pi}$. The power transferred to the inverter can be calculated with:

$$p_i(t) = u_i(t) \cdot i(t) \tag{5.3}$$

Based on Equation 5.3, an active damping power component with natural frequency Ω can therefore be achieved by modifying the inverter voltage $v_i(t)$ or the DC-link current $i(t)$. The available current control loop would therefore be the preferred point of connection for the active damping loop, but the control bandwidth of the current control loop typically only allows effective frequency modulation in the lower frequency range, up to 5..10 Hz, too low for a general implementation scheme for frequencies in the sub-harmonic range, but easily applicable and therefore preferred for active damping of natural frequencies below these limits.

$d\beta$-Modulation

The inverter voltage can be influenced with the firing angle β, which is typically not derived from a closed loop control, only adapted by looking it up on a table based on the DC-link current magnitude to achieve power factor values which are as high as possible (Section 2.3.1). The dynamic required for the equidistant firing angle control is than realized in hardware. One approach of implementing the active damping loop into a load-commutated inverter control design therefore modifies the β-angle by exchanging a $d\beta$ signal between damping control loop and load-commutated inverter hardware (see Figure 2.15). The $d\beta$ signal is modified based on a signal derived from measurements. The measurement is filtered to contain just the relevant natural frequency Ω of the connected mechanical drive train. Equation 5.3 modified by the $d\beta = \hat{\beta}_0 cos(\Omega t)$ signal can be written as:

$$p_i(t) = k \cdot V_{ACi} cos(\beta + d\beta) \cdot i(t) \tag{5.4}$$

Equation 5.4 is only true with a DC-link current $i(t)$ not influenced by the $d\beta$ modulation for an ideal closed loop current control implementation. A more appropriate implementation of Equation 5.3 when applying $d\beta$-modulation can therefore be formulated as:

$$p_i(t) = u_i(t) \cdot i(t) = (V_{dc} + \hat{v}_\Omega cos(\Omega t)) \cdot (I_{dc} + \hat{i}_\Omega cos(\Omega t + \phi)) \tag{5.5}$$

$\hat{u}_\Omega$ is calculated with:

$$\hat{u}_\Omega = V_{dc} \left| cos(\beta + \hat{\beta}_0) - cos(\beta - \hat{\beta}_0) \right|$$

$\hat{i}_\Omega$ is influenced by the size of the smoothing inductor, but also by the current control performance and can't be written in simple equations. It will be evaluated for different control settings in a subsequent section. The current control performance also influences the source of the modulated power: Two extremes can be derived: (I) ideal current control, constant DC-link current, no energy at the modulation frequency drawn from the "energy

storage" DC-link inductor ($E = 1/2Li^2$), i.e. the damping power comes form the utility grid, and (II) very slow current control, no power exchanged with the power system, complete energy drawn from DC-link inductor. The reality is somewhere in between which is also acceptable because of very limited power requirements for torsional mode damping. The $d\beta$-modulation will only be performed on a small signal base, so as not to influence the normal operation of the drive control and electrical machine. Acting only at the resonance frequency requires very limited power. Neglecting the terms including $\hat{i}_\Omega \cdot \hat{u}_\Omega$, Equation 5.5 can be reduced to:

$$p_i(t) = \{V_{dc} \cdot I_{dc}\} + \left\{V_{dc} \cdot \hat{i}_\Omega cos(\Omega t + \phi)\right\} + \{I_{dc} \cdot \hat{u}_\Omega cos(\Omega t)\} \tag{5.6}$$

The first term in Equation 5.6 represents the steady state operation, the second and third term, the effect of the small signal $d\beta$ active damping power modulation. Sufficient $d\beta$ magnitudes have been found to be below 3^o.

Transmission losses are typically proportional to the square of the current, $p_{loss} \sim I^2$. Therefore, typical high power converter designs have relative high voltage vs. current ratios, up to $V_{DC}/I_{DC} < 8$ are typical for load-commutated inverters in the $> 10\ MW$ range for variable speed applications. For this reason, the second term $V_{dc}\hat{i}_\Omega cos(\Omega t + \phi)$ in Equation 5.6 can have significant influence on the active power modulation, even if it is not initially desired.

A phasor representation can be chosen to quantify the impact of the two active power components in Equation 5.6; both components depend only on the natural frequency Ω.

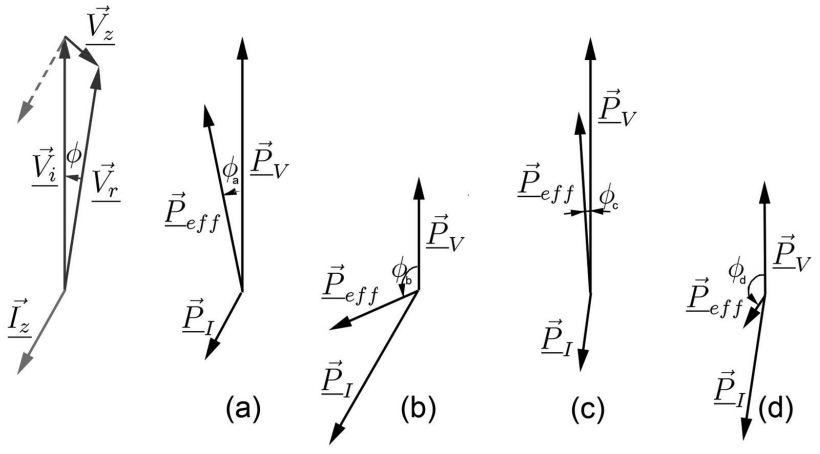

Figure 5.7: Phasor diagram representing the two relevant power components identified in Equation 5.6.

Different effects on the modulated power $\vec{P}_{eff}$, derived in Equation 5.6 can be observed

in Figure 5.7. The different length of the voltage and current phasor $\underline{\vec{V_i}}$,$\underline{\vec{V_r}}$ and $\underline{\vec{I_z}}$ can be explained by possibly different operation conditions for variable speed drives. The terminal voltage of the electrical machine is typically proportional to the rotational speed, to achieve constant flux operation; the motor current is proportional to the mechanical torque. Phasor diagram (a) can be applied for operations close to nominal speed, with relatively large $\underline{\vec{V_r}}$ magnitudes. (b) can be applied to low speed, high torque applications. The angle ϕ depends on the DC-link impedance, but also on the current controller settings. Faster current control results in smaller ϕ angle values. (c) repeats case (a); (d) repeats (b) for smaller ϕ values. The modulated damping power is almost negligible for case (d), which is not a serious limitation, as this operation point is an exception in the high power range. Figure 5.8 indicates the relative effects on modulation power components and effective damping power for a given modulation angle (e.g. $d\beta = 2^o$) with different control settings and operation conditions, and for a specific drive train application. The resulting values are normalized to the maximum achievable value. It is obvious, that the influence of the applied torque on $V_{dc}\hat{i}_\Omega cos(\Omega t + \phi)$ is small compared to the influence of speed and current control settings on the same damping power component. The current control performance of the power electronic converter is indicated with $CtrlSetD$: The performance is varied between $D = 0.5$ for fast or aggressive current control action and $D = 0.9$ for comparable slow current control action. The current control performance observed in field measurements with large line commutated inverter systems is mostly between these two settings, and typically much closer to the slower performance assumption.

The effective damping characteristic depends mainly on the rotational speed and the current control performance for the investigated design; it could look different with variations in the drive design. The current control setting is typically fixed for a certain drive train arrangement, and not the full toque-speed characteristic is applicable for typical load characteristics.

A summary of the phasor diagram Figure 5.7 and Figure 5.8 is presented in Figure 5.9, with the predicted effective damping mesh and the measured effective damping power for the different operation points during the string test of a $30MW$ drive train.

Even more than the magnitude of the active power $\underline{\vec{P}_{eff}}$, the different phase relations between the reference modulation angle in phase with $\underline{\vec{V_i}}$ and the angle of the effective modulation angle in phase with $\underline{\vec{P}_{eff}}$ must be considered in the design of the damping control, effecting the overall delay time to achieve the optimum damping at a phase lag of $+\frac{\pi}{2}$, (see Equation 4.4). Figure 5.3 shows the different components in the closed loop influencing the phase delay. Figure 5.10 illustrates the effect of speed and torque on the calculated delay at different operation points. The delay time (phase shift) is the most

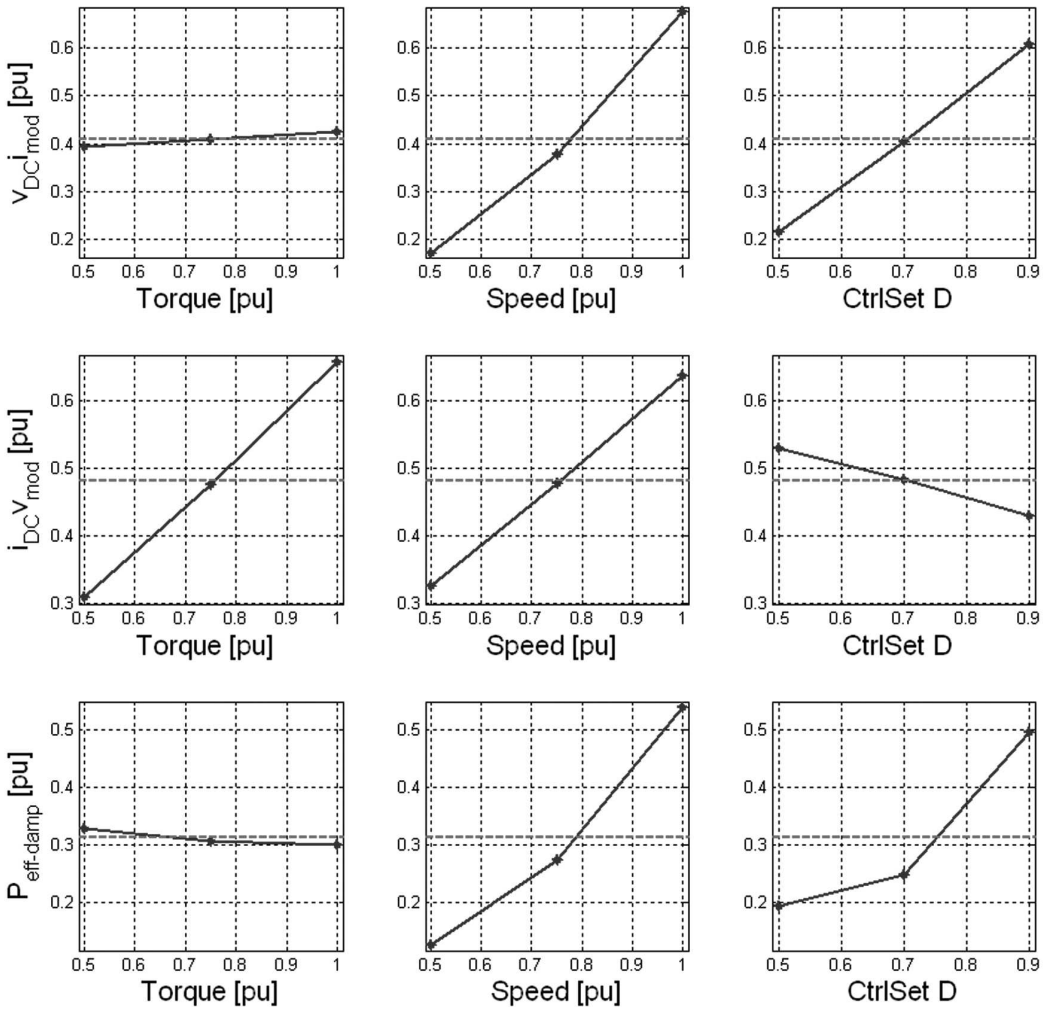

Figure 5.8: Experimental Setup result with full factorial design: Influence of torque, speed operation points and control-settings on the modulation power components Equation 5.6 and the resulting effective damping. Mean values are indicated with dashed lines.

important parameter for optimum performance of the damping loop. The characteristic was calculated and successfully applied to a $30MW$ compressor drive train with extended variable speed operation and comparably slow current control settings. The variation t_{var} corresponds to a significant variation in phase of $\sim 105^o$.

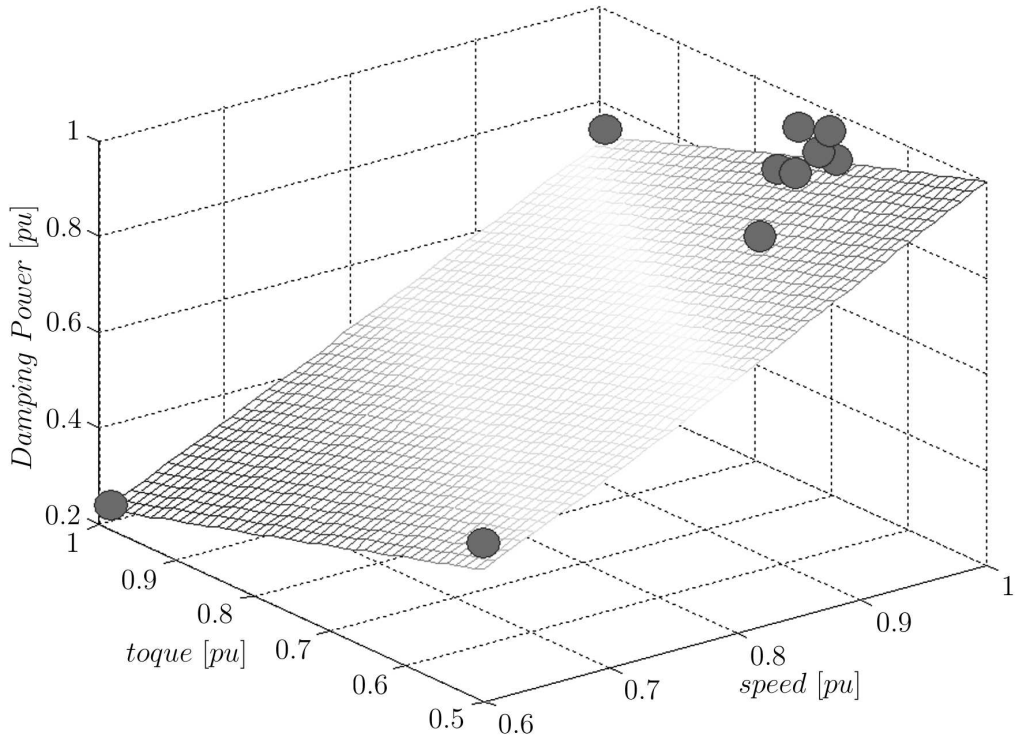

Figure 5.9: Predicted damping power $P_{damp} = f(v, T)$ and verified operation points (gray dots) for a $30MW$ drive train, with comparably slow current control settings ($D_c = 0.9$) of the drive system.

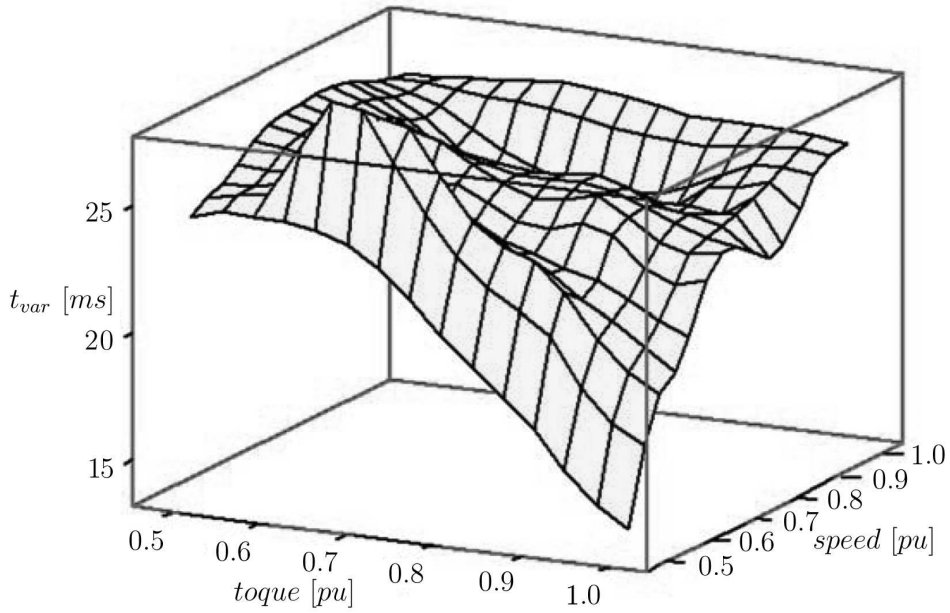

Figure 5.10: $t_{del} = f(T, v)$, required delay in the damping control for optimum damping performance

Modulation Signal Characteristic

Another important aspect to be considered for a $d\beta$-modulation implementation in a load-commutated inverter is the fact that the β-angle is typically as high as possible because of the relation to the power factor (Equation 2.39). A sufficient margin for commutation needs to be considered because of the commutation overlap angle μ and extinction delay angle δ to prevent re-conduction of the "turned off" semiconductor. A typical maximum for the β-angle is between 140^o and 155^o, dependent on the semiconductor used, the commutation inductance and the current to be commutated. This requirement makes it necessary to modify the modulation signal $d\beta$ to act only in one direction, away from the operational limit.

Two different shapes have been identified as applicable for the control scheme, which has been developed: (a) ideal sine waveform modulation and (b) half sine wave modulation, cutting the negative components of a pure sine wave. Both modulation signals have advantages, the ideal sine waveform in the frequency domain, and the half-sine wave modulation in the implementation.

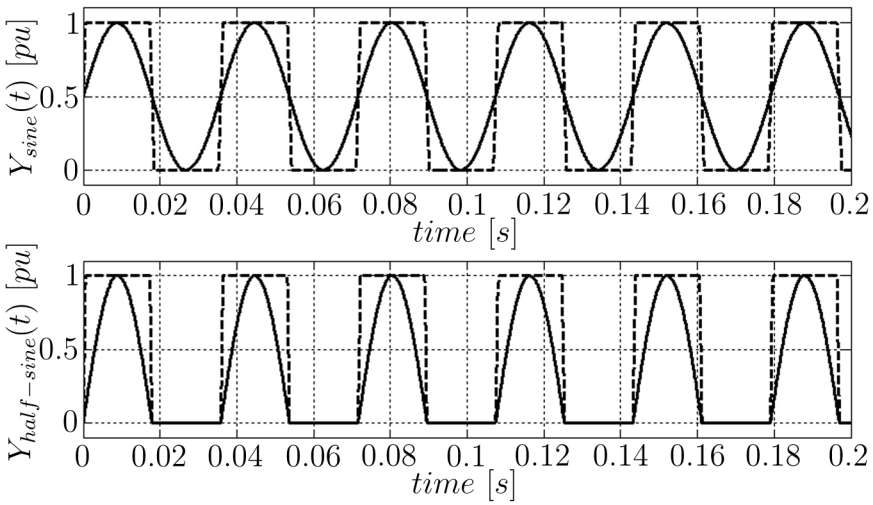

Figure 5.11: Time domain modulation signal for unipolar $d\beta$-modulation. Subplot 1: Ideal modulation waveform, dashed: Modulation signal in saturation. Subplot 2: Half sine wave modulation, dashed: Modulation signal in saturation. Amplitudes normalized to $\hat{y} = 1$.

The pure sine wave, as indicated in Figure 5.11, upper plot, consists of two parts: An AC and a DC-part, which has to be adapted based on the amplitude of the alternating part (Equation 5.7).

$$Y_{sin}(t) = \frac{\hat{y}}{2} + \frac{\hat{y}}{2} sin(\omega_0 t) \tag{5.7}$$

The frequency domain for this plot can be identified in Figure 5.13, upper left plot. The DC-offset is responsible for a very limited modification of the power angle, dependent on the required damping power Figure 5.12.

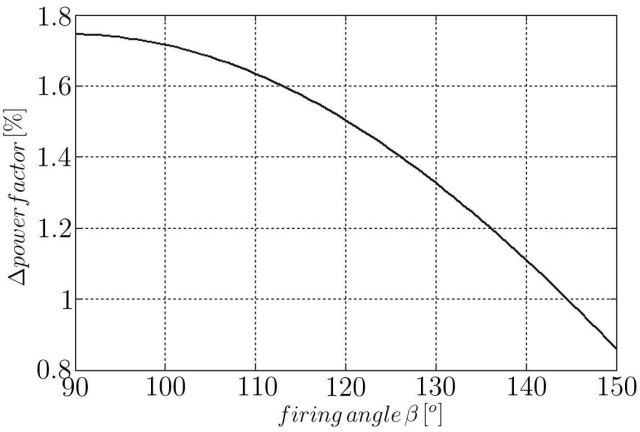

Figure 5.12: Influence of DC-offset on effective power factor, maximum damping power with an allowed modulation angle of 2^o assumed.

The second, easier to implement, alternative can be seen in Figure 5.11, lower plot, which can be analyzed by calculating the Fourier series, resulting in:

$$Y_{half-sin}(t) = \frac{\hat{y}}{\pi} + \frac{\hat{y}}{2} sin(\omega_0 t) - \frac{2\hat{y}}{\pi} \sum_{k=1}^{\infty} \frac{cos(2k\omega_0 t)}{(2k-1)(2k+1)} \tag{5.8}$$

The DC-component in the modulation signal is reduced, but there are additional, even harmonics produced, e.g. the 2^{nd}, 4^{th}..., see also Figure 5.13, lower left characteristic. This can be a clear disadvantage, e.g. in case that the second natural frequency is exactly two times the first natural frequency. The signals shown in Figure 5.11 demonstrate only a snapshot of the modulation signal. The real modulation signal changes the magnitude dynamically, dependent on the alternating torque magnitude in the mechanical shaft. They can reach lower, but also higher magnitudes, which then result in a saturated signal waveform unless an anti-windup is implemented. Figure 5.11 gives an idea of saturated signal waveforms (dashed lines). The saturated waveform results for both proposed shapes, in case of an infinitely high gain, into a pure rectangular shape with its Fourier series:

$$Y_{sat}(t) = \frac{\hat{y}}{\pi} + \frac{2\hat{y}}{\pi} \sum_{k=1}^{\infty} \frac{sin((2k-1)\omega_0 t)}{2k-1} \tag{5.9}$$

This waveform includes only odd harmonics, e.g. 3^{rd}, 5^{th}.... Figure 5.13, upper and lower right, shows the resulting harmonics for the two proposed waveforms in saturation.

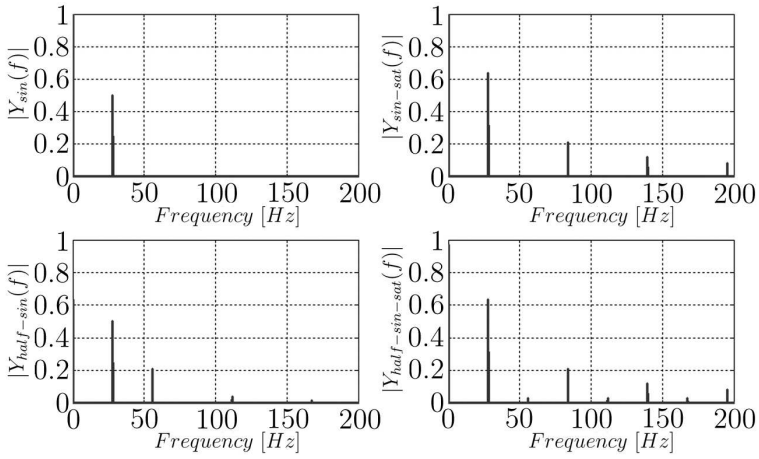

Figure 5.13: Frequency domain of the signals introduced in Figure 5.11. Amplitudes are normalized to $\hat{y} = 1$.

The characteristic of the harmonic content in the modulation signal is shown for an increasing degree of saturation in Figure 5.14. It can be seen that the amplitude of the fundamental frequency also increases with increased saturation degree.

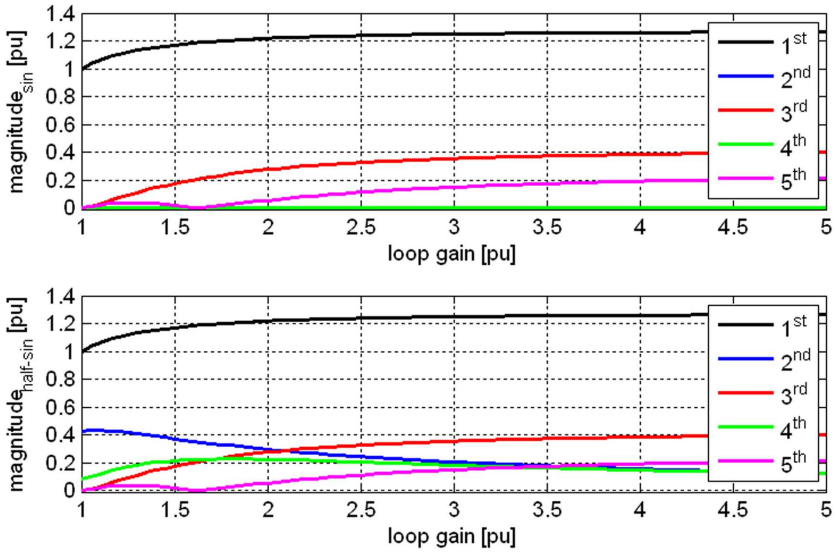

Figure 5.14: Harmonics content in the modulation signal, dependent on the degree of saturation. An amplitude of $\hat{y} = 2$ is applied for the modulation signal to "start" with "1" for the first (desired) harmonic in the not saturated case.

Both options have been tested (e.g. sine - Figure 5.24, half sine - Figure 4.7), and show similar performance, as long as no sensitive natural frequency is coincident with a multiple of another natural frequency of the mechanical system. An anti-windup - scheme could be implemented to avoid the saturation, with the cost of additional control loop complexity.

Implementation Optimization

Both described LCI-implementations can be optimized. The significant components of the active power in the DC-link have been identified in Equation 5.6, with two relevant active damping power terms relevant for the phase and performance in the active control loop. The term

$$V_{dc} \cdot \hat{i}_{\Omega} cos(\Omega t + \phi) \tag{5.10}$$

is initially not desired because of the difficulty in predicting the impact of the current controller on this term. One way to eliminate this effect is to modulate not only the β-angle, but also the α-angle to achieve a DC-link current not influenced by the $d\beta$-modulation and a resulting non-observability for the current control loop. The goal is to achieve a constant voltage across the DC-link inductor $v_z(t)$, (Figure 5.6) to achieve a DC-link current not influenced by the active power modulation at the natural frequency.

$$v_z(t)|_{\Omega} = const \tag{5.11}$$

The α-angle modulation needs to be adapted based on the effective β-angle to achieve a constant current, and can be derived based on Equation 5.1 and 5.2, for small signal variation calculated with:

$$\frac{dv_r(t)}{dt} = \frac{dv_i(t)}{dt} + \frac{dv_z(t)}{dt} \text{ with } \frac{dv_z(t)}{dt} = 0 \tag{5.12}$$

resulting in:

$$d\alpha = \frac{V_{ACi} sin(\beta)}{V_{ACr} sin(\alpha)} d\beta \tag{5.13}$$

A disadvantage is the need for a second interface to the drive control, i.e. additional hardware. Figure 5.15 shows the effective damping power with α- and β-modulation applied for the given LCI configuration. The effective damping is significantly increased, even though the current ripple is not reduced to zero, as based on theory. There is still an effective damping variation with speed variation, $V_{dc} \cdot \hat{i}_{\Omega} cos(\Omega t + \phi)$, but reduced by factor of two compared to the base case.

More important than the effective damping is the variation in phase for different operation points (Figure 5.10). This influence is compared to the base scenario reduced by a factor of 5 to $\sim 22^o$ phase variation for all control settings, for the slow control settings by a factor of 10, resulting in $\sim 12^o$ phase variation over the whole operation range. Another approach to reduce Equation 5.5 to only one term is to utilize only the α-angle. This approach would bring theoretically the $I_{dc} \cdot \hat{u}_{\Omega} cos(\Omega t)$ term to zero.

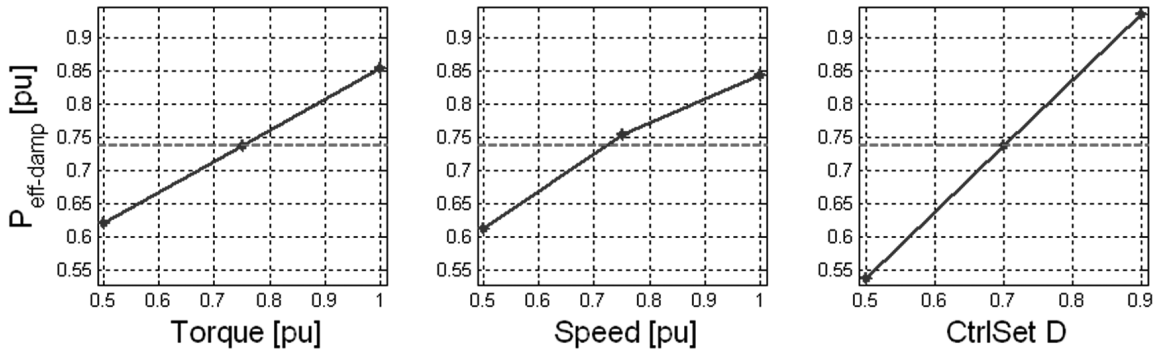

Figure 5.15: Influence of different operation conditions and control settings on effective damping, α- and β-modulation as described in Equation 5.13. Same base case as with pure β-modulation.

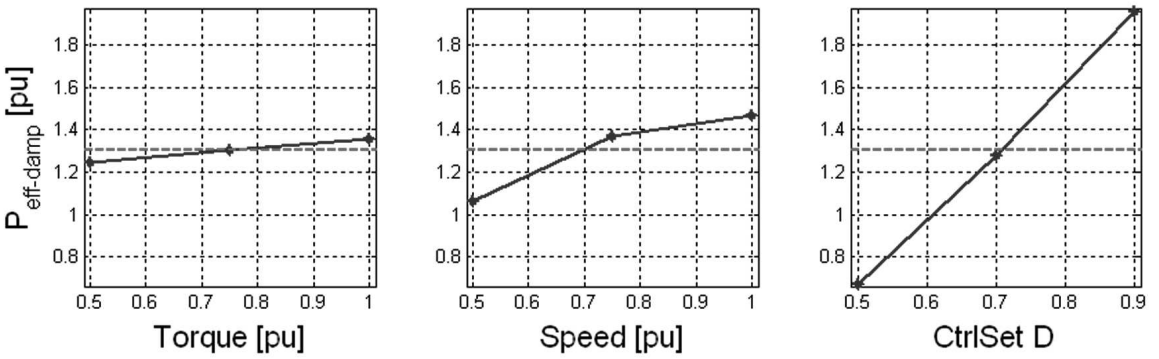

Figure 5.16: Active damping with pure α-angle modulation applied. The $I_{dc} \cdot \hat{u}_{\Omega} cos(\Omega t)$ component is significantly reduced. The shown effective damping is better than with pure β-modulation, but does not include relevant power system effects.

Figure 5.16 shows the trend of a pure α-angle modulation, but without any effect of the power system strength, which would a) reduce the damping effect on the machine side, and b) potentially excite power generation units in the power system, if their natural frequency is close to the modulation frequency. The damping effect with α-angle-modulation depends strongly on the current control settings, as the α-modulation is a disturbance for the current controller.

Figure 5.17 indicates the result of applying the active damping with current reference modulation, which is typically not available because of limited bandwidth for large drive trains. The current control setting slightly influences the effective damping performance: As higher the control bandwidth, as better the damping performance. Basically, this is the only variation in which the current control does not fight against the modulation

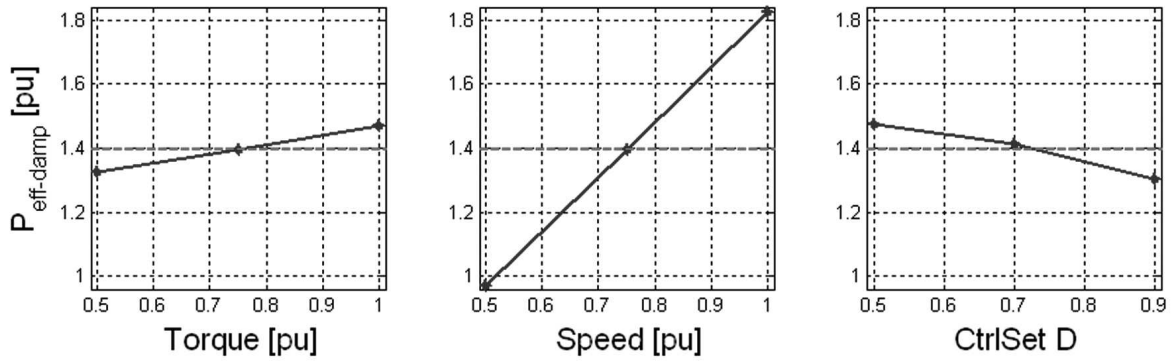

Figure 5.17: Active damping utilizing current reference modulation. The results are similar to the alpha angle modulation; the effect of different control settings is almost eliminated.

required for the active damping purpose. The effective phase variation is, with 27^o for the whole operation range and 6.2^o for one set of control settings, very low compared to the beta modulation. The question to be answered, also for this variation, is how much damping power will be modulated with the electrical motor, and how much modulated power is exchanged with the power system.

The results, with variations in the implementation, have shown that both components (Equation 5.6) always act on the effective damping, but with different impact. Modifying the α-side firing angle (by modifying the current reference or directly the α-angle) seems to be more effective, with the uncertainty of the influence of the power system on the effective damping and the potential excitation of power generation units in the power system. The significant advantage is the reduced effect of phase variation when using the α-side firing angle modulation, which could be important for units, which operate in a wide operation speed range. But the phase variation can be compensated in monitoring the operational speed and torque values when using pure β-modulation.

Control Loop Operation

A very good performance of the damping device during operation at critical speeds can be observed in simulation and measurements (Section 5.5, 5.5.2, 5.5.3). The damping loop also causes some steady-state alternating torque levels next to those at critical speeds, but they do not affect the lifetime of the shaft at all. It might be possible to reduce or eliminate these unnecessary torque components. One advantage of having the damping device permanently enabled is that it gives a direct feedback on the status of the damping loop. A malfunction of the damping circuit can easily be detected, e.g. by observing the combined beta angle signal, and countermeasures could be taken to avoid operation at

critical speeds during the down time of the damping loop.
Eliminating the effect of the damping loop for operational points away from critical conditions can be achieved by disabling the damping loop in those conditions. One approach is to utilize a speed measurement to activate the damping loop around critical speeds, which is easy to implement, but relies on an additional speed measurement. Calculating an RMS equivalent of the measured shaft torque and applying a hysteresis for enabling and disabling of the damping loop is a potential solution, but it can easily result in undesirable non-continuous operation with beating torques close to critical speeds.
Having the damping loop permanently enabled is the preferred way of operation, because of the advantages described before. There is no harm to the drive train in this mode of operation, and it reduces the complexity of the overall damping control loop.

Control Loop Gain

Another optimization degree of freedom is the closed loop gain of the damping loop. Two operational conditions can be distinguished: (a) operation at a high alternating torque level, e.g. at critical speeds, and (b) operation at a small alternating torque level. High damping loop gain is desired in (b), as it is difficult to distinguish between enabled and disabled operation of the damping loop in this condition. The proportional characteristic of the damping loop results in relatively large output signals for condition (a); the loop often operates at the fixed limits. A lower gain could be desired for this operation condition, to reduce the amount of harmonics produced due to saturation (Figure 5.14). Increased modulation margin, e.g. instead of 2^o an interface with 5^o, would be advantageous for the active damping loop, but would possibly affect the steady state operation of the converter. A useful optimization could therefore be to adapt the effective gain for the integrated torsional mode damping device in an inverse proportional behavior to the RMS equivalent of the measured shaft torque.

5.4 Independent Protection

Active damping utilizing the natural frequency of a sensitive mechanical drive train is very powerful, but can also be dangerous if applied incorrectly, with a wrong phase adjustment. Although the modulated power is limited to small values, the corresponding alternating torques can cause mechanical damage if continuously applied over a long time. An independent protection algorithm is therefore applied to disable the active damping loop for alternating mechanical torques, which are higher than a specified threshold. The threshold is a value that should not be reachable for a correctly working damping loop.

The proposed and tested algorithm implemented into an embedded control can be formulated with:

$$T_{lim} > \frac{1}{T_s} \sum_{n=0}^{\infty} \left[\left(\frac{T_n \cdot k_t}{2^8} \right)^2 - T_{sav} \right] \tag{5.14}$$

The algorithm results in a time-dependent protection limit (Figure 5.18). The relevant constants are the controller sampling time T_s, T_{sav} and k_t considering e.g. the signal resolution applied in the real-time controller, and a maximum allowable alternating torque, e.g. $T_{lim} = 50kNm$. The controller continuously calculates the torque T_n over time (Equation 5.14) and compares it with the adjusted limit T_{lim}. Exceeding the limiting value is used to disable the active damping control.

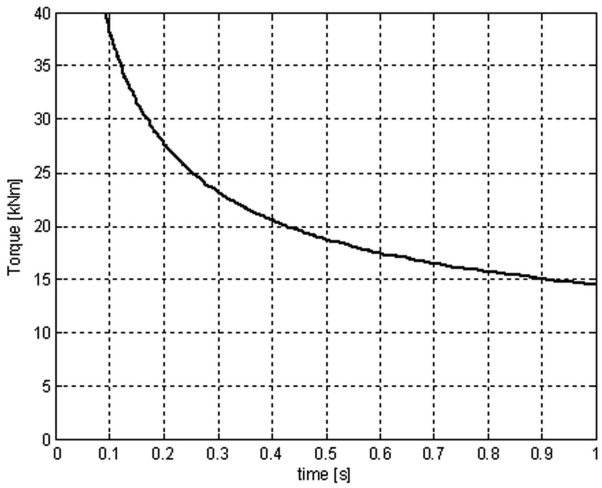

Figure 5.18: Time-dependent protection limit for the alternating torque value T_{lim}. Every calculated value above the limit triggers the damping control loop to be disabled.

The implementation of the active damping scheme into existing line-commutated inverters with high-rated power was successfully tested with LCI designs of three different suppliers.

5.5 Application Examples

Several industrial application examples with potential torsional interaction are discussed within this section. A comparison of operation with and without active damping is performed with appropriate simulations and validated against measurements performed in several tests with multi-megawatt drive trains.

5.5.1 Damping Results for Variable Speed Drives

The successful application of the developed damping method for large industrial drive trains is an important achievement within the thesis. The various implementation steps have been discussed in previous sections. Simulation results for a $30MW$ drive train will now be discussed and compared to measurements. An LCI produces variable pulsating torque components in variable speed operation, based on Figure 2.19. The effect on the mechanical drive train will be shown in the following simulation and measurement results.

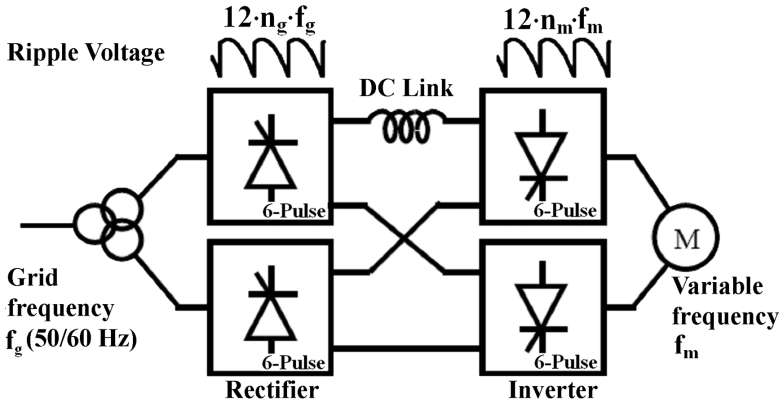

Figure 5.19: 12/12-Pulse LCI design feeding a 6-phase synchronous motor

A single line diagram of the electrical system investigated within this subsection is given in Figure 5.19. A 12-pulse LCI is utilized to allow operation in a wide speed range of 50% to 105% of nominal speed at nominal torque. Several critical speeds are within this operation range.

Figure 5.20 illustrates the reaction of the mechanical system to a constant speed ramp with 2.5 rpm/s when running through a critical speed (speed = $0.952p.u.$). The alternating torque amplitude increases before and after the resonance point, as the quality of the resonance is not infinite. The magnitude of the alternating torque and therefore the stress level depends on the speed ramp applied. A lower speed ramp results in more periods of excitation at the natural frequency; higher magnitudes can be observed. In the given arrangement, the magnitude already exceeds the allowed continuous alternating torque level of the coupling. The speed reference is usually set by the process, e.g. by the required operational temperature and pressure of a Liquid Natural Gas compression train. Running through critical speeds or even operation at critical speed can therefore not always be prevented for variable speed operation (Campbell Diagram - Figure 3.1), with potential negative effects for the mechanical drive train. The alternating torque

does not continuously decrease after passing the natural frequency, which is caused by the interharmonic content with increasing frequency: A beating effect excites and damps the torsional oscillation depending on the phase relation between the harmonic, which increases in frequency, and the present torsional oscillation at the mechanical natural frequency. The effective alternating torque decreases with increasing distance between the interharmonic frequency and the natural frequency of the mechanical system.

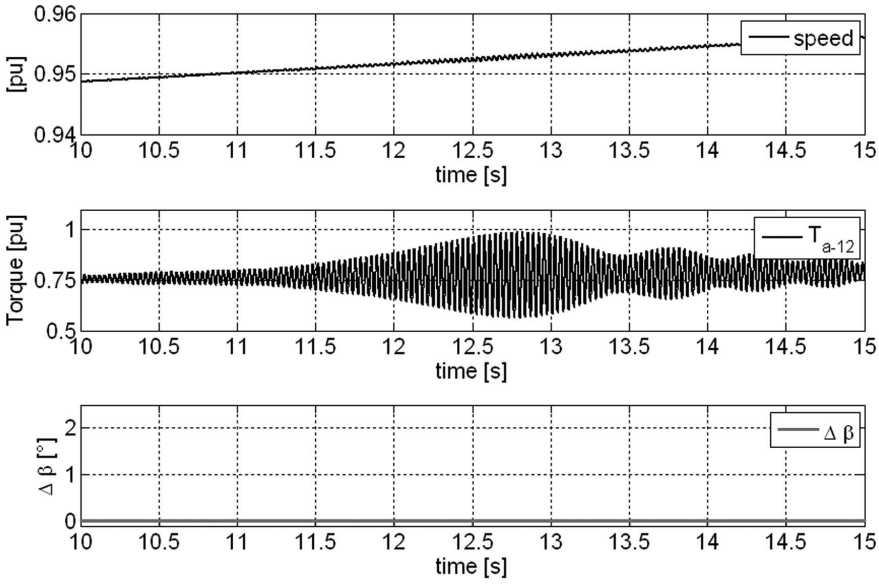

Figure 5.20: Simulation result: Variable speed operation of an electrically driven drive train. An increased level of dynamic torques can be detected while passing a critical speed.

A waterfall calculation applied to the mechanical torque enables the identification of the interharmonics responsible for the torsional interaction - Figure 5.21. The abscissa axis represents the time measured in seconds, the ordinate axis the frequency content and the color in the diagram represents the amplitude of the frequency components, with larger amplitude for colors with larger wavelength. It can clearly be seen, that the electrical frequency component with $|12f_g - 12f_m|$ crosses the natural frequency at $29Hz$, resulting in high alternating torque components at that frequency around $t = 12s$. Running through a critical speed with the same ramp as before, but with torsional damping device enabled after $t = 12.5s$, is investigated in Figure 5.22 and Figure 5.23. The damping device would typically always be enabled during operation; this run is only for demonstration of the damping performance. The alternating torque at natural frequency is almost gone after activation of the damping device. A kind of "white noise" around the critical speed can be identified in the frequency plot.

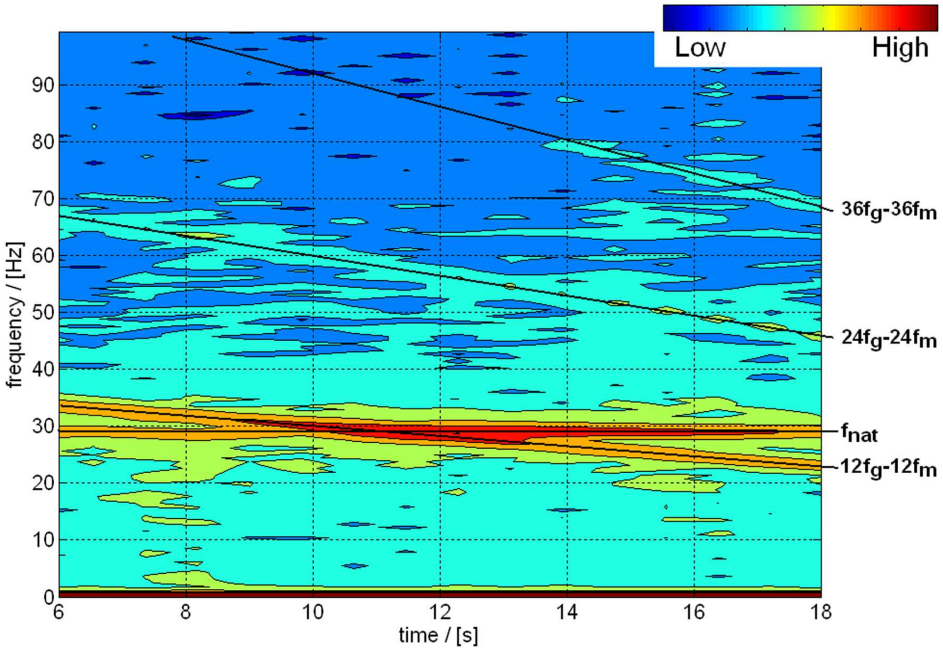

Figure 5.21: Waterfall diagram of the shaft torque while running through a critical speed.

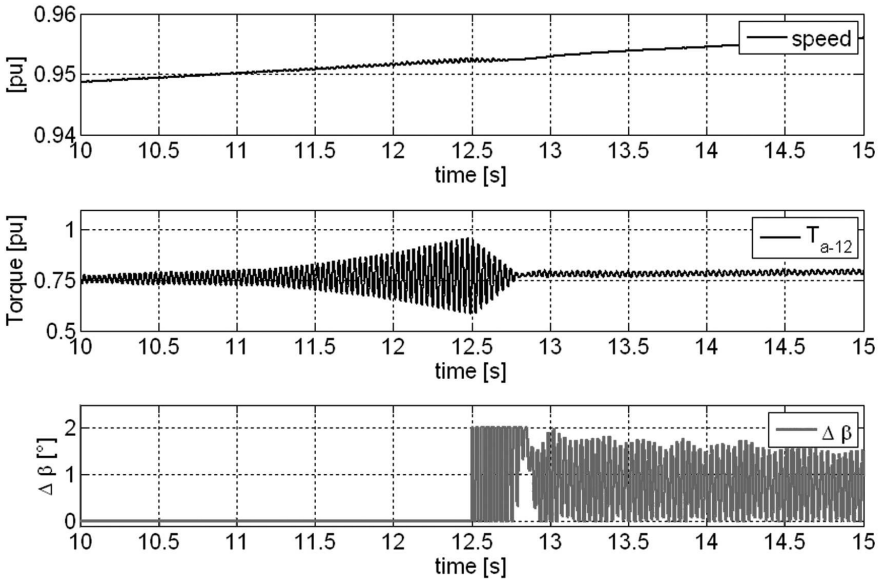

Figure 5.22: Simulation result: Variable speed operation of an electrically driven drive train. An increased level of dynamic torques can be detected while passing a critical speed. Active damping, enabled after 12.5s, decreases the dynamic torque components significantly over time.

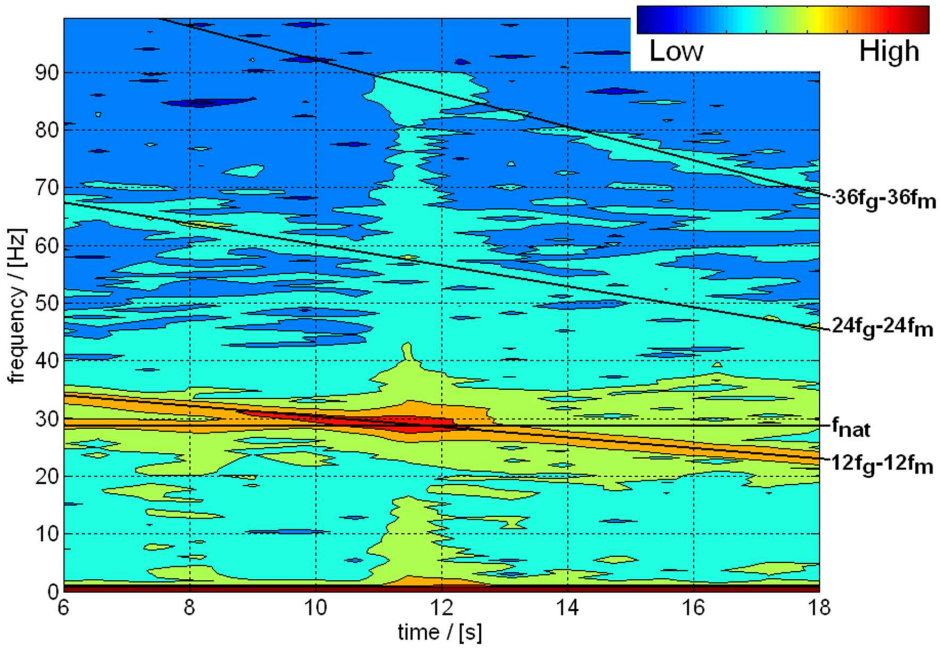

Figure 5.23: Waterfall diagram of the shaft torque while running through critical speed, with active damping enabled for $t >= 12.5s$.

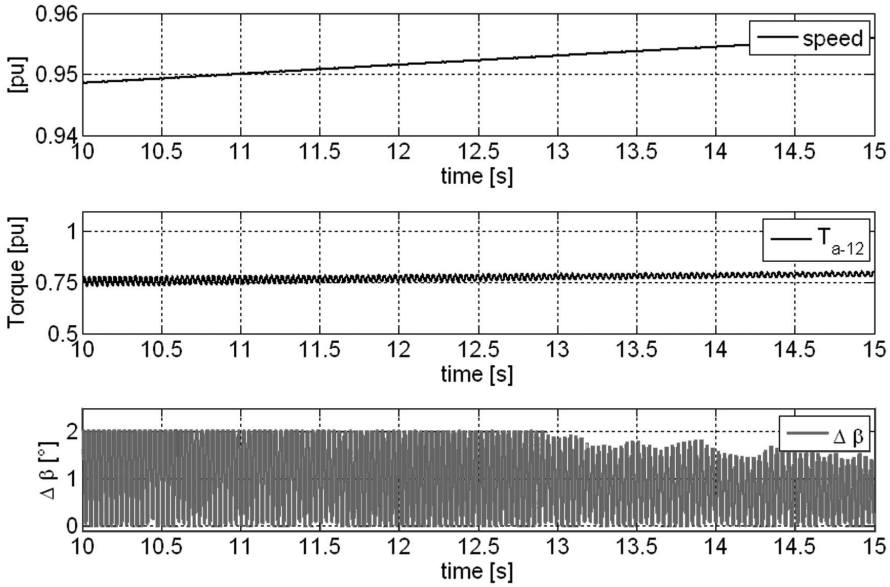

Figure 5.24: Simulation result: Variable speed operation of an electrically driven drive train. Passing critical speed does not impact the level of dynamic torques.

The run through critical speed with damping fully enabled is shown in Figure 5.24. The alternating torque is limited to a value well within the limits set for permanent operation. The same series of runs has been performed with a real $30MW$ synchronous motor driven compressor train during a string test. The effective alternating torque corresponds well to the simulated result shown in Figure 5.20.

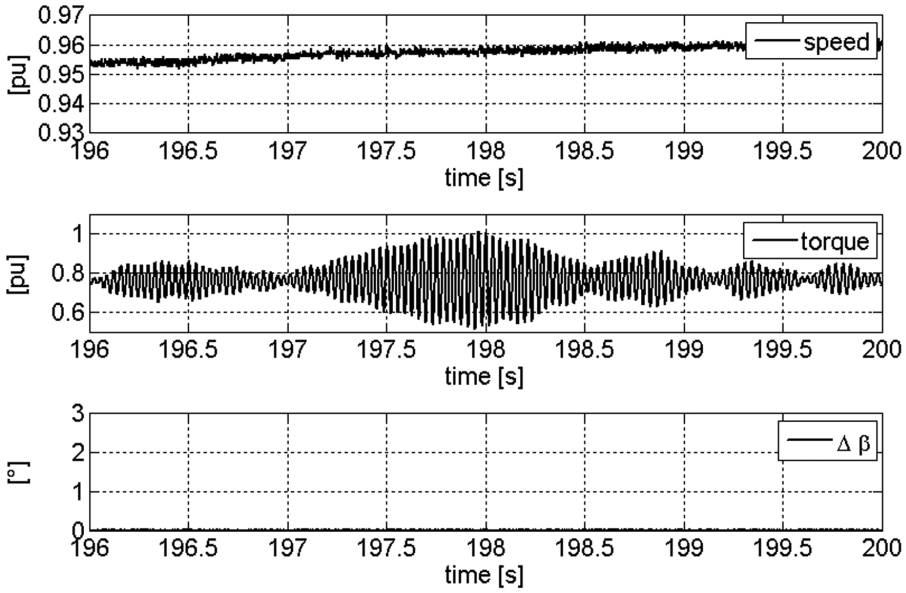

Figure 5.25: Measurement result: Variable speed operation through critical speed (below nominal speed): The dynamic torque level is increasing to unacceptable values.

Figure 5.25 illustrates the run through a critical speed with the damping device disabled. The alternating torque is increasing to unacceptable values within a second. The same run performed with active damping enabled is shown in Figure 5.26. The alternating torque is significantly reduced. The reduction is lower than in the simulation because a lower gain has been applied in the tests. Such strong damping effects are not required in real systems. The damping device is meant to provide additional damping at critical speeds to be able to run through, or even at critical speed while staying well below the alternating torque limit of the drive train, and not reducing the alternating torque to zero. The difference between simulation and reality can be found with different gains in the damping control loop, but is also due to the existence of additional "converter torque noise" in the real system, e.g. due to switching effects, which have been measured in all operation conditions. Lower alternating torque could be achieved with higher damping power and higher gain in the damping loop. The string tests performed with a $30MW$ compression train with ITMD control also included fault analyses for the damping control.

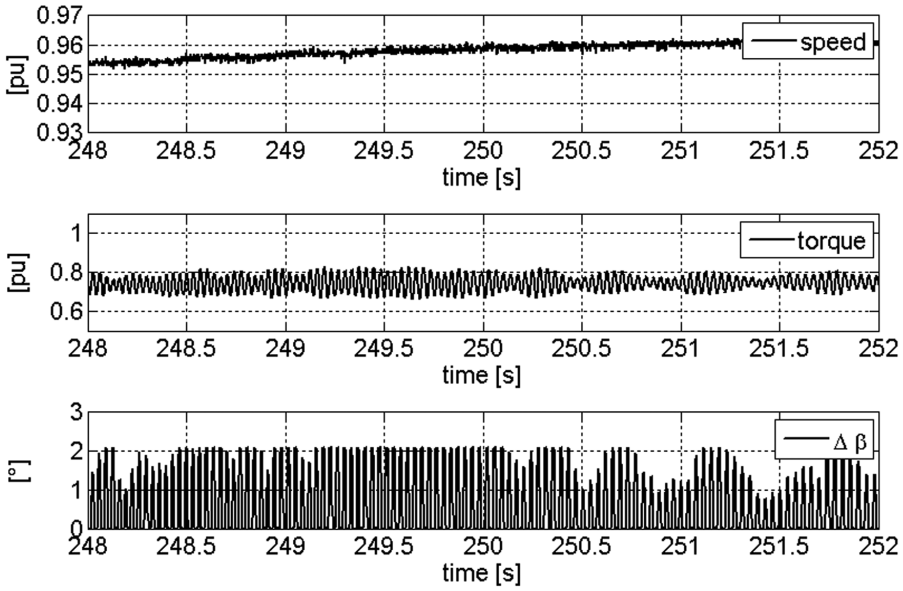

Figure 5.26: Measurement result: Variable speed operation through a critical speed (below nominal speed) with active damping enabled: The dynamic torque level is well within the limits.

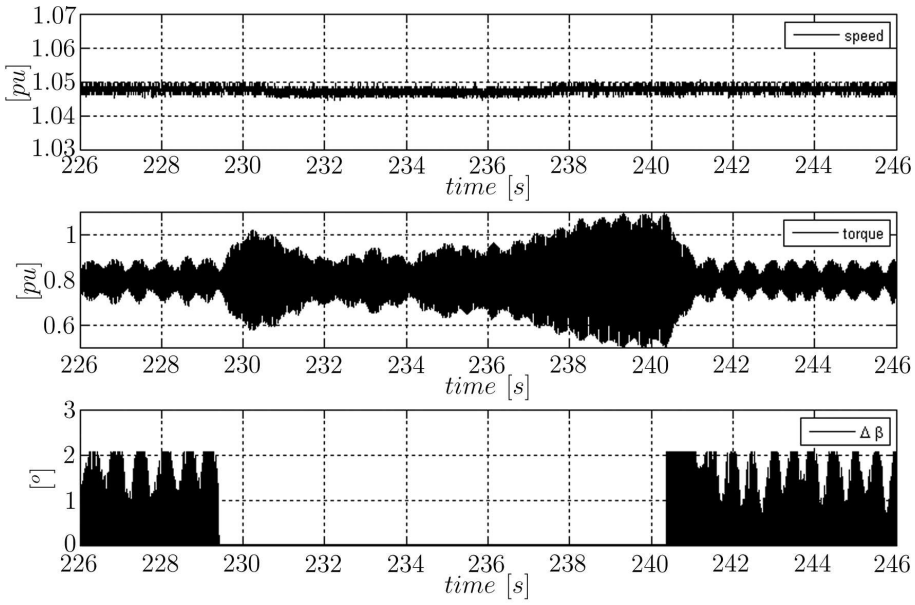

Figure 5.27: Measurement result: Operation at a critical speed with and without active damping enabled.

For instance as shown in Figure 5.27, the effect on the dynamic torque value when operating the train at a critical speed and the ITMD control is switched off for a few seconds and

then back on. In this experiment, the speed reference was kept at a constant value. The exact actual speed strongly influences the dynamic torque amplitude during resonance excitation, but only during the $11s$ for which the ITMD control was turned off. When the ITMD control was reactivated at $t = 240.3s$, less than one second was needed to damp the dynamic torque components down to values that are well within the alternating torque limits of the shaft. The damping device enables the large drive train to operate even at critical speed without any reduction in lifetime of the mechanical train.

5.5.2 Active Damping in Island Power Systems

The probability of torsional interaction between power electronic devices and large rotational machinery depends on (a) the Q-factor of the sensitive drive train and (b) the probability of excitation by harmonics at the natural frequency with sufficient magnitude [53]. Item (b) is influenced by (I) the ratio of the installed power of power electronic devices to the nominal power of electrically close power generation units, (II) the percentage of the harmonics produced at nominal power, but also (III) the power system environment around the disturbance source. (I) and (II) are most relevant in island or island-like power systems, because of the level of harmonics and interharmonics which excite electrically close-coupled power generation units. Significant influence on (III) can be expected from the short circuit ratio (SCR) of the external power system, compared to the SCR of the local system. The effect of the external power system strength on the disturbance power is indicated in Figure 5.28.

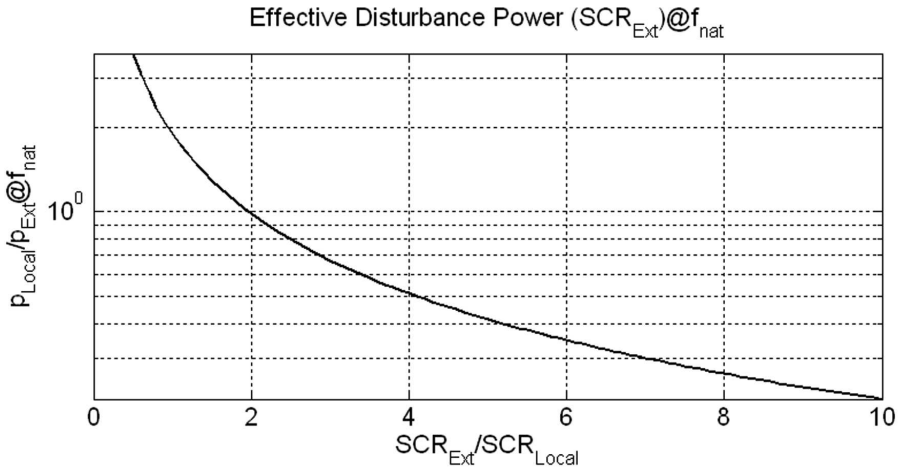

Figure 5.28: The effect of the disturbance power as a function of the short-circuit ratio of the external power system to the local short circuit ratio.

A large external power system (high SCR_{Ext}/SCR_{Local} -ratio) absorbs most of the distur-

bance, and hence reduces the probability of exciting local generation units. On the other hand, there is a high probability that island-like systems with weak interconnections will be excited by local power electronic devices. Another important factor to (III) is the type of load connected to the island-like power system. A typical load can be of the constant impedance type (Z, $P \sim V^2$), constant current type (I, $P \sim V$) or constant power type (P). A way of representing the characteristic is to use a polynomial representation:

$$P = P_0(p_1 V^2 + p_2 V + p_3) \tag{5.15}$$

$p_1..p_3$ are constants defining the proportions. A load frequency dependency is not relevant for the effect on the disturbance power. Industrial systems usually achieve a high penetration of power electronic loads with characteristics of constant current (LCI) or constant power (VSC). These loads typically do not affect the disturbance power, except for control interaction problems known especially for constant power operation. Constant impedance loads can interact with the disturbance power contribution, mainly by absorbing and hence reducing the effect of excitation, as the voltage is distorted by the disturbance power.

An exemplary torsional vibration measurement performed on a synchronous generator shaft (Figure 5.29) illustrates the sensitivity of power generation units for torsional interaction.

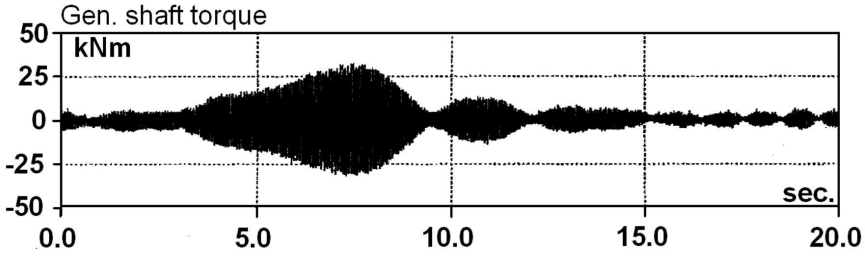

Figure 5.29: Alternating torque measurement on a generator shaft in an island like power system (Figure 3.2) [7].

Torsional interaction in an island-like power system can be counteracted with the two approaches described in Subsection 5.2 and 5.3. The effectiveness of the counter-measure on the rotational drive train is also influenced by the described factors. The effect can be improved with an installation as electrically close as possible to the sensitive generator so that the damping power is as least as efficient as the disturbance source.

Redundant operation in island-like environments requires $n + 1$ generating units for n redundancy. Figure 3.2 shows a typical arrangement, with two identical generators (Main

Generator A and B) connected to one bus. Increasing the damping behavior of a single generator is already shown; two, or in general n, generators of the same type act in the same way in case of a harmonic excitation. Not fully identical units are more common in real applications and will be investigated in this section. The mechanical system of generator B is analyzed in Section 2.1.5 - Figure 2.9. The mechanical system of generator A is assumed to have its first natural frequency 1.5% below generator B's first natural frequency.

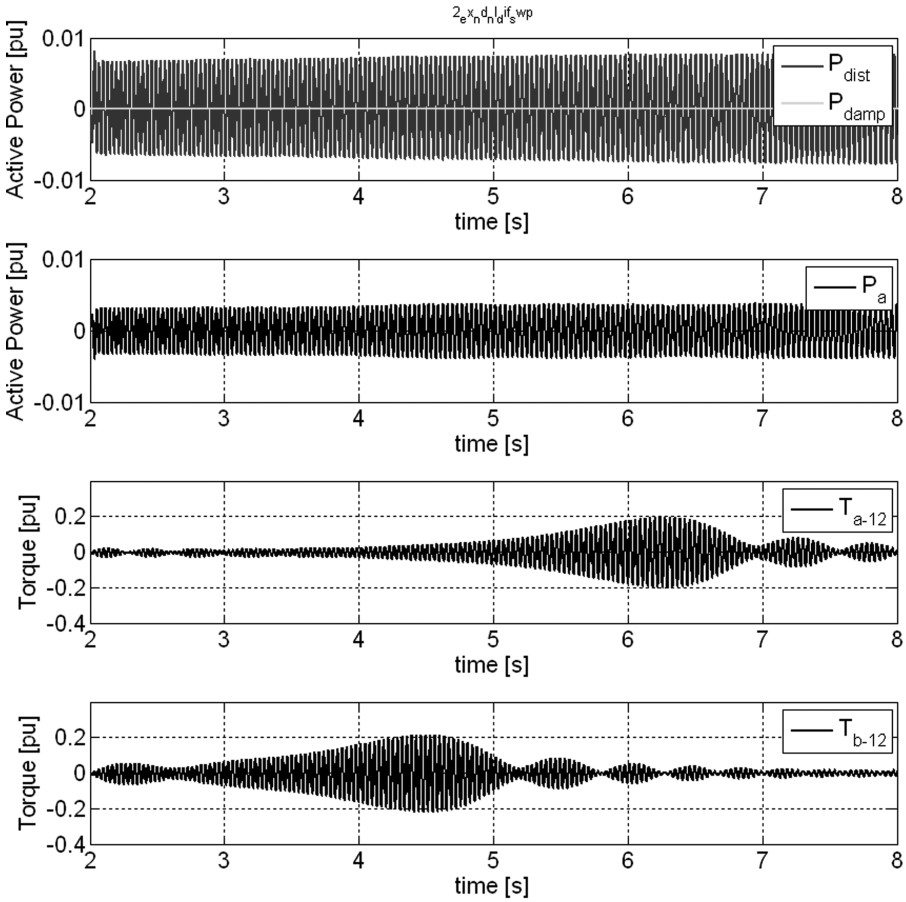

Figure 5.30: Variable speed drive acts on speed reference change with $2.5\,rpm/s$ and thus producing interharmonics, which excites the two generators at their natural frequency. $f_{nat(b)}$ is reached after $\sim 4s$, $f_{nat(a)}$ after $\sim 4.2s$. Active Damping disabled.

A variable speed drive produces harmonics with $\sim 0.5\%$ of the nominal power of generator (a) or (b). This variable speed drive acts on a speed reference change request with a constant rate of $2.5\,rpm/s$, resulting in a variable frequency disturbance power (Figure 5.30 - subplot 1, blue). The effective air-gap torque is indicated for generator (a) in subplot 2; the alternating torque in generator coupling (a) and (b) are shown in subplot

3 and 4. The harmonic with varying frequency affects the alternating torque and excites the two generator trains at their natural frequency. The disturbance chosen is very small, but still excites the alternating torque to $40\%_{pk-pk}$ in both drive trains, which could be already the continuous duty limit of the mechanical system. The same run with the external damping device enabled, based on Section 5.2 (configuration a-e-f) with a damping resistor, is shown for both generators in Figure 5.31.

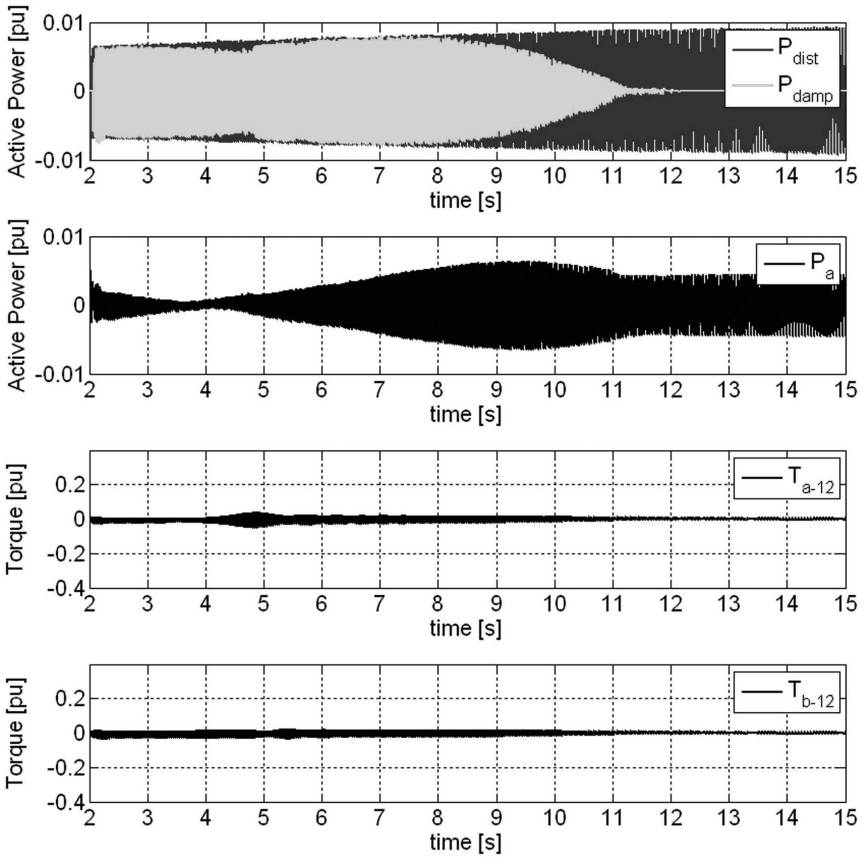

Figure 5.31: Same run as in Figure 5.30, but with active damping enabled: The dynamic torque level is significantly reduced in both mechanical systems.

The maximum of the alternating torque is shifted; the damping power is partially compensated and thus less effective at the new maximum due to anti-phase of the alternating torque components. The new maximum is not a natural frequency, and will not grow to the alternating torque magnitudes of the case, which is not damped. The air-torque increases due to the increasing filter phase lag, with increasing frequency. The modulated air-gap torque component reaches, therefore, a higher magnitude. At non-critical frequencies the modulated air-gap torque harmonic does not have any impact on the mechanical drive train. The amplitude will die out with increasing interharmonic frequency due to

the low pass characteristic of the filter, which has been applied. This effect could even be improved with more advanced filter approaches, as mentioned in previous sections. The overall alternating mechanical torque is significantly reduced.

Separate Device for Torsional Mode Damping - Optimization

The question of how to operate the separate, torsional mode damping device in power systems is more critical compared to the integrated version, especially with utilizing simple resistors to modulate active power with the sensitive electrical machine. In this case, damping means heating a resistor, to dissipate energy. As already discussed, very little power is needed for the damping operation, typically less than one percent of the nominal power. The proportional behavior of the damping loop results in much lower energy converted into heat at low alternating torque levels. The damping device can be disabled for non-critical operation(s). Or the damping loop gain can be adapted, dependent on the mechanical system to be protected, to use low gain in non-critical operation, and higher gain for critical operation. This is contrary to the optimization approach of the integrated torsional mode implementation. Optimizing the damping loop requires more complex control routines, with potential negative impact on the reliability. Therefore, separate damping devices should always be based on a modular approach. Each module can be controlled autonomously, so that sufficient damping power can also be generated if a single damping module fails.

5.5.3 Damping of Multiple Modes

Damping multiple natural modes of a single machine is an extension of the previous section, with the difference being the larger distance between the different natural modes compared to identical units. The first mode is usually the most critical in terms of TI. The probability of this mode to be in the subsynchronous range is high for large drive trains, and the damping of that mode is typically very low. But there are also drive train examples, especially very long drive trains, where more than one mode is sensitive to interact with electrical system harmonics.

Figure 5.32 illustrates a typical configuration of an LNG drive train, fed by a gas turbine. The electrical machine is fed by a VSD in order to start the drive train, but also to support it during high ambient temperatures, where the gas turbine is not able to provide the full power, e.g. $\sim 100MW$. Those drive trains can have lengths of $30m$ or more, and multiple natural frequencies below $50Hz$. An increased damping at multiple natural frequencies can be achieved, as described before. The separation of the multiple modes is key, and can be achieved e.g. in using different torque measurement locations for different

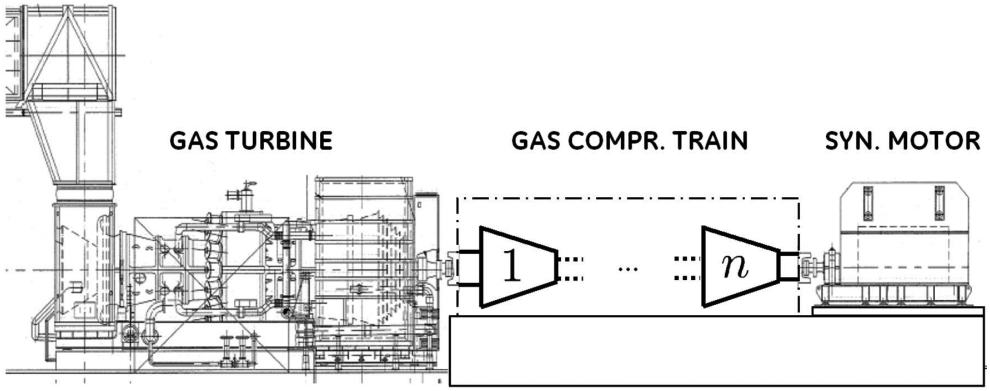

Figure 5.32: Typical configuration of an LNG compression train with several compressor stages.

torsional natural frequencies, based on the calculated mode shapes. An observer can be used if classical filters and different locations do not allow separating the critical modes sufficiently.

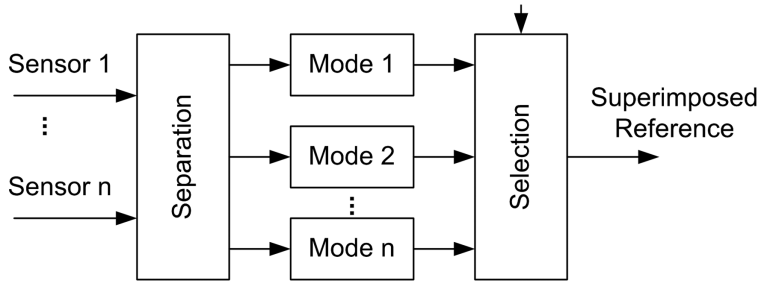

Figure 5.33: General block diagram - damping multiple modes with a single damping control.

The general block diagram (Figure 5.33) describes the implementation for damping several modes simultaneously. The dedicated modes will be treated separately, and will finally be superimposed to the modulation reference signal. Adaptive weighting functions, dependent on the expected modes to be present for the actual operation condition, can be necessary if the separation part is not able to perfectly decouple the different modes.
Example simulation results are shown in Figure 5.34 and Figure 5.35, assuming that two of the torsional modes are excited at $t > 2.5s$. These two figures show time histories of the simulated shaft torque at different locations of the compression train of Figure 5.32: T_{GT-C1} is the torque at the gas turbine coupling; T_{C3-EM} can be measured at the motor coupling; T_{C1-C2} and T_{C2-C3} represent shaft torque between compressor stages.

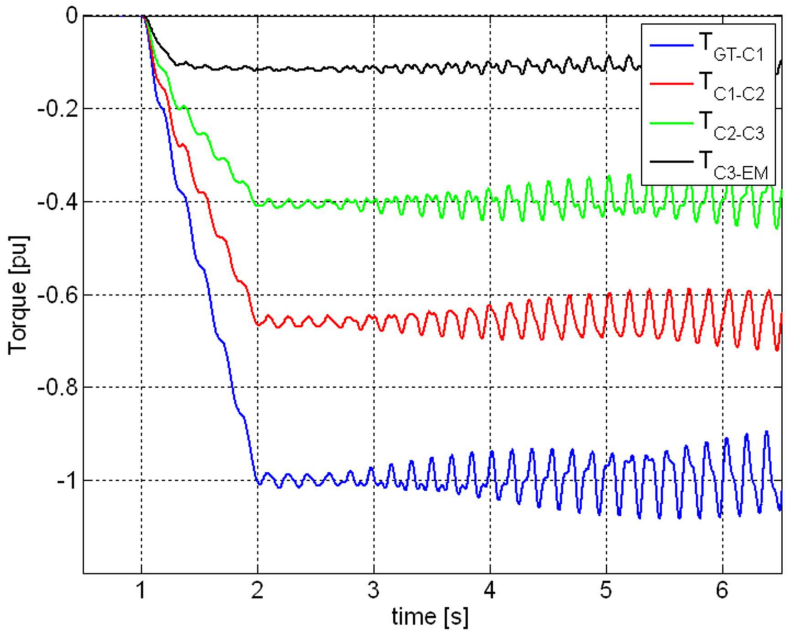

Figure 5.34: Excitation of the first two natural frequencies of an LNG compressor train.

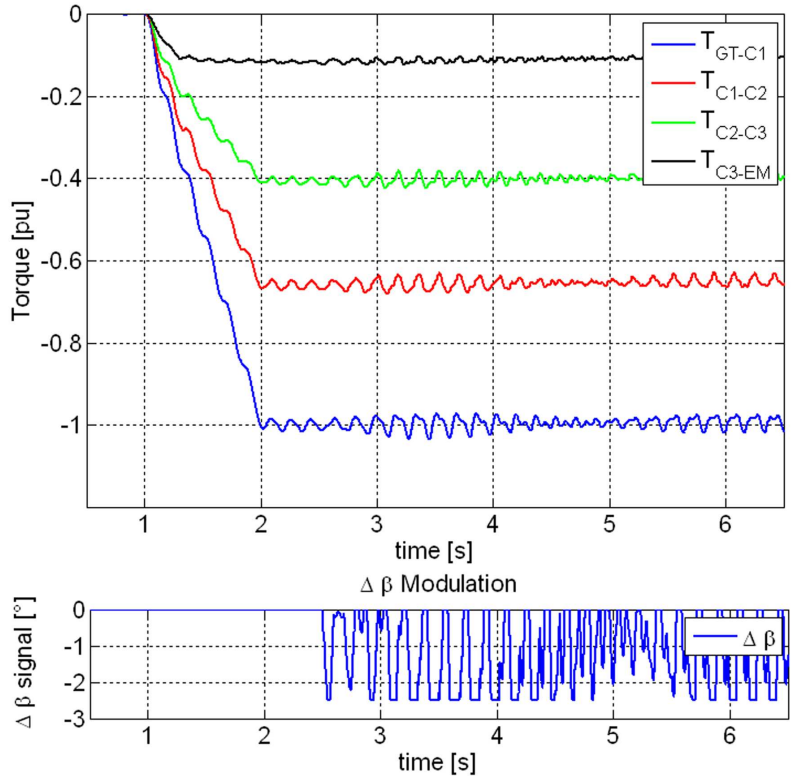

Figure 5.35: Excitation of the first two natural frequencies of an LNG compressor train, damping circuit enabled for $t \geq 2.5s$.

It is unlikely that two modes will be simultaneously excited, but this case was investigated to ensure that several modes could be damped without nuisance interactions. Additional simulations were performed to ensure that satisfactory torsional mode damping can be achieved in cases where either single modes and up to three modes are excited by motor air-gap torque harmonics.

5.5.4 Wind Turbine Emergency Stop

An emergency stop (E-stop) brings a wind turbine to complete stop as fast as possible. The wind turbine control system orders an E-stop in case of grid loss, excessive vibration, excessive over speed, excess temperature, etc. Several actions are automatically initiated when an E-stop is requested: The blade pitch control has to turn the blades out of the wind, the main converter is switched off, the mechanical brake is activated etc. Immediately pitching the blades and activating the mechanical brake is required in order to ensure that the wind turbine does not run into excessive over speed.

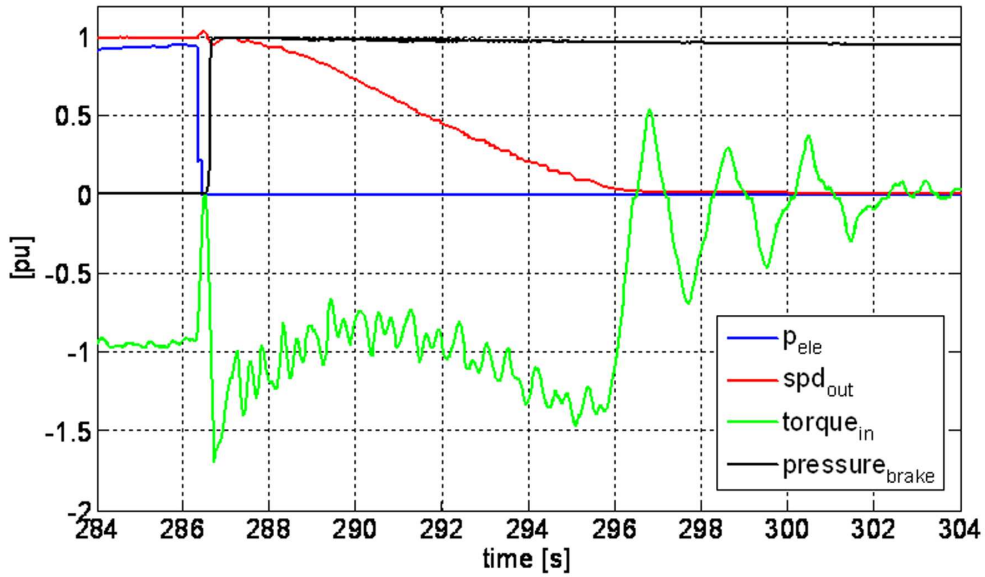

Figure 5.36: Emergency stop event measurement of a wind turbine [54].

The emergency stop is characterized by a sudden drop in the generator torque P_{ele} (blue line in Figure 5.36), followed by a torque step on the shaft when the mechanical brake is applied $torque_{brake}$ / $pressure_{brake}$ (black). The turbine accelerates (spd_{geno}, red) after tripping the converter because of the time delay due to dynamic constraints of the mechanical brake system. This time delay results in a dynamic torque response of the shaft ($torque_{in}$ (green)). The first peak clearly exceeds the nominal torque of the shaft, and is

followed by alternating torque oscillations at the first natural frequency of the turbine, until the turbine is at zero speed. There are several torque reversals before the E-stop event is completed.

The emergency stop represents a severe load cycle, responsible for a significant reduction of gearbox lifetime [55]. Improvements in the past were mainly characterized by modifications to the mechanical brake system to react faster or to be better controllable to achieve a smoother torque response.

Torsional Rotor Dynamics

Wind turbines have complex drive trains, consisting of many torsional components (Figure 5.37). The dimension of the rotor shaft system is similar to the dimension of drive trains in the Oil & Gas industry described previously. The main natural frequencies of a wind turbine are typically between $1Hz < f_1 < 3Hz$, which is, for nominal operation, well within the bandwidth of the available torque controller. There are typically several modes below the synchronous frequency.

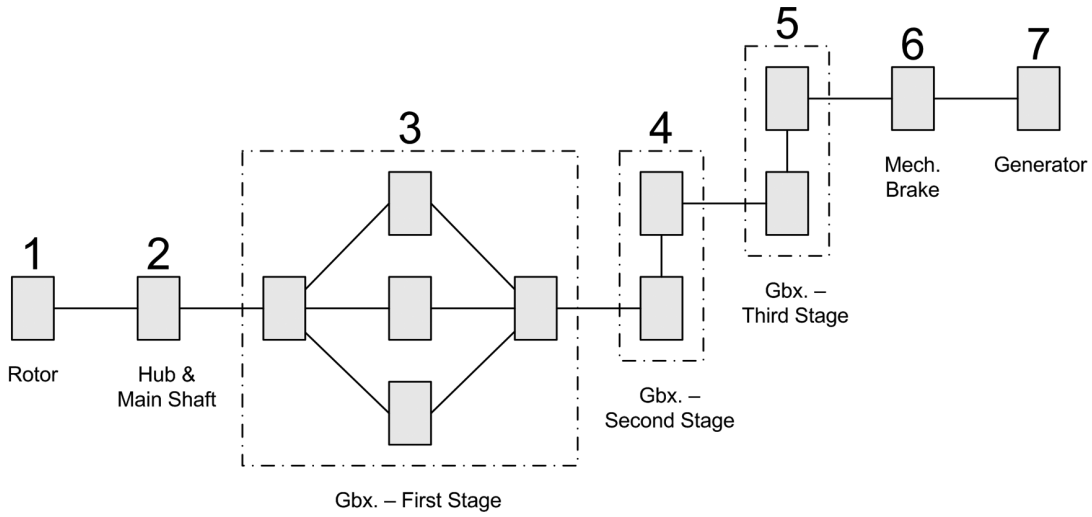

Figure 5.37: Wind turbine rotational system representation, reduced to a 7^{th} order mass-system.

A mechanical system representation model of a wind turbine was built as shown in Figure 5.37 to show benefits of having an additional dynamic electromagnetic brake supporting the mechanical brake during the E-stop event. The E-stop event, with available dynamic brake, can be split into two stages, (1) a transition smoothing part to avoid torsional excitation, and (2) a torsional mode damping part to increase the damping of the drive train at the relevant natural frequency of the drive train.

The additional dynamic brake will be based on a similar hardware design as described in Section 5.2, and takes care of the dynamic requirements for the overall brake system.

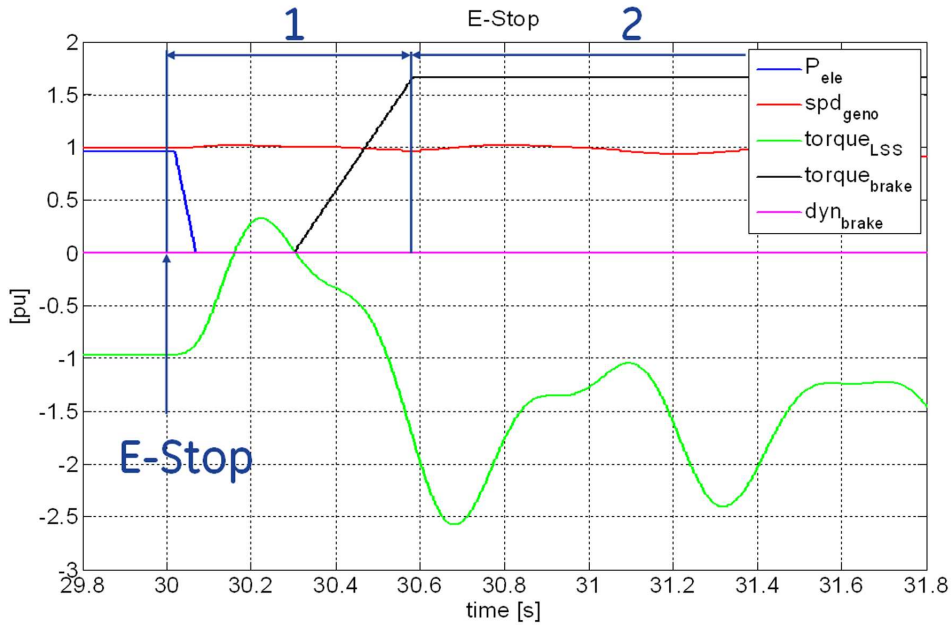

Figure 5.38: E-Stop event split into two parts, (1) smoothing transition, (2) torsional mode damping.

The power electronic hardware can be directly connected to the generator terminals. The brake torque in Figure 5.38 and Figure 5.39 is normalized to the nominal torque on the high-speed shaft to indicate the torque transition between the normal operation and the braking event.

The smoothing transition part (1) can be achieved with a feed forward reference that considers the active power produced before the E-stop event occurrence, or with closed loop control e.g. based on speed or torque information of the shaft. Torsional mode damping reference (2) is derived as described in Section 4.2, and requires, because of the closed loop implementation, a sensed signal from the mechanical system, e.g. from a torque sensor connected to the main shaft. The effect of the dynamic brake is demonstrated in Figure 5.39, where the response of the system after an E-stop is shown with a conventional mechanical brake (dashed) and with additional dynamic electromagnetic brake (solid). The dynamic torque component is significantly reduced.

Total excitation avoidance can only be achieved when the generator torque before the E-stop event is equal to the brake torque during the E-stop event. This is not possible if we assume that the brake torque is higher than the nominal generator torque. The intention of the dynamic brake is to support the main mechanical brake to achieve better overall braking behavior, resulting in very compact design for the brake resistor. The energy dissipation and the required dump resistor size can be estimated by calculating the

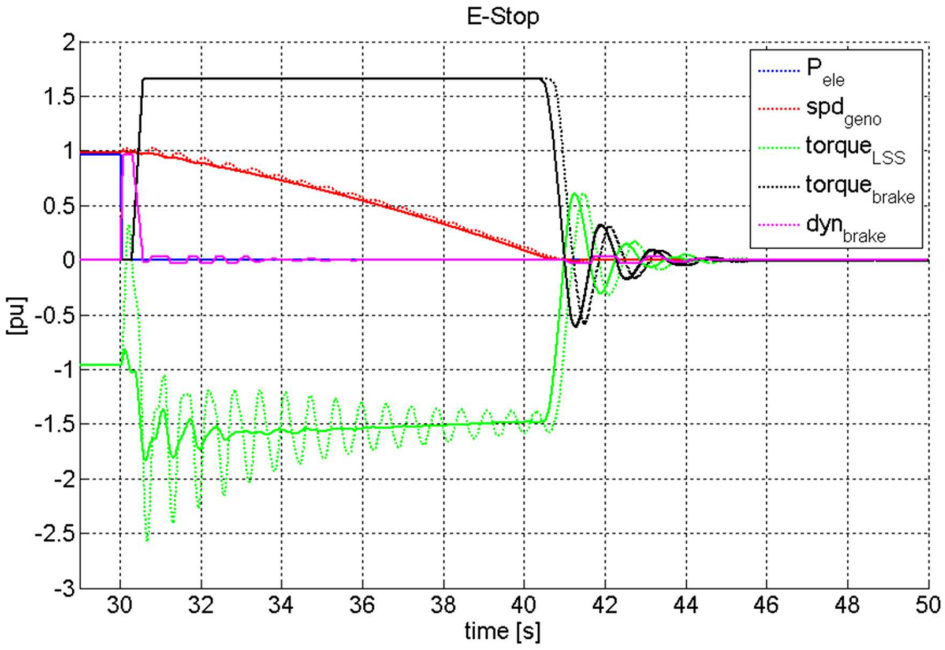

Figure 5.39: Simulation of the resulting torque during an E-Stop event with and without dynamic brake.

surface below the magenta dynamic brake line. The major energy needs to be dissipated during the initial smoothing transition phase, where the dynamic brake power can reach the nominal power. The smoothing phase typically lasts less than $500ms$. The power electronic and the dump resistor can be designed with a certain overload capability, to withstand the peak power without rating it to nominal power. The torsional mode damping has much lower power requirements, as it operates at natural frequency of the modes to be damped. Using a different shape, e.g. applying a reference to try to smooth the mechanical brake's torque step, does not change the overall system response; the torque step, while effectively activating the brake, can't be reduced significantly.

An even better brake system response during an emergency event can only be achieved by a modified mechanical brake, or by introducing a different dynamic brake design, e.g. by using energy storage, which is, at this time, very costly with respect to the required size and therefore has not been considered further.

5.6 Economic Aspects of Torsional Mode Damping

An economic decision whether or not to implement the developed torsional mode damping system requires comparing (a) the effort and effectiveness of conventional counter-measures, as discussed in Section 4.1 and/or the cost of potential outages of the drive train during operation with (b) the effort to implement one of the developed torsional mode damping approaches (Section 5.2 or 5.3). Several aspects have to be considered for the economic evaluation:

- Implementation: Is the counter-measure considered in the design phase, or is a retrofit-implementation needed? Is the sensitive drive train a prototype (true for most large drive trains) or an off the shelf product?
- Sensing: How difficult is it to sense the torsional oscillation, how does the mode shape distribution look like? Which sensors are available?
- Control: Is appropriate control hardware available to add the functionality as discussed in Section 4.2.2? What type of signal processing is needed (based on available sensing opportunities)?
- Active Power Modulation: Can the damping converter be based on available hardware? Do owner and manufacturer of the available hardware support the implementation?
- Mechanical Drive Train: Is the rating of drive train components done based on dynamic loads caused by torsional oscillations (and thus sufficiently overrated)?
- Operation of the Mechanical Drive Train: Is continuous operation at critical speeds expected?

The pure costs associated with the implementation of the developed and discussed methods differ significantly depending on the answers given to the questions above. Conservative cost estimations for torsional mode damping will be performed within this section based on the discussed application examples:

1. Variable Speed Drive Application (Section 5.5.1)
2. Damping in Power Systems (Section 5.5.2)
3. Wind Turbine Emergency Stop (Section 5.5.4)

The main components needed for the implementation are a sensor measuring a signal representative of shaft torque, control hardware and a power converter unit to exchange a controlled amount of active power with the drive train.

The integrated torsional mode damping implementation (1.) can be built based on commercially available torque sensors (e.g. $\sim 6k\$$ [49]). The controller used for that application is based on a Real-time Processor / FPGA Hardware, including software for torsional mode damping operation, -tuning and -protection. The cost for the controller can be assumed with $\sim 5k\$$ [56]. The interface to the available converter is assumed to be prepared within one day. The associated costs are estimated at $2k\$$. The total cost of the hardware for an integrated torsional mode damping solution can therefore be assumed to be below $15k\$$. Redundancy requirements could increase this cost assumption; using available control hardware would reduce it. Using a different type of converter to potentially mitigate the effect of torsional interaction instead would increase the total cost by several million Dollars.

The implementation of damping torsional oscillation in power systems (2.) would potentially result into additional requirements, mainly the need of a damping converter. The converter discussed in Section 5.2 with a nominal power rating of $300kW$ peak power can be assumed with $\sim 15k\$$, the required transformer would add $\sim 10k\$$. The total cost of the torsional damping solution would than be $\sim 50k\$$ (including auxiliary equipment) for a generator with a nominal power of $\sim 30MW$. A $24h$ power outage of that generator caused by torsional interaction would result in significant loss of energy production exceeding the costs associated with the torsional mode damping implementation.

The hybrid braking solution proposed for wind turbine implementation requires basically a converter specified for pulse mode operation. Typical converters can be overloaded by factor of five for short time operation up to 5 seconds. The required converter for a $2MW$ wind turbine can be estimated with $\sim 15k\$$, the available speed sensor and control hardware limits the costs for such implementation. The replacement of a damaged gearbox can be estimated to be at least $100k\$$.

Mechanical systems are typically overrated based on empiric knowledge to withstand certain amount of alternating torque. A more lightweight design is possible with considering the developed damping method already during the design stage of the drive train. The costs associated with the implementation of the developed torsional mode damping method are comparably low, also for a retrofit implementation.

5.7 Summary - Field of Application

The number of applications proposed for the developed active damping method has shown clear benefits of this method. Some of these applications have already been implemented and tested in the field. Two main categories of implementation have been discussed: Utilizing existing power electronic devices for modulating active power with the mechanical drive trains, and adding dedicated converters for the same purpose. Both implementations benefit from the comparably low power requirement with this active damping method, one percent of the drive trains nominal power has been identified to be sufficient in many cases. Both implementations allow retrofit applications, many issues with torsional interaction are detected only during commissioning or operation.

The possibility to access already existing power electronic device for an integration of torsional mode damping serves as a risk mitigation, and can be specified already during the design phase of the power electronic converter. The damping control does not influence the inherent operation of the converter, because of the very limited power requirement for this active damping method. The additional costs for the implementation are typically low compared to the total cost of the system. It has been shown with LCIs from different manufacturers that it is possible to successfully include this interface into their systems.

Using a dedicated damping converter to support sensitive mechanical drive trains has been discussed for power system applications. It is beneficial to use separate devices in cases, where suitable power electronic converters are not available, or where reliability and redundancy requires dedicated and potentially distributed damping converters.

A single power electronic converter can be used for several drive trains with potential torsional issues, or to increase the damping of several natural frequencies of a single drive train. The main task is to measure and to isolate the relevant natural frequencies, which can be achieved with available sensing and signal processing methods. The power electronic design of a dedicated converter or the interface to an available converter is not influenced by this extension of functionality.

The developed method enables the design of even larger mechanical systems, or even more complex power systems, e.g. full electric plants, without having the operational constraints of torsional interaction. All this functionality can be provided at comparably low cost.

6

Summary

This thesis seeks to increase the reader's sensitivity to new torsional interaction phenomena caused by an increased number of large variable-speed drives, especially in weakly connected power systems. Large mechanical drive trains have some unique properties that make them very sensitive to torsional interaction, e.g. low inherent mechanical damping properties at their natural frequencies. The natural frequencies can already be found below the synchronous frequency because of the dimensions and torsional stiffness of the large systems. A calculation of the mode shapes, the modal distribution of the torsion angle along the mechanical system, can be used to identify natural frequencies sensitive to torsional interaction. Power electronic converters, used to operate electric motor driven trains at variable speed, contribute significantly to torsional interactions due to their production of harmonics and interharmonics that potentially excite critical torsional modes in case of coincidence with these frequencies. The variable speed driven motors, but also power generation units that are installed in proximity to the variable speed drives, can be affected by harmonic excitation. The resulting dynamic torque levels can have significant impact on the lifetime of the mechanical system.

A variety of methods for reducing torsional oscillations are described in literature. Different power levels require a diversity of methods, because of different technical properties and requirements in low and high power systems. Solutions applied in low power applications, e.g. for servo-drives, cannot be applied with multi-megawatt systems, as explained in more detail in Section 4.1.2. The sensing of torsional oscillations is already a challenge in high power applications because of the high torsional stiffness of the rotor shaft system. Even high precision speed encoders used in very dynamic servo-drive applications

are not sensitive enough for monitoring torsional oscillation in high power applications. They require observer based speed sensing or direct torque sensing methods, e.g. based on measuring the shaft stress or strain.

High power electronic converters can be designed to generate air-gap torque harmonics with amplitudes that stay below one percent of the nominal torque at critical frequencies, which is very low, but still sufficient to excite natural frequencies of multi-megawatt drive trains. Avoiding critical speeds is a suitable approach for some variable speed drive (VSD) applications, but leads to limitations in the operating range and it cannot be applied to avoid torsional interactions with multiple VSDs and nearby generators.

Therefore, new methods of solving torsional interaction issues for large drive trains have been developed, analyzed, and verified by numerical simulations and tests. The torsional mode damping methods are based on increasing the damping property of a mechanical drive train at its natural frequencies without modifying the mechanical design. The developed method exchanges active power at the natural frequency of the mechanical system in-between a power electronic converter and the sensitive mechanical drive train, based on a feedback signal from the mechanical system. The active power modulation is done in such a way that the effect is the same as an increased mechanical damping. The requirements for the power electronic converter are comparably low, as the required power is typically less than one percent of the nominal power of the critical drive train. The developed method can cope with dead-times, e.g. due to the control implementation into an existing power electronic hardware, without significant effect on the achieved damping performance. This enables implementation of this damping solution as a retrofit to existing drive systems. The developed solution is very robust, so that any minor changes to the drive train's mechanical system do not affect the effectiveness of the damping device. Several applications for this damping control approach have been proposed in this thesis. Generally, the proposed method allows the design and production of even larger drive trains based on low cost power electronics, e.g. line commutated converters. Without active damping control, self-commutated converters with a significantly higher number of active devices would be required, in order to minimize critical air-gap torque harmonics, because of decreasing torsional damping parameters with increasing size of the mechanical trains.

One potential field of further research is the improvement of the implementation of the torsional mode damping topology, especially the sensing part and the filter. The developed torsional mode damping system was successfully tested in several string tests with multi-megawatt drive trains.

List of Figures

Bibliography

[1] A. T. D. Almeida, F. J. T. E. Ferreira, and P. Fonseca, "VSDs for Electric Motor Systems," 2000.

[2] V. Hütten, R. M. Zurowski, and M. Hilscher, "Torsional Interharmonic Interaction Study of 75MW Direct Driven VSDS Motor Compressor Train for LNG Duty," No. 37, (Turbomachinery Laboratory, Texas A&M University, College Station, Texas), Turbomachinery Symposium, 2008.

[3] T. Feese and R. Maxfiedl, "Torsional Vibration Problem with Motor/ID Fan System Due to PWM Variable Frequency Drive," No. 37, (Turbomachinery Laboratory, Texas A&M University, College Station, Texas), Turbomachinery Symposium, 2008.

[4] K. T. Andersen, "Torsional Oscillation in Drive Systems," 2005.

[5] F. Joswig and S. Kulig, "Perception about new kinds of subsynchronous resonances," (Rio de Janeiro), IPST, 2001.

[6] P. Kundur, *Power System Stability and Control.* No. 978-0070359581, New York: McGraw-Hill, 1994.

[7] M. Hernes, "Risk for interaction between components in power grids containing a high percentage of converter loads," 2002.

[8] "API Standard 617 - Axial and Centrifugal Compressors and Expander-Compressors for Petroleum, Chemical and Gas Industry Services," 2002.

[9] H. Dresig and F. Holzweißig, *Maschinendynamik.* No. 978-3540876939 in 7, Berlin: Springer Verlag, 2006.

[10] J. Huster and A. Ziegler, "Simulation der Beanspruchungen der Wellen und langen Niederdruck Schaufeln grosser Dampfturbinensatze mit geschweissten ND-Trommelrotoren in thermischen Kraftwerken bei elektrischen Stoerfallen," vol. 1749, 2003.

[11] M. A. Corbo, "Torsional Vibration Analysis of Synchronous Motor-Driven Turbomachinery," No. 29, (Turbomachinery Laboratory, Texas A&M University, College Station, Texas), Turbomachinery Symposium, 2000.

[12] C. Sihler, "A novel torsional exciter for modal vibration testing of large rotating machinery," vol. 20, pp. 1725–1740, Mechanical Systems and Signal Processing, 2006.

[13] C. Sihler, S. Schramm, J. Song-Manguelle, P. Rotondo, S. D. Puglia, and E. Larsen, "Torsional Mode Damping For Electrically Driven Gas Compression Trains In Extended Variable Speed Operation," No. 38, (Turbomachinery Laboratory, Texas A&M University, College Station, Texas), pp. 81–92, Turbomachinery Symposium, 2009.

[14] H. Holzer, *Die Berechnung der Drehschwingungen.* No. 978-1161070880, Berlin: Springer Verlag, 1912.

[15] E. I. Rivin, "Methode zur Verminderung der Freiheitsgrade in Berechungsmodellen verketteter und verzweigter Systeme," pp. 38–41, Vestnik Masinostronenija, 1966.

[16] P. N. Di, *Beitrag zur Reduktion diskreter Schwingunsketten auf ein Minimalmodell.* PhD thesis, TU Dresden, 1973.

[17] M. Bressani, A. Odorico, and M. Sica, "High-Speed, Large-Power Induction Motors for Direct Coupling to Variable Speed Gas Compressors," vol. Fifth European Conference on Power Electronics and Applications, 1993.

[18] W. Wenzke, "Zur Ableitung der dynamischen Kennlinie des Asynchronmotors im Hinblick auf die Berechnung von Schwingungserscheinungen in Antriebsanlagen," pp. 517–523, Wiss. Zeitschrift der TU Magdeburg, 1970.

[19] C. M. Ong, *Dynamic Simulation of Electric Machinery using Matlab/ Simulink.* No. 978-0137237852, Prentice Hall, 1999.

[20] T. Bödefeld, *Elektrische Maschinen.* No. B0000BGNS8, Springer Verlag, 1949.

[21] B. K. Bose, *Power Electronics and Motor Drives Advances and Trends.* No. 978-0120884056, Academic Press, 2006.

[22] N. G. Hingorani and L. Gyugyi, *Understanding Facts.* No. 978-0780334557, IEEE press, 2000.

[23] E. Morris, "A Guide to Standard Medium Voltage Variable Speed Drives," ABB Industrie AG, 2008.

[24] R. Klug and A. Mertens, "Reliability of Megawatt Drive Concepts," vol. 2, pp. 636–641, IEEE International Conference on Industrial Technology, 2003.

[25] A. Siebert, A. Troedson, and S. Ebner, "AC to DC Power Conversion Now and in the Future," vol. 38, IEEE Transactions on Industry Applications, 2002.

[26] W. Leonhard, *Control of Electrical Drives*. No. 978-3540418207, Berlin: Springer Verlag, 1997.

[27] J. J. Simond, A. Sapin, M. T. Xuan, R. Wetter, and P. Burmeister, "12-Pulse LCI Synchronous Drive for a 20 MW Compressor - Modeling, Simulation and Measurements," pp. 2302–2308, IEEE Transactions On Industry Applications, 2005.

[28] A. Adachi, K. Tanaka, and Y. Fukushima, "Torsional Lateral Coupled Vibration of Centrifugal Compressor System at Interharmonic Frequencies Related to Control Loop Frequencies in Voltage Source PWM Inverter," No. 38, (Turbomachinery Laboratory, Texas A&M University, College Station, Texas), Turbomachinery Symposium, 2009.

[29] P. M. Anderson, B. L. Agrawal, and J. E. V. Ness, *Subsynchronous Resonance in Power Systems*. No. 978-0780353503, Technology & Engineering, 1999.

[30] S. Kulig and D. Lambrecht, "Resonant Excitation of Turbine Generator Shaft," (Stuttgart), The Road-Vehicle-System and Related Mathematics Workshop, 1985.

[31] S. Kulig, *Über die Auswirkungen von Störfällen in elektrischen Energieübertragungsnetzen auf Kraftwerksturbosätze*. PhD thesis, FU Hagen, 1987.

[32] M. Humer, *Erfassung und Bewertung von Torsionsschwingungen in Wellensträngen von Kraftwerksturbosätzen*. PhD thesis, Universität Dortmund, 2004.

[33] D. Lee and P. Kundur, "Advanced Excitation Controls for Power System Stability Enhancement," vol. 38-01, (Paris), CIGRE, 1986.

[34] "Std 1204-1997 - Guide for Planning DC Links Terminating at AC Locations Having Low Short-Circuit Capacities, PartI: AC/DC Interaction Phenomena," 1997.

[35] K. Mortensen, E. V. Larsen, and R. J. Piwko, "Field Tests and Analysis of Torsional Interaction Between the Coal Creek Turbine-Generators and the CU HVDC System," IEEE transaction on power apparatus and systems, 1981.

[36] R. J. Piwko and E. V. Larsen, "HVDC System Control For Damping Subsynchronous Oscillation," vol. PAS-101, IEEE transaction on power apparatus and systems, 1982.

[37] A. Abedini, G. Mandic, and A. Nasiri, "Wind power smoothing using rotor inertia aimed at reducing grid susceptibility," No. 34th, pp. 1445–1451, 2008,.

[38] T. Feese and C. Hill, "Prevention of Torsional Vibration Problems in Reciprocating Machinery," No. 38, (Turbomachinery Laboratory, Texas A&M University, College Station, Texas), pp. 213–239, Turbomachinery Symposium, 2009.

[39] H. Müller, M. Pöller, A. Basteck, M. Tilscher, and J. Pfister, "Grid Compatibility of Variable Speed Wind Turbines with Directly Coupled Synchronous Generator and Hydro-Dynamically Controlled Gearbox," vol. 6, (Delft, NL), Workshop on International Large Scale Integration of Wind Power and Transmission Networks for Offshore Wind Farms, 2006.

[40] D. E. Walker, C. Bowler, R. Jackson, and D. Hodges, "Results of SSR Tests at Mohave," vol. PAS-94, pp. 1878–1889, IEEE Transactions, 1975.

[41] M. Perrin, G. Kohn, S. Mugford, and G. Seggewiss, "Induction motors, reciprocating compressors and variable frequency drives," vol. 44, (Banff, Alta.), The Institute of Electrical and Electronics Engineers Incorporated Industry Applications Society - Petroleum and Chemical Industry Conference, 1997.

[42] GEEnergy, *Turbine-Generator Torsional Stress Analyzer (TSA).* http://www.gepower.com/.../downloads/10088.pdf, 2004.

[43] "Countermeasures to Subsynchronous Resonance Problems," 1980.

[44] N. Olgac, "Delayed Resonator as active absorber," 1995.

[45] D. Schröder, *Elektrische Antriebe-Regelung von Antriebssystemen.* No. 978-3540419945, Springer Verlag, 2001.

[46] T. Kakinoki, R. Yokoyama, G. Fujita, K. Koyanagi, and T. Funabashi, "Evaluation technique of turbine shaft fatigue in private-generation systems using consumption rate of shaft life cycle," pp. 779–783, IEEE International Conference on Power System Technology, 2002.

[47] E. V. Larsen, "Applying Power System Stabilizers, Part I-III," vol. PAS-100, IEEE Transaction on Power Apparatus and Systems, 1981.

[48] R. J. Piwko, C. A. Wegner, S. J. Kinney, and J. D. Eden, "Subsynchronous Resonance Performance Tests of the Slatt Thyristor-Controlled Series Capacitor," vol. 11, pp. 1112–1119, IEEE Transactions on Power Delivery, 1996.

[49] A. Wirsen and S. Kulig, "A Contact-Less Torque Sensor for Online Monitoring of Torsional Oscillations," 2007.

[50] C. Sihler and A. M. Miri, "A Stabilizer for Oscillating Torques in Synchronous Machines," vol. 41, IEEE Transaction on Industry Applications, 2005.

[51] T. Zöller, A. M. Miri, and T. Leibfried, "Power Electronic Devices for Damping Torsional Vibrations," No. 7, International Conference on Power Electronics and Drive Systems, 2007.

[52] S. Schramm, "Torsional Mode Damping in Island Power Systems," Master's thesis, Munich University of Applied Sciences, 2006.

[53] S. Schramm, C. Sihler, J. Song-Manguelle, and P. Rotondo, "Damping Torsional Interaction Effects of Large Drives," vol. 25, pp. 1090–1098, IEEE Transactions on Power Electronics, 2010.

[54] J. Hemmelmann, "Latest Results On Transmission and Conversion," (Brussels), 2008.

[55] A. Heege, "Computation of Dynamic Loads of Wind Turbine Power Trains," vol. XXVI, (Còrdoba, Argentina), pp. 2985–3004, Mecànica Computational, 2007.

[56] "CompactRIO-PAC-Hardware," (www.ni.com/pac/d/crio.htm), National Instruments, 2009.